Supplementary Information (SI) for Chemical Science.
This journal is © The Royal Society of Chemistry 2025

Supporting Information

Bio-inspired total synthesis of daphnepapytone A

Joan Pereira,[a] Nicolas Casaretto,[b] Gilles Frison,[c] Bastien Nay*[a]

[a] Laboratoire de Synthèse Organique, Ecole Polytechnique, ENSTA Paris, CNRS, Institut Polytechnique de Paris, Route de Saclay, F-91128 Palaiseau Cedex, France

[b] Laboratoire de Chimie Moléculaire, Ecole Polytechnique, CNRS, Institut Polytechnique de Paris, Route de Saclay, F-91128 Palaiseau Cedex, France

[c] Laboratoire de Chimie Théorique, Sorbonne Université, CNRS, F-75005 Paris, France

Table of content

1 Supplementary Tables and Figures in support to the discussion 3
Table S1. Catalyst or reagent screening the allenic Pauson-Khand reaction 3
Table S2. Optimisation of the allenic Pauson-Khand reaction catalyzed with a Rh^{I}-based catalyst ...3
Table S3. Optimisation attempts of the allenic Pauson-Khand reaction using chloroform as a CO source in the COware 4
Table S4. Comparison of ^{1}H and ^{13}C NMR spectra ($CDCl_3$) of natura and synthetic oleodaphnone (**3**) 5
Table S5. Comparison of ^{1}H and ^{13}C NMR spectra ($CDCl_3$) of the natural and synthetic daphnenicillata W (structure **11**) 6
Table S6. Comparison of ^{1}H and ^{13}C NMR spectra (DMSO-d_6) of the natural and synthetic diarthroncha C (structure **10**), highlighting inconsistencies 7
Table S7. Comparison of ^{1}H and ^{13}C NMR spectra (DMSO-d_6) of the natural diarthroncha C and synthetic daphnenicillata W (structure **11**) 8
Table S8. Attempts of formation of a dienol silyl ether in view of a vinylogous Rubottom reaction for the γ-hydroxylation of substrate **2** 9
Table S9. Attempts of direct γ-hydroxylation of substrate **2** 9
Table S10. Optimisations of the C-H oxidation reactions in presence of CrO_3.....9
Table S11. Comparison of ^{1}H and ^{13}C NMR spectra (CD_3OD) of natural and synthetic daphnepapytone A 10
Table S12. Computed relative Gibbs free energy (in kJ/mol) between $\mathbf{TS_{ax}}$ and $\mathbf{TS_{eq}}$ at various level of calculations. 29
Table S13. Absolute electronic energies and thermal corrections (in a.u.) for all molecules (B3LYP-D3 geometry optimisation). 31
Table S14. Absolute electronic energies and thermal corrections (in a.u.) for $\mathbf{TS_{ax}}$ and $\mathbf{TS_{eq}}$ (M06-2X geometry optimisation).....31
Table S15. Absolute electronic energies (in a.u.) of $\mathbf{TS_{ax}}$ and $\mathbf{TS_{eq}}$ computed at various level.....31
Table S16. Crystal data and structure refinement for compound **1** (CCDC 2418571).....32
Table S17. Crystal data and structure refinement for compound **2** (CCDC 2419407).....33
Table S18. Crystal data and structure refinement for compound **3** (CCDC 2418579).....34
Table S19. Crystal data and structure refinement for compound **9b** (CCDC 2419409) 35
Table S20. Crystal data and structure refinement for Compound **13** (CCDC 2419408) 36
Table S21. Crystal data and structure refinement for compound **14** (CCDC 2428644).....37
Table S22. Crystal data and structure refinement for compound **15** (CCDC 2418568).....38
Table S23. Crystal data and structure refinement for compound **19** (CCDC 2423044).....39

Figure S1. X-ray crystallographic structure of **3** showing an equimolar distribution of two conformers in the crystal, with a pseudo-equatorial (left) or a pseudo-axial orientation (right) of the isopropenyl group. 11
Figure S2. Key HMBC (H✂C) correlations observed for compound **2** (a) and compound **13** (b), and key NOESY correlation (blue) demonstrating the stereochemistry of C-4 in compound **13**.[10] 11
Figure S3. Copy of the ^{1}H NMR spectrum ($CDCl_3$) of the crude extract of the photochemical [2+2] cycloaddition of **3** under visible light and comparison with pure compound **2**.[a] 11
Figure S4. Optimised structures of $\mathbf{TS_{ax}}$ and $\mathbf{TS_{eq}}$ at the B3LYP-D3 and M06-2X level with the 6-311++G(d,p) basis set. 28
Figure S5. Optimised transition state structures for the reduction of **15** by $NaBH_4$ for the three different CO groups and their two faces. Relative free energies with respect to the separated fragments (**15** and $NaBH_4(MeOH)_3$) computed at the SMD(methanol)-M06-2X/aug-cc-pVTZ//SMD(methanol)-B3LYP-D3/6-311++G(d,p) level. 30
Figure S6. Reaction mechanism for the $NaBH_4$ reduction of **15**, including three explicit solvent molecules, computed at the SMD(methanol)-M06-2X/aug-cc-pVTZ//SMD(methanol)-B3LYP-D3/6-311++G(d,p) level through A) transition state $\mathbf{TS^1_{C\text{-}9}}$ and B) transition state $\mathbf{TS_{ax}}$. 30
Scheme S1. Resume of the synthetic route performed during this work. 12
2 General experimental data 12
Scheme S1. Resume of the synthetic route performed during this work. 12
3 Synthetic procedures and compound characterizations 13
4 Computational details 28
Figure S4. Optimised structures of $\mathbf{TS_{ax}}$ and $\mathbf{TS_{eq}}$ at the B3LYP-D3 and M06-2X level with the 6-311++G(d,p) basis set. 28
Table S12. Computed relative Gibbs free energy (in kJ/mol) between $\mathbf{TS_{ax}}$ and $\mathbf{TS_{eq}}$ at various level of calculations. 29
Figure S5. Optimised transition state structures for the reduction of **15** by $NaBH_4$ for the three different CO groups and their two faces. Relative free energies with respect to the separated fragments (**15** and $NaBH_4(MeOH)_3$) computed at the SMD(methanol)-M06-2X/aug-cc-pVTZ//SMD(methanol)-B3LYP-D3/6-311++G(d,p) level. 30
Figure S6. Reaction mechanism for the $NaBH_4$ reduction of **15**, including three explicit solvent molecules, computed at the SMD(methanol)-M06-2X/aug-cc-pVTZ//SMD(methanol)-B3LYP-D3/6-311++G(d,p) level through A) transition state $\mathbf{TS^1_{C\text{-}9}}$ and B) transition state $\mathbf{TS_{ax}}$. 30
Table S13. Absolute electronic energies and thermal corrections (in a.u.) for all molecules (B3LYP-D3 geometry optimisation). 31
Table S14. Absolute electronic energies and thermal corrections (in a.u.) for $\mathbf{TS_{ax}}$ and $\mathbf{TS_{eq}}$ (M06-2X geometry optimisation). 31
Table S15. Absolute electronic energies (in a.u.) of $\mathbf{TS_{ax}}$ and $\mathbf{TS_{eq}}$ computed at various level. 31
5 X-Ray crystallographic data 32
Table S16. Crystal data and structure refinement for compound **1** (CCDC 2418571) 32
Table S17. Crystal data and structure refinement for compound **2** (CCDC 2419407) 33
Table S18. Crystal data and structure refinement for compound **3** (CCDC 2418579) 34
Table S19. Crystal data and structure refinement for compound **9b** (CCDC 2419409) 35
Table S20. Crystal data and structure refinement for Compound **13** (CCDC 2419408) 36
Table S21. Crystal data and structure refinement for compound **14** (CCDC 2428644) 37
Table S22. Crystal data and structure refinement for compound **15** (CCDC 2418568) 38
Table S23. Crystal data and structure refinement for compound **19** (CCDC 2423044) 39
6 Copies of spectra 40
7 References 76

1 Supplementary Tables and Figures in support to the discussion

Table S1. Catalyst or reagent screening the allenic Pauson-Khand reaction

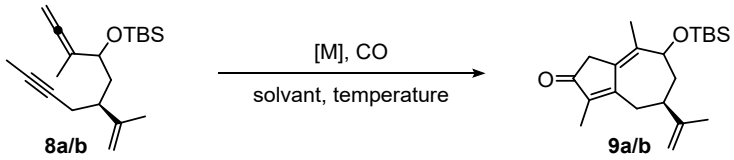

Substrate	Cat	Addition time	Concentration	Temperature	Overall time	Yield (9a/9b)
8a/8b (1:1.5)[a]	$IrCl(CO)(PPh_3)_2$[1]	3h00	[0.04M]	120 °C	3h30	36%
8a/8b (1:1.5)[b]	$Mo(CO)_6$[2]	-	[0.05M]	120 °C	17h00	degradation
8a/8b (1:1.3)[c]	$Co_2(CO)_8$[3]	-	[0.1M]	r.t.	23h	No reaction
8a/8b (1:1.5)[d]	**$[Rh(CO)_2Cl]_2$**	**3h30**	**[0.011M]**	**110 °C**	**4h30**	**78%**

[a] Chamber A: COgen (2.5 equiv), $PdCl_2(cod)$ (10 mol%), TTBP.HBF_4 (10 mol%), Cy_2NMe (4.0 equiv), Chamber B: $IrCl(CO)(PPh_3)_2$ (5 mol%), 3h addition time of allene-yne substrate, xylene [0.04 M].
[b] $Mo(CO)_6$ (1.5 equiv), DMSO (10 equiv), toluene [0.05 M].
[c] $Co_2(CO)_8$ (1.2 equiv), NMO (6 equiv), CH_2Cl_2 [0.1 M]
[d] Chamber A: COgen (2.5 equiv), $PdCl_2(cod)$ (10 mol%), TTBP.HBF_4 (10 mol%), Cy_2NMe (4.0 equiv), Chamber B: $[Rh(CO)_2Cl]_2$ (5 mol%), 3h30 addition time of allene-yne substrate, toluene [0.011 M].

Table S2. Optimisation of the allenic Pauson-Khand reaction catalyzed with a Rh^I-based catalyst

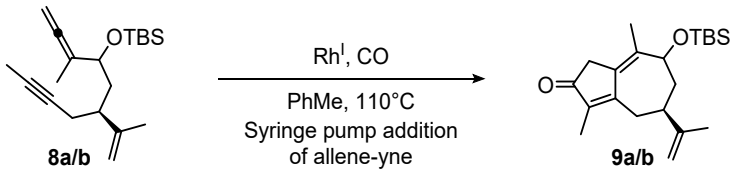

Substrate	Scale (mmol)	Cat	Addition time	Concentration	Overall time	Yield
8a[a]	0.10	$[Rh(CO)_2Cl]_2$	1h30	[0,016M]	1h45	66% (**9b**)
8b[a]	0.10	$[Rh(CO)_2Cl]_2$	1h30	[0,016M]	1h45	20% (**9a**)
8b[a]	0.05	$[Rh(CO)_2Cl]_2$	3h00	[0,011M]	4h	80% (**9a**)
8b[a]	0.037	$[Rh(CO)(dppp)_2]Cl$	3h00	[0,011M]	4h	54% (**9a**)
8b[a]	0.19	$[Rh(CO)_2Cl]_2$	3h00	[0,011M]	4h	51% (**9a**)
8b[b]	0.27	$[Rh(CO)_2Cl]_2$	15h00	[0,02M]	15h30	75% (**9a**)
8a/8b (1:1.3)[b]	**1.87**	**$[Rh(CO)_2Cl]_2$**	**20h00**	**[0.019M]**	**20h30**	**75%** (**9a/9b**)

[a] Chamber A: COgen (2.5 equiv), $PdCl_2(cod)$ (10 mol%), TTBP.HBF_4 (10 mol%), NDCHMA (4.0 equiv), Chamber B: cat (5 mol%), addition time of allene-yne substrate, concentration of toluene.
[b] Chamber A: COgen (2.0 equiv), $PdCl_2(cod)$ (10 mol%), TTBP.HBF_4 (10 mol%), NDCHMA (4.0 equiv), Chamber B: cat (5 mol%), addition time of allene-yne substrate, concentration of toluene.

Table S3. Optimisation attempts of the allenic Pauson-Khand reaction using chloroform as a CO source in the COware

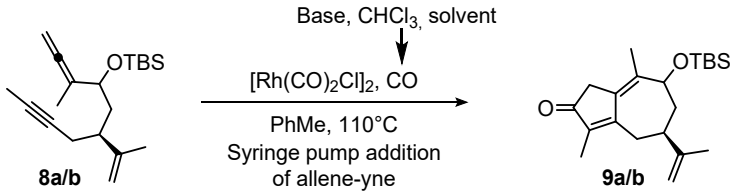

8a/b **9a/b**

Substrat	Scale (mmol)	Base	$CHCl_3$	Solvant	Addition time	Concentration	Overall time	Yield (9a/9b)
8a/8b (1:1.3)	0.15	KOH (48 equiv)	[0.03M]	-	3h00	[0.011M]	3h30	54%
8a/8b (1:1.3)	0.40	KOH crushed (15 equiv)	[1M]	-	19h50	[0.011M]	20h00	54%
8a/8b (1:1)	0.33	$CsOH.H_2O$ (3 equiv)	$CHCl_3$ (10 equiv)	toluene [0.1M]	16h00	[0.02M]	16h30	42%
8a/8b (1:1.3)	0.30	**KOH crushed 10 equiv**	**30 equiv**	**toluene [0.05M]**	**16h00**	**[0.02M]**	**16h30**	**55%**

Table S4. Comparison of ^{1}H and ^{13}C NMR spectra ($CDCl_3$) of natural[4] and synthetic oleodaphnone (3)

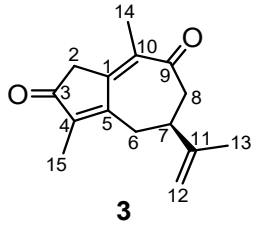

3

#	Natural oleodaphnone ^{1}H (400 MHz)	Synthetic oleodaphnone ^{1}H (400 MHz)	Δδ/ppm (natural–synthetic)	Natural oleodaphnone ^{13}C (100 MHz)	Synthetic oleodaphnone ^{13}C (100 MHz)	Δδ/ppm (natural–synthetic)
1	-	-	-	144.1	144.3	-0.2
2	3.08 (21.0) 3.15 (21.0)	3.06 d, (21.1) 3.13 d, (21.1)	0.02 0.02	41.1	41.3	-0.2
3	-	-	-	201.9	201.9	0
4	-	-	-	144.8	145.0	-0.2
5	-	-	-	162.8	162.8	0
6	2.99, br t (14.7) 2.76, dd (14.7, 12.6)	2.98, m 2.76, m	0.01 0	35.4	35.6	-0.2
7	2.73, br t (12.6)	2.72, m	0.01	39.0	39.2	-0.2
8	2.89, m	2.88, m 2.87, m	0.01	49.8	49.9	-0.1
9	-	-	-	200.7	200.7	0
10	-	-	-	131.6	131.7	-0.1
11	-	-	-	147.0	147.2	-0.2
12	4.82, s 4.79, s	4.82, app p (1.4) 4.78, m	0 0.01	111.1	111.3	-0.2
13	1.79, s	1.78, s	0.01	20.2	20.3	-0.1
14	1.98, s	1.97, s	0.01	17.4	17.6	-0.2
15	1.88, s	1.87, s	0.01	9.0	9.1	-0.1

Table S5. Comparison of ^{1}H and ^{13}C NMR spectra ($CDCl_3$) of the natural[6] and synthetic daphnenicillata W (structure 11)

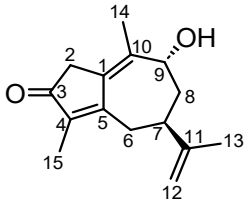

11

#	Natural daphnenicillata W ^{1}H (600 MHz)	Synthetic daphnenicillata W ^{1}H (400 MHz)	Δδ/ppm (natural–synthetic)	Natural daphnenicillata W ^{13}C (150 MHz)	Synthetic daphnenicillata W ^{13}C (100 MHz)	Δδ/ppm (natural–synthetic)
1	-	-	-	132.6	132.5	0.1
2	2.98, d (20.6) 2.93, d (20.6)	2.98, d (20.8) 2.91, d (20.8)	0 0.02	41.2	41.2	0
3	-	-	-	204.0	204.1	-0.1
4	-	-	-	140.5	140.4	0.1
5	-	-	-	165.2	165.3	-0.1
6	2.93, overlapped 2.59, dd (17.1, 11.4)	2.94, overlapped 2.59, dd (17.0, 11.5)	-0.01 0	36.5	36.5	0
7	2.69, m	2.69, m	0	37.6	37.6	0
8	2.15, ddd (14.4, 6.2, 3.2) 2.02, ddd (14.4, 9.3, 3.0)	2.14, dddd, (14.4, 6.2, 3.1, 1.6) 2.01, ddd (14.3, 9.1, 3.1 Hz, 1H)	0.01 0.01	41.5	41.5	0
9	4.49, m	4.48, m	0.01	72.5	72.5	0
10	-	-	-	134.9	135.1	-0.2
11	-	-	-	149.5	149.5	0
12	4.80, d (1.5) 4.78, d (1.5)	4.79, m 4.77, m	0.01 0.01	110.0	109.9	0.1
13	1.80, s	1.80, s	0	20.5	20.5	0
14	1.97, s	1.97, s	0	21.0	21.0	0
15	1.77, s	1.77, s	0	8.7	8.7	0

Table S6. Comparison of ^{1}H and ^{13}C NMR spectra (DMSO-d_6) of the natural[5] and synthetic diarthroncha C (structure 10), highlighting inconsistencies (see Table S7 for structure revision)

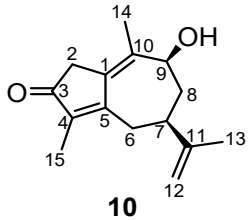

10

#	Natural diarthroncha C ^{1}H (600 MHz)	Synthetic diarthroncha C ^{1}H (400 MHz)	Δδ/ppm (natural–synthetic)	Natural diarthroncha C ^{13}C (150 MHz)	Synthetic diarthroncha C ^{13}C (100 MHz)	Δδ/ppm (natural–synthetic)
1	-	-	-	138.2	130.0	8.2
2	3.20, m 2.90, m	2.98, d (20.7) 2.84 d (20.7)	0.22 0.06	40.4	40.5	-0.01
3	-	-	-	202.8	202.7	0.01
4	-	-	-	137.3	138.4	-1.1
5	-	-	-	165.5	165.2	0.3
6	2.80, m 2.63, m	2.77, m 2.68, m	0.03 -0.05	35.3	34.7	0.6
7	2.65, m	2.36, m	0.29	37.2	39.6	0.6
8	1.93, m 1.89, m	2.07, m 1.72, m	0.14 0.17	41.0	42.2	-1.2
9	4.33, m	4.16, m	0.17	70.0	71.6	-1.6
10	-	-	-	130.4	138.6	-8.2
11	-	-	-	149.8	149.5	0.3
12	4.76, s 4.71, s	4.76, m 4.70, m	0 0.01	110.1	109.5	0.6
13	1.75, s	1.73, m	0.02	20.2	19.8	0.4
14	1.87, s	1.87, br s	0	17.0	20.2	-3.2
15	1.66, s	1.66, br s	0	8.2	8.2	0

Table S7. Comparison of ^{1}H and ^{13}C NMR spectra (DMSO-d_6) of the natural[5] diarthroncha C and synthetic daphnenicillata W (structure 11)

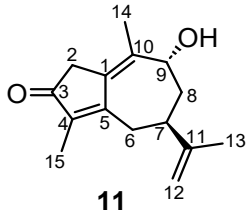

11

#	Natural diarthroncha C ^{1}H (600 MHz)	Synthetic daphnenicillata W ^{1}H (400 MHz)	Δδ/ppm (natural–synthetic)	Natural diarthroncha C ^{13}C (150 MHz)	Synthetic daphnenicillata W ^{13}C (100 MHz)	Δδ/ppm (natural–synthetic)
1[a]	-	-	-	138.2	130.5	7.7[a]
2	3.20, m[b] 2.90, m	2.92, d (21.0) 2.86, d (21.0)	0.28 0.04	40.4	40.4	0
3	-	-	-	202.8	202.8	0
4	-	-	-	137.3	138.2	-0.9
5	-	-	-	165.5	165.4	0.1
6[c]	2.80, m 2.63, m	2.66, m 2.62, m	0.14[c] 0.01	35.3	37.2	-1.9[c]
7[c]	2.65, m	2.80, m	-0.15[c]	37.2	35.2	1.9[c]
8	1.93, m 1.89, m	1.94, m 1.89, m	-0.01 0	41.0	41.0	0
9	4.33, m	4.33, m	0	70.0	70.0	0
10[a]	-	-	-	130.4	137.3	-6.9[a]
11	-	-	-	149.8	149.8	0
12	4.76, s 4.71, s	4.76, m 4.71, m	0 0	110.1	109.3	0.8
13	1.75, s	1.75, m	0	20.2	20.4	-0.2
14	1.87, s	1.86, br s	0.01	17.0[b]	20.1	3.1
15	1.66, s	1.66, br s	0	8.2	8.2	0

[a] Permuted attribution compared to the literature, between positions 1 and 10.

[b] Remaining inconsistency, likely due to solvent impurity. The copy of spectra for the natural product was not available.

[c] Permuted attribution compared to the literature, between positions 6 and 7.

Table S8. Attempts of formation of a dienol silyl ether in view of a vinylogous Rubottom reaction for the γ-hydroxylation of substrate 2

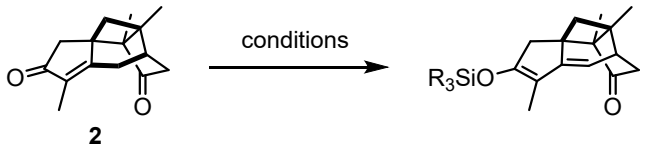

2

Entry	Conditions	Result
1	TBSOTf (1.1 eq), NaHMDS (1.0 eq), THF [0.04M]	degradation
2	TMSCl (1.1 eq), Et_3N (1.1 eq), NaI (1.1 eq), MeCN [0.1M]	no reaction
3	$FeCl_3$ (0.15 eq); MeMgBr (2 eq), TMSCl (2 eq), Et_3N (2 eq), THF [0.08M]	no reaction

Table S9. Attempts of direct γ-hydroxylation of substrate 2

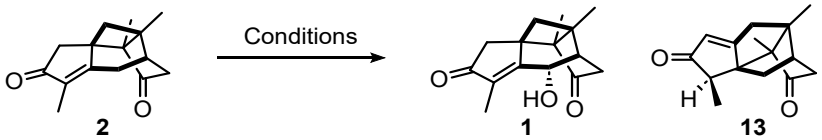

2 **1** **13**

Entry	Conditions	Result
1[7]	O_2, hν (440nm), Na_2-eosyn Y (5 mol%), MeCN	degradation
2	O_2, hν (440nm), methylene blue (5 mol%), MeOH	no reaction
3[8]	O_2 (air), Cu-Al Ox, tBuOK (2 equiv), EtOH	40% (**13**)[a]
4	O_2 (air), 10% KOH in MeOH	17% (**13**)
5	SeO_2 , tBuOOH, CH_2Cl_2	no reaction
6	LiHMDS, Davis reagent, THF	Starting material + complex mixture

[a] Compound **13** could be obtained in a 67% yield from **2** in presence of tBuOK (2 equiv) in EtOH.

Table S10. Optimisations of the C-H oxidation reactions in presence of CrO_3

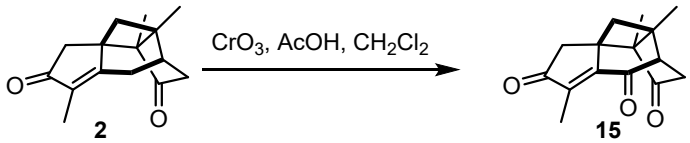

2 **15**

Entry	CrO_3 (equiv)	Additive (equiv)	AcOH	Temperature	Time	Work-up	Yield
1	20	3,5-dimethylpyrrazole (20)	-	0°C to r.t.	21h		26%
2	5	AcOH (30)	-	reflux	1h30		9%
3	5	-	[0.1M]	r.t.	23h		30%
4	5	-	[0.1M]	r.t.	68h		6%
5	5	celite	[0.1M]	r.t.	16h	filtration through a pad of celite	25%
6	5	-	[0.1M]	r.t.	18h	filtration through a pad of silica	32%
7	5	-	[0.1M]	r.t.	20 h	add [1M] citric acid aq. solution	21%
8	5	-	[0.1M]	r.t.	20 h	add [0.1M] NaOH aq. solution	26%
9	5	-	[0.1M]	r.t.	16 h	add 10 equiv pyridine	24%
10	5	MS 4 Å	[0.1M]	r.t.	16 h	-	27%
11	**5**	**MS 4 Å**	**[0.1M]**	**r.t.**	**38 h**	**-**	**62%**
12	10	MS 4 Å	[0.1M]	r.t.	20h	-	59%
13	15	MS 4 Å	[0.1M]	r.t.	15h		32%

Table S11. Comparison of ^{1}H and ^{13}C NMR spectra (CD_3OD) of natural[9] and synthetic daphnepapytone A

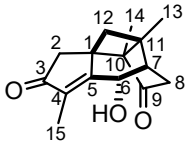

#	Natural daphnepapytone A ^{1}H (500 MHz)	Synthetic daphnepapytone A ^{1}H (400 MHz)	Δδ/ppm (natural–synthetic)[a]	Natural daphnepapytone A ^{13}C (125 MHz)	Synthetic daphnepapytone A ^{13}C (100 MHz)	Δδ/ppm (natural–synthetic)[a]
1	-	-	-	54.4	55.7	-1.3
2	2.37, d (19.4) 2.15, d (19.4)	2.35, d (19.4) 2.13, dd (19.4, 1.4)	0.02 0.02	38.8	40.2	-1.4
3	-	-	-	208.3	209.7	-1.4
4	-	-	-	135.3	136.7	-1.4
5	-	-	-	174.8	176.2	-1.4
6	5.31, d (6.1 Hz)	5.29, d, (6.5)	0.02	67.9	69.3	-1.4
7	2.61 ddd (9.0, 6.1, 4.1)	2.58, dd (6.8, 6.8)	0.03	45.5	46.7	-1.2
8	2.78, dd (18.0, 4.1) 2.40, dd (18.0, 9.0)	2.77, d (18.1) 2.39, ddd (18.1, 7.2, 1.4)	0.01 0.01	39.8	41.2	-1.4
9		-	-	219.8	221.3	-1.5
10	-	-	-	60.8	62.2	-1.4
11	-	-	-	44.4	45.8	-1.4
12	2.24 d (10.0) 2.20 d (10.0)	2.22, d (10.0) 2.18, d (10.0)	0.02 0.02	34.7	36.1	-1.4
13	1.17, s	1.15, s	0.02	17.0	18.5	-1.5
14	1.14, s	1.12, s	0.02	9.3	10.7	-1.4
15	1.84, s	1.82, d (1.9)	0.02	6.7	8.1	-1.4

[a] Calibration used for CD_3OD in ref. 9: δH = 3.33 and δC = 48.0; our calibration: δH = 3.31 and δC = 49.0. Taking these calibration differences into account, the Δδ are reduced to ~0 for ^{1}H NMR and to ~0.4 for ^{13}C NMR.

Figure S1. X-ray crystallographic structure of **3** showing an equimolar distribution of two conformers in the crystal, with a pseudo-equatorial (left) or a pseudo-axial orientation (right) of the isopropenyl group.

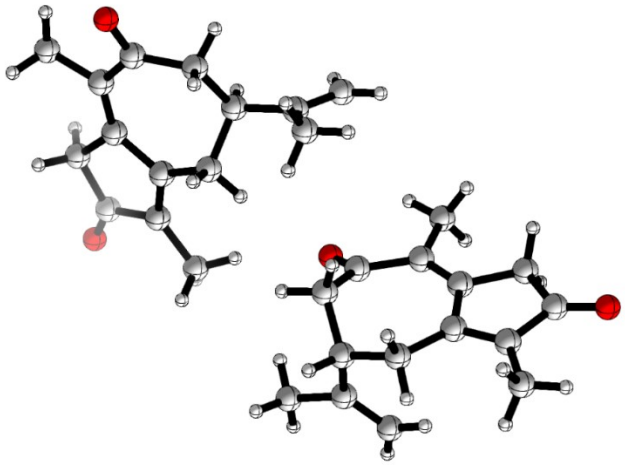

Figure S2. Key HMBC (H✂C) correlations observed for compound **2** (a) and compound **13** (b), and key NOESY correlation (blue) demonstrating the stereochemistry of C-4 in compound **13**.[10]

a.

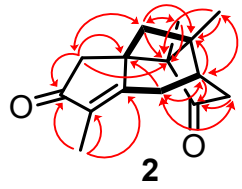

b.

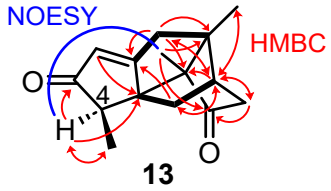

Figure S3. Copy of the ^{1}H NMR spectrum ($CDCl_3$) of the crude extract of the photochemical [2+2] cycloaddition of **3** under visible light and comparison with pure compound **2**.[a]

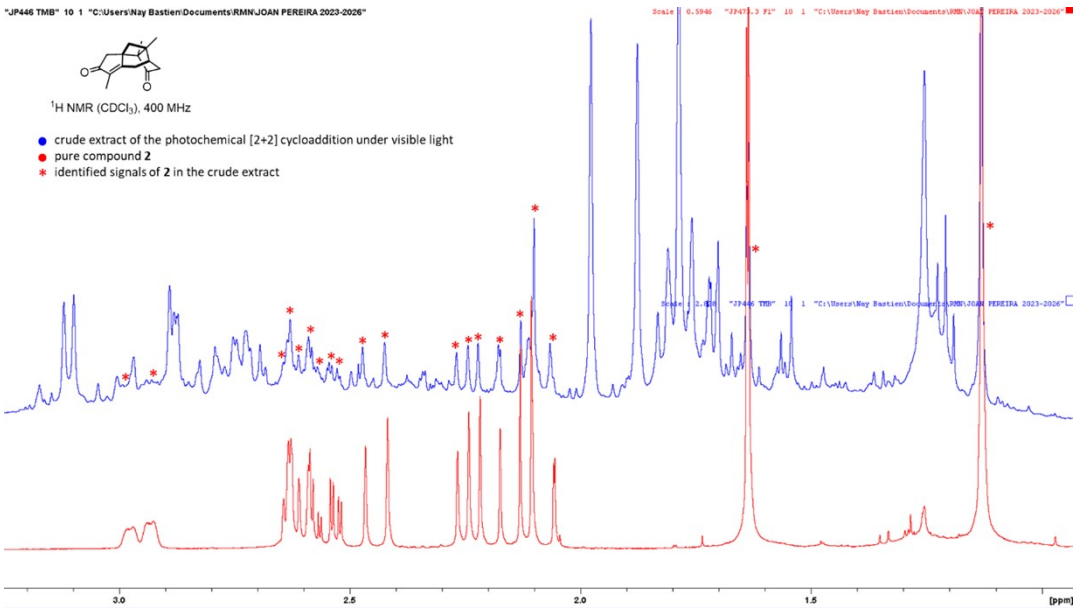

Method: into an NMR tube, oleodaphnone **3** (4.4 mg, 0.019 mmol, 1 equiv) was dissolved in 0.5 mL of $CDCl_3$. The solution was irradiated with a white LED for 18 days. Then, 1,3,5-trimethoxybenzene (1 mg, 0.0063 mmol) was added as an internal standard. NMR analysis indicated a 10% NMR yield for compound **2**.

2 General experimental data

All reactions were carried out in oven-dried vessels under an atmosphere of argon and in anhydrous solvents unless stated otherwise. Dichloromethane (DCM) and tetrahydrofurane (THF) were purified using a MB-SPS 800 Solvent purification system (MBraun). Toluene was distillated over CaH_2 as dessicant. Anhydrous acetonitrile was purchased from Carlo Erba. Analytical thin-layer chromatography (TLC) was carried out using aluminum TLC plates coated with F254 silica gel 60 (Merck), which were visualized by exposure to ultraviolet light and/or exposure to vannilin stain followed by heating. Flash chromatography was carried out on silica gel 60 (40-63 µm).

Infrared (IR) spectra were recorded on an FTIR PerkinElmer Spectrum Two equipped with a Jasco ATR. Absorption maxima (ν) are reported in wavenumbers (cm^{-1}). High-resolution mass spectra (HRMS) were obtained on a Bruker tims-TOF mass spectrometer (ESI+), and reported as m/z. Optical rotations were measured on an Anton Paar MCP 100 polarimeter. Nuclear magnetic resonance spectra (^1H NMR and ^{13}C NMR) were recorded at 25 °C on a Bruker 400 MHz Avance I (^1H at 400 MHz, ^{13}C at 100 MHz) or a Bruker 300 MHz Avance II (^1H at 300 MHz, ^{13}C at 75 MHz). Chemical shifts in $CDCl_3$, CD_3OD and DMSO-d6 solutions are reported as parts per million (ppm) referenced to residual protium or carbon of the solvent (for $CDCl_3$: δH = 7.26 and δC = 77.1; for CD_3OD: δH = 3.31 and δC = 49.0; for DMSO-d_6: δH = 2.50 and δC = 39.5). Coupling constants are reported in Hertz (Hz). Data for ^1H NMR spectra are reported as follows: chemical shift in ppm (multiplicity [the following abbreviations are used for spin multiplicity: s = singlet, d = doublet, t = triplet, q = quartet, m = multiplet], coupling constants [Hz], integration).

Compound numbers are reminded in Scheme S1.

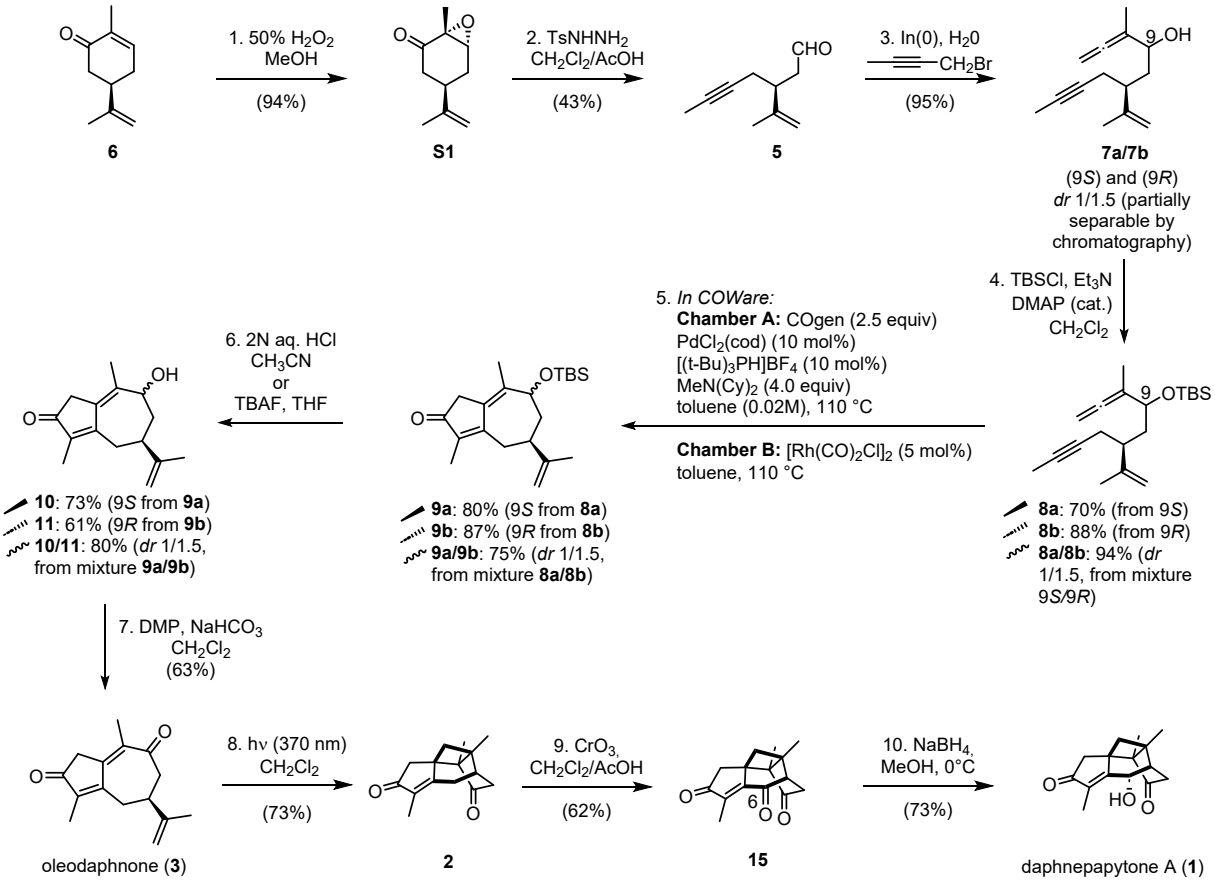

Scheme S1. Resume of the synthetic route performed during this work.

3 Synthetic procedures and compound characterizations

(1*R*,4*R*,6*R*)-1-Methyl-4-(prop-1-en-2-yl)-7-oxabicyclo[4.1.0]heptan-2-one (S1)

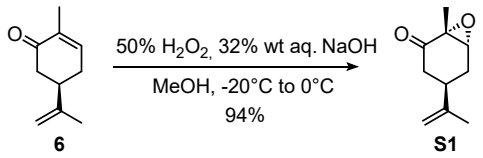

According to a known literature procedure[11] : To a solution of (*R*)-carvone (10 g, 66.6 mmol, 1 equiv) in 150 mL of MeOH (non distilled) at -20 °C, aq. NaOH (32 wt%, 2.5 mL, 20 mmol, 0.3 equiv) was added, followed by the dropwise addition of aq. H_2O_2 (35 wt%, 8.5 mL, 175 mmol, 2.63 equiv). The resulting mixture was stirred at 0 °C for 3h30. Then, the reaction was carefully quenched sat. aq. $Na_2S_2O_3$ and extracted three times diethyl ether. The combined organic phases were washed with brine, dried over anhydrous $MgSO_4$ and concentrated under vacuum to afford 10.33 g (94 %) of **S1** as a colorless oil.

Spectroscopic data were consistent with those of the literature.[11]

Rf: 0. 59 (petroleum ether : AcOEt = 8:2)

^{1}H NMR (400 MHz, $CDCl_3$): δ 4.78 (apparent pd, *J* = 1.4, 0.5 Hz, 1H), 4.72 – 4.70 (m, 1H), 3.44 (dd, *J* = 3.1, 1.2 Hz, 1H), 2.76 – 2.67 (m, 1H), 2.58 (ddd, *J* = 17.7, 4.7, 1.4 Hz, 1H), 2.37 (dddd, *J* = 14.8, 4.4, 3.0, 1.4 Hz, 1H), 2.02 (dd, *J* = 17.6, 11.6 Hz, 1H), 1.89 (ddd, *J* = 14.8, 11.1, 1.2 Hz, 1H), 1.72-1.70 (m, 3H), 1.41 (s, 3H).

^{13}C NMR (100 MHz, $CDCl_3$): δ 205.6, 146.5, 110.6, 61.5, 59.0, 41.9, 35.2, 28.9, 20.7, 15.4.

$[\alpha]_D^{20}$ = +84.2 (c = 1.9, $CHCl_3$) [Lit:[11] $[\alpha]_D^{20}$ = +85.6 (c = 1.7, $CHCl_3$)]

(*S*)-3-(Prop-1-en-2-yl)hept-5-ynal (5)

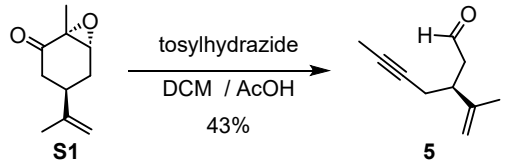

According to a known literature procedure[11] : To a solution of epoxycarvone **S1** (10.33 g, 62.15 mmol, 1 equiv) in CH_2Cl_2/AcOH (1:1 v/v, 88 mL) at 0 °C, *p*-toluensulfonyl hydrazide (12.15 g, 65.25 mmol, 1.05 equiv) was added portion wise. After 15 minutes, all the hydrazide was dissolved, giving a clear solution. The resulting mixture was allowed to warm at 10 °C for 3h. Then, ice cold water was added and the mixture was extracted three times with diethyl ether. The combined organic phases were carefully washed with ice-cold sat. aq. $NaHCO_3$, brine, then dried over anhydrous $MgSO_4$ and concentrated under vacuum. The residue was purified by flash chromatography on silica (95/5 pentane/Et_2O) to afford 3.96 g (43%) of **5** as a yellow volatile oil.

Spectroscopic data were consistent with those of the literature.[11]

Rf: 0. 68 (petroleum ether : AcOEt = 8:2)

^{1}H NMR (400 MHz, $CDCl_3$): δ 9.72 (dd, *J* = 2.6, 1.8 Hz, 1H), 4.84 (apparent p, *J* = 1.5 Hz, 1H), 4.79 (apparent pd, J = 2.5, 0.8 Hz, 1H), 2.85 – 2.77 (m, 1H), 2.70 (ddd, *J* = 16.6, 6.0, 1.8 Hz, 1H), 2.53 (ddd, *J* = 16.6, 8.4, 2.6 Hz, 1H), 2.38 – 2.30 (m, 1H), 2.26 – 2.17 (m, 1H), 1.77 (apparent t, *J* = 2.6 Hz, 3H), 1.72 (ddd, J = 1.5, 0.8, 0.3 Hz, 3H).

^{13}C NMR (100 MHz, $CDCl_3$): δ 202.1, 145.8, 112.2, 78.1, 76.7, 46.5, 40.8, 23.9, 20.3, 3.6.

$[\alpha]_D^{20}$ = -22.3 (c = 0.52, $CHCl_3$) [Lit[11] $[\alpha]_D^{20}$ = -18.1, c = 0.52, $CHCl_3$]

(4*S*,6*S*)- and (4*R*,6*S*)-3-Methyl-6-(prop-1-en-2-yl)deca-1,2-dien-8-yn-4-ol (7a and 7b, respectively)

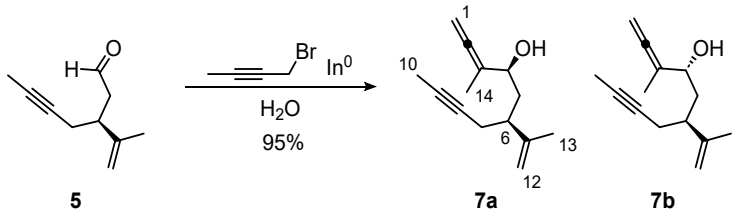

To a solution of aldehyde **5** (1.26 g, 8.4 mmol, 1 equiv) in 8.5 mL of at room temperature, 1-bromobutyne (16.8 mmol, 2.0 equiv) was added, followed by the portion wise addition of indium (16.8 mmol, 2.0 equiv). The resulting mixture was stirred vigorously for 2h30. Then, the mixture was extracted three times diethyl ether. The combined organic phases were washed two times with water, brine, then dried over anhydrous $MgSO_4$ and concentrated under vacuum. The residue was purified by flash chromatography on silica (95/5 pentane/Et_2O) to afford a 1/1.5 mixture of **7a** and **7b** (1.33 g), and pure fractions of the diastereoisomers **7a** (136 mg) and **7b** (169 mg) as colorless oils (95% yield).

Nota bene: The diastereoisomerically pure fractions were used for the total synthesis of diarthroncha C and daphnenicillata W. See the following general procedure for the diastereoselective allenation leading to **7a** or **7b**.

Data for the 4*S* product (7a)

Rf: 0. 28 (petroleum ether : diethylether = 8:2)

^{1}H NMR (400 MHz, $CDCl_3$): δ 4.83 – 4.80 (m, 1H, H-12a), 4.80 – 4.78 (m, 1H, H-12b), 4.78 – 4.68 (m, 2H, H-1) 4.15 – 4.08 (m, 1H, H-4), 2.40 – 2.31 (m, 1H, H-6), 2.25 – 2.19 (m, 2H, H-7), 1.87 (ddd, *J* = 13.9, 6.9, 5.4 Hz, 1H, H-5a), 1.77 (apparent t, *J* = 2.5 Hz, 3H, H-10), 1.72 (apparent t, *J* = 3.2 Hz, 3H, H-14), 1.71 – 1.70 (m, 3H, H-13), 1.68 (dd, *J* = 5.4, 1.4 Hz, 1H, H-5b).

^{13}C NMR (100 MHz, $CDCl_3$): δ 205.9 (C-2), 147.5 (C-11), 112.0 (C-12), 101.3 (C-3), 77.6 (C-9), 77.0 (C-8), 76.0 (C-1), 71.7 (C-4), 43.5 (C-6), 37.8 (C-5), 24.0 (C-7), 19.5 (C-13), 13.9 (C-14), 3.6 (C-10).

ν_{max} (ATR) : 3334, 3073, 2919, 1958, 1645, 1436, 1375, 1238, 1019, 995, 892, 843, 738 cm^{-1}.

HRMS (ESI+) *m/z*: calculated for $[M+H]^+$ $C_{14}H_{21}O^+$: 205.1587; found: 205.1581.

$[\alpha]_D^{25}$ = -51.7 (c = 0.84, $CHCl_3$)

Data for 4*R* product (7b)

Rf: 0. 38 (petroleum ether : diethylether = 8:2)

^{1}H NMR (400 MHz, CDCl3): δ 4.86 – 4.84 (m, 1H, H-12a), 4.84 – 4.83 (m, 1H,H-12b), 4.80 – 4.74 (m, , 2H, H-1), 4.04 – 3.96 (m, 1H, H-4), 2.58-2.50 (m, 1H, H-6), 2.28-2.14 (m, 2H, H-7), 1.77 (apparent t, J = 2.6 Hz, 3H, H-10), 1.73 – 1.71 (m, 1H, H-5a), 1.71 (apparent td, J = 3.2, 0.5 Hz, 3H, H-14), 1.69 – 1.68 (m, 3H, H-13), 1.63 (dd, J = 6.0, 1.8 Hz, 1H, H-5b).

^{13}C NMR (100 MHz, $CDCl_3$): δ 204.9 (C-2), 146.9 (C-11), 112.6 (C-12), 102.5 (C-3), 77.6 (C-9), 77.0 (C-8), 77.0 (C-1), 70.5 (C-4), 43.1 (C-6), 38.0 (C-5), 24.4 (C-7), 19.0 (C-13), 14.8 (C-14), 3.7 (C-10).

ν_{max} (ATR) : 3353, 3073, 2918, 1957, 1645, 1436, 1374, 1294, 1073, 1040, 993, 891, 845 cm^{-1}.

HRMS (ESI+) *m/z*: calculated for $[M+H]^+$ $C_{14}H_{21}O^+$: 205.1587; found: 205.1580.

$[\alpha]_D^{25}$ = +0.9 (c = 0.62, $CHCl_3$)

General procedure for the diastereoselective allenation leading to 7a and 7b[12]

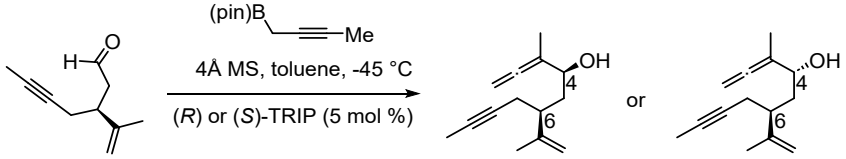

5 | **7a** (from (*R*)-TRIP) 75%, dr : 95/5 | **7b** (from (*S*)-TRIP) 72%, dr : 96/4

The chiral phosphoric acid (*R*)-TRIP or (*S*)-TRIP (0.005 mmol, 5 mol%), was added to a reaction flask equipped with a stirring bar and containing freshly activated 4Å molecular sieves (50 mg). A solution of the aldehyde **5** (0.1 mmol, 1.0 equiv) in toluene (0.3 mL) was added dropwise with vigorous stirring. The mixture was then cooled to –45 °C, and a solution of propargylic boronate[12] (0.14 mmol, 1.4 equiv) in toluene (0.3 mL) was slowly introduced. The reaction was stirred overnight at –45 °C and then quenched at 0 °C by adding saturated aqueous $NaHCO_3$ (0.6 mL). Next, 50% aq. H_2O_2 (0.1 mL) was added dropwise, and the mixture was stirred for an additional hour at the same temperature. The mixture was extracted three times diethyl ether. The combined organic phases were washed with brine, dried over anhydrous $MgSO_4$ and concentrated under vacuum. The residue was purified by flash chromatography on silica (95/5 pentane/Et_2O) to afford a colorless oil. Allenols **7a** (15.2 mg, 75% yield, *dr* 95:5 measured by ^{1}H NMR) and **7b** (14.8 mg, 72% yield, *dr* 96:4 measured by ^{1}H NMR) were prepared following this procedure, in presence of (*R*)-TRIP or (*S*)-TRIP, respectively.

***tert*-Butyldimethyl(((4*S*/*R*,6*S*)-3-methyl-6-(prop-1-en-2-yl)deca-1,2-dien-8-yn-4-yl)oxy)silane (8a and 8b, respectively)**

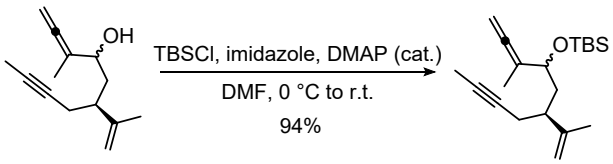

7a/7b dr 1:1.5 | **8a/8b**

To a solution of a diastereomeric mixture of allenols **7a/7b** (708 mg, 3.46 mmol, 1 equiv, dr 1:1.6) in 17 mL of DMF at 0 °C, imidazole (710 mg, 10.43 mmol, 3.0 equiv), DMAP (23 mg, 0.19 mmol, 5.5 mol%) and TBSCl (783 mg, 5.2 mmol, 1.5 equiv) were added. The resulting mixture was stirred, and let warm to room temperature overnight. Then, the mixture was quenched with NH_4Cl and extracted three times with diethyl ether. The combined organic phases were washed two times with water, NH_4Cl, brine, then dried over anhydrous $MgSO_4$ and concentrated under vacuum. The residue was purified by flash chromatography on silica (90/10 petroleum ether/CH_2Cl_2) to afford 1.03 g of **8a/8b** (94%, dr = 1:1.5) as a colorless oil.

Nota bene: This procedure was used for the total synthesis of oleodaphnone toward daphnepapytone A.

Synthesis of 4*S* silyl ether 8a

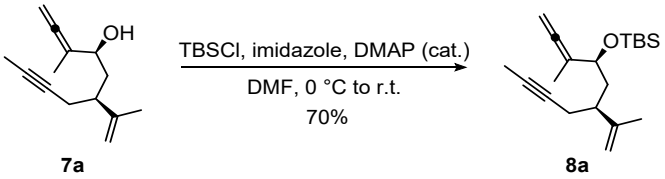

7a **8a**

To a solution of allenol **7a** (55 mg, 0.27 mmol, 1 equiv) in 1.4 mL of DMF at 0 °C, imidazole (56 mg, 0.82 mmol, 3.0 equiv), DMAP (3.5 mg, 0.029 mmol, 10 mol%) and TBSCl (70.7 mg, 0.47 mmol, 1.74 equiv) were added. The resulting mixture was stirred, and let warm at room temperature overnight. Then, the mixture was quenched with NH_4Cl and extracted three times with diethyl ether. The combined organic phases were washed two times with water, NH_4Cl, brine, then dried over anhydrous $MgSO_4$ and concentrated under vacuum. The residue was purified by flash chromatography on silica (90/10 petroleum ether/CH_2Cl_2) to afford 60 mg of **8a** (70%) as a colorless oil.

Nota bene: This procedure was used for the total synthesis of diarthroncha C (**10**).

Rf: 0.30 (petroleum ether : diethyl ether = 9:1, v/v)

^{1}H NMR (400 MHz, $CDCl_3$): δ 4.80 (apparent pd, *J* = 1.5, 0.6 Hz 1H, H-12a), 4.75 – 4.72 (m, 1H, H-12b), 4.64 – 4.51 (m, 3H, H-1), 4.14 (dd, *J* = 9.1, 5.3 Hz, 1H, H-4), 2.21 – 2.12 (overlapped signals, m, 3H, H-7+ H-6), 1.87 – 1.79 (m, 1H, H-5), 1.77 (apparent t, *J* = 2.4 Hz, 3H, H-10), 1.68-1.67 (m, 3H, H-13), 1.64 (apparent t, *J* = 3.1 Hz, 3H, H-14), 1.61 – 1.57 (m, 1H, H-5), 0.88 (s, 9H, $SiMe_2(C\underline{Me}_3)$), 0.04 (br s, 3H, H-$Si\underline{Me}_2(CMe_3)$), 0.02 (br s, 3H, H-$Si\underline{Me}_2(CMe_3)$).

^{13}C NMR (100 MHz, $CDCl_3$): δ 206.7 (C-2), 146.7 (C-11), 112.0 (C-12), 99.9 (C-3), 77.4 (C-9), 76.7 (C-8), 73.8 (C-1), 72.8 (C-4), 42.9 (C-6), 38.4 (C-5), 26.0 (C-$SiMe_2(C\underline{Me}_3)$), 24.3 (C-7), 19.4 (C-13), 11.9 (C-14), 3.6 (C-10), -4.5 (C-$SiMe_2(\underline{C}Me_3)$), -4.9 (C-$Si\underline{Me}_2(CMe_3)$).

ν_{max} (ATR): 2952, 2928, 2856, 1472; 1435, 1250, 1062, 1004, 891, 834, 773 cm^{-1}.

HRMS (ESI+) *m/z*: calculated for $[M+H]^+$ $C_{20}H_{35}OSi^+$: 319.2452; found: 319.2452.

$[\alpha]_D^{20}$ = -80.9 (c = 0.19, $CHCl_3$)

Synthesis of 4*R* silyl ether 8b

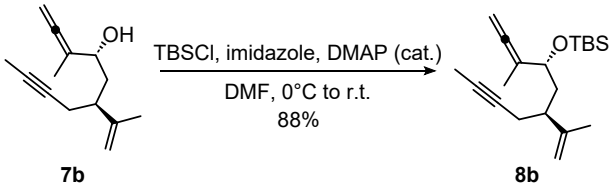

7b **8b**

To a solution of allenol **7b** (240 mg, 1.17 mmol, 1 equiv) in 6 mL of DMF at 0 °C, imidazole (250 mg, 3.67 mmol, 3.1 equiv), DMAP (11 mg, 0.09 mmol, 7.8 mol%) and TBSCl (277 mg, 1.84 mmol, 1.57 equiv) were added. The resulting mixture was stirred and let warm at room temperature overnight. Then, the mixture was quenched with NH_4Cl and extracted three times with diethyl ether. The combined organic phases were washed two times with water, NH_4Cl, brine, then dried over anhydrous $MgSO_4$ and concentrated under vacuum. The residue was purified by flash chromatography on silica gel (90/10 petroleum ether/CH_2Cl_2) to afford 210 mg of **8b** (88%) as a colorless oil.

Nota bene : This procedure was used for the total synthesis of daphnenicillata W (**11**).

Rf: 0.36 (petroleum ether : diethylether = 8:2, v/v)

^{1}H NMR (400 MHz, $CDCl_3$): δ 4.80 (apparent pd, *J* = 1.5, 0.6 Hz 1H, H-12), 4.78 – 4.76 (m, 1H, H-12), 4.65 – 4.54 (m, 2H, H-1), 4.15 (dd, *J* = 8.1, 5.1 Hz, 1H, H-4), 2.35 – 2.27 (m, 1H, H-6), 2.23 – 2.18 (m, 2H, H-7), 1.85 - 1.74 (m, 1H, H-5), 1.77 (apparent t, *J* = 2.5 Hz, 3H, H-10), 1.68-1.67 (m, 3H, H-13), 1.63 (apparent t, *J* = 3.1 Hz, 3H, H-14), 1.58 (ddd, *J* = 13.7, 8.4, 5.1 Hz, 1H, H-5), 0.89 (s, 9H, H-SiMe$_2$(CMe$_3$)), 0.04 (br s, 3H, H-SiMe$_2$(CMe$_3$)), 0.03 (br s, 3H, H-SiMe$_2$(CMe$_3$)).

^{13}C NMR (100 MHz, $CDCl_3$): δ 206.1 (C-2), 146.9 (C-11), 112.0 (C-12), 101.1 (C-3), 77.6 (C-9), 77.4 (C-8) 74.1 (C-1), 72.8 (C-4), 42.6 (C-6), 38.9 (C-5), 26.0 (C-SiMe$_2$(CMe$_3$)), 24.0 (C-7), 19.7 (C-13), 12.4 (C-14), 3.7 (C-10), -4.5((C SiMe$_2$(CMe$_3$)), -5.0 (C-SiMe$_2$(CMe$_3$)).

ν_{max} (ATR): 2953, 2927, 2856, 1472, 1373, 1250, 1076, 1053, 891, 833, 773 cm^{-1}.

HRMS (ESI+) *m/z*: calculated for $[M+H]^+$ $C_{20}H_{35}OSi^+$: 319.2452; found: 319.2443.

$[\alpha]_D^{20}$ = -23.1 (c = 0.26, $CHCl_3$)

(7S,9*S*/*R*)-9-((*tert*-Butyldimethylsilyl)oxy)-4,10-dimethyl-7-(prop-1-en-2-yl)-6,7,8,9-tetrahydroazulen-3(2*H*)-one (9a and 9b)

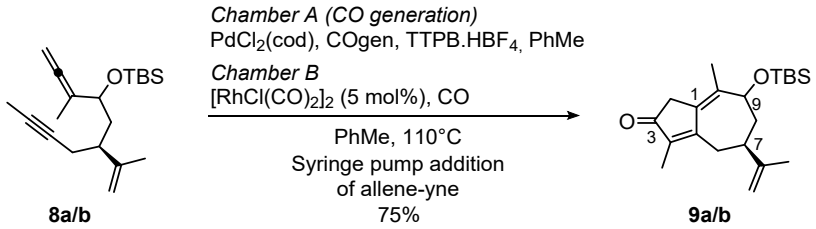

*APK reaction on the 1:1.5 diastereomeric mixture of **8a/8b** (1.87 mmol scale)*

In a dry two-chamber (A and B; a representative picture of the system is shown) system with a total capacity of 400 mL, **chamber A** was charged with COgen® or 9-methyl-9*H*-fluorene-9-carbonyl chloride (932 mg, 3.76 mmol, 2.0 equiv), $PdCl_2$(cod) (53 mg, 0.186 mmol, 10 mol%), TTBP·HBF_4 (53 mg, 0.183 mmol, 9.8 mol%), and 50 mL of PhMe. **Chamber B** was charged with $[Rh(CO)_2Cl]_2$ (37 mg, 0.095 mmol, 5 mol%) and 50 mL of PhMe. The system was sealed using screw caps and Teflon® coated silicon seals. To ensure safety, the setup was covered with a blast shield before heating. Lastly, *N,N*-dicyclohexylmethylamine (1.6 mL, 7.50 mmol, 4.0 equiv) was introduced to **chamber B**. The two-chamber system was then dived into a preheated 110 °C oil bath and stirred. A solution of allene-yne **8a**/**8b** (596 mg, 1.87 mmol, 1 equiv) in 50 mL of PhMe, was added dropwise over a period of 20h with a syringe pump into the **chamber B**. After the addition, the mixture was further stirred for 30 min, then Teflon® coated silicon seal of **chamber A** was carefully pierced with a thin needle to release excess CO gas, in a controlled manner through a bubbler, while ensuring that the sash of the fume hood remained as closed as possible. The **chamber B** was then concentrated under vacuum. The residue was purified

by flash chromatography on silica (95/5 petroleum ether/AcOEt) to afford 486 mg of guaiane derivative **9a**/**9b** (75%, dr 1:1.5).

Data for **9a** and **9b** are separately described hereafter.

APK reaction in the COware with CO generation from chloroform

In a dry two-chamber (A and B) system with a total capacity of 100 mL, **chamber A** was charged with KOH crushed with a mortar and pestle (516 mg, 9.2 mmol, 30 equiv) and 6 mL of PhMe . **Chamber B** was charged with $[Rh(CO)_2Cl]_2$ (6 mg, 0.0157 mmol, 5 mol%) and 8 mL of PhMe. The system was sealed using screw caps and Teflon® coated silicon seals. To ensure safety, the setup was covered with a blast shield before heating. Lastly, $CHCl_3$ (0.25 mL, 10 equiv) was introduced to **chamber A**. The two-chamber system was then heated and stirred at 80 °C during 2h. Then, **chamber B** was heated at 110 °C, while ensuring that **chamber A** was cooled down (here using a stream of compressed air). A solution of allene-yne **8a**/**8b** (98 mg, 0.308 mmol, 1 equiv) in 8 mL of PhMe, was added dropwise over 16 h with a syringe pump into the **chamber B**. After the addition, the mixture was further stirred for 30 min, then the Teflon® coated silicon seal of **chamber A** was pierced with a thin needle to release excess CO gas in a controlled manner into a bubbler, while ensuring that the sash of the fume hood remained as closed as possible. The **chamber B** was then concentrated under vacuum. The residue was purified by flash chromatography on silica (95/5 petroleum ether/AcOEt) to afford 58.3 mg of **9a**/**9b** (55%, dr 1:1.5).

(7*S*,9*S*)-9-((*tert*-Butyldimethylsilyl)oxy)-4,10-dimethyl-7-(prop-1-en-2-yl)-6,7,8,9-tetrahydroazulen-3(2*H*)-one (9a)

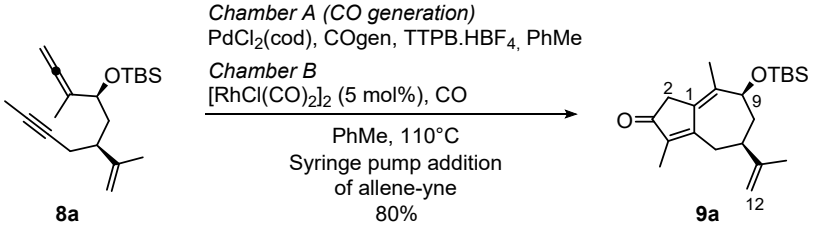

In a dry two-chamber (A and B) system with a total capacity of 20 mL, **chamber A** was charged with COgen® or 9-methyl-9*H*-fluorene-9-carbonyl chloride (31 mg, 0.126 mmol, 2.5 equiv), $PdCl_2$(cod) (1.4 mg, 0.049 mmol, 10 mol%), TTBP·HBF_4 (1.8 mg, 0.062 mmol, 12 mol%), and 2.5 mL of PhMe. **Chamber B** was charged with $[Rh(CO)_2Cl]_2$ (1 mg, 0.0026 mmol, 5 mol%) and 1.9 mL of PhMe. The system was sealed using screw caps and Teflon® coated silicon seals. To ensure safety, the setup was covered with a blast shield before heating. Lastly, *N,N*-dicyclohexylmethylamine (0.04 mL, 0.2 mmol, 4 equiv) was introduced to **chamber B**. The two-chamber system was then dived into a preheated 110 °C oil bath and stirred. A solution of allene-yne **8a** (16 mg, 0.050 mmol, 1 equiv) in 2.5 mL PhMe was added dropwise over 3h with a syringe pump into **chamber B**. After the addition, the mixture was stirred for further 30 min, then Teflon® coated silicon seal of **chamber A** was pierced with a thin needle to release excess CO gas in a controlled manner into a bubbler, while ensuring that the sash of the fume hood remained as closed as possible. The **chamber B** was then concentrated under vacuum. The residue was purified by flash chromatography on silica (95/5 petroleum ether/AcOEt) to afford 14 mg of **9b** (80%) as an amorphous colorless solid.

Rf: 0.39 (petroleum ether : AcOEt = 8:2)

^{1}H NMR (400 MHz, $CDCl_3$): δ 4.76 – 4.73 (m, 1H, H-12), 4.72 (apparent p, J = 1.5 Hz, 1H, H-12), 4.34 (dd, *J* = 8.1, 4.0 Hz, 1H, H-9), 3.01 – 2.86 (overlapped signals 3H: 2.97, d, *J* = 20.0 Hz, 1H, H-2a; 2.97-2.90, m,

1H, H-6a; 2.89, d, *J* = 20.0 Hz, 1H, H-2b), 2.69 (dd, *J* = 16.3, 3.2 Hz, 1H, H-6b), 2.46 – 2.36 (m, 1H, H-7), 2.11 (dddd, *J* = 14.0, 6.1, 4.3, 1.1 Hz, 1H, H-8a), 1.92 – 1.83 (overlapped signals 4H: 1.89, br s, 3H, H-14; 1.92 – 1.83, m, 1H, H-8b), 1.78 – 1.75 (overlapped signals 6H: 1.77-1.74, m, 3H, H-13; 1.77-1.74, m, 3H, H-15), 0.89 (s, 9H), 0.10 (br s, 3H, H-TBS), 0.07 (br s, 3H, H-TBS).

^{13}C NMR (100 MHz, $CDCl_3$): δ 204.5 (C-3), 166.5 (C-5), 149.4 (C-11), 139.5 (C-4), 137.5 (C-10), 131.9 (C-1), 109.9 (C-12), 74.1 (C-9), 42.2 (C-8), 41.1 (C-2), 40.8 (C-7), 34.4 (C-6), 26.0 (C-TBS), 21.1 (C-14), 20.0 (C-13), 8.6 (C-15), -4.3 (C-TBS), -4.6 (C-TBS).

ν_{max} (ATR): 2929, 1685, 1252, 1041, 1020, 1005, 893, 870, 832, 812 cm^{-1}.

HRMS (ESI+) *m/z*: calculated for $[M+H]^+$ $C_{21}H_{35}O_2Si^+$: 347.2401; found: 347.2392.

$[\alpha]_D^{20}$ = +23.9 (c = 0.25, $CHCl_3$)

(7S,9*R*)-9-((*tert*-Butyldimethylsilyl)oxy)-4,10-dimethyl-7-(prop-1-en-2-yl)-6,7,8,9-tetrahydroazulen-3(2*H*)-one (9b)

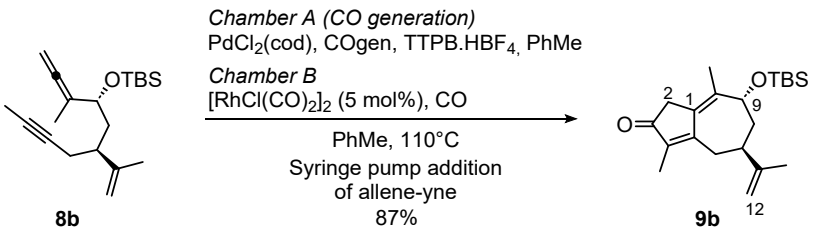

In a dry two-chamber (A and B) system with a total capacity of 100 mL, **chamber A** was charged with COgen® (82 mg, 0.33 mmol, 2.0 equiv), $PdCl_2$(cod) (5 mg, 0.017 mmol, 10 mol%), TTBP·HBF_4 (5 mg, 0.017 mmol, 10 mol%), and 4.2 mL of PhMe. **Chamber B** was charged with $[Rh(CO)_2Cl]_2$ (3 mg, 0.008 mmol, 5 mol%) and 6.4 mL of PhMe . The system was sealed using screw caps and Teflon® coated silicon seals. To ensure safety, the setup was covered with a blast shield before heating. Lastly, *N,N*-dicyclohexylmethylamine (0.14 mL, 0.668 mmol, 4 equiv) was introduced to **chamber B**. The two-chamber system was then dived into a preheated 110 °C oil bath and stirred. A solution of allene-yne **8b** (53 mg, 0.167 mmol, 1 equiv) in 6.4 mL of PhMe was added dropwise over a period of 16h30 with a syringe pump into the **chamber B**. After the addition, the mixture was stirred for an additional 30 min, then the Teflon® coated silicon seal of **chamber A** was pierced with a thin needle to release excess CO gas in a controlled manner into a bubbler, while ensuring that the sash of the fume hood remained as closed as possible. The **chamber B** was then concentrated under vacuum. The residue was purified by flash chromatography on silica (95/5 petroleum ether/AcOEt) to afford 50.3 mg of **9b** (87%) as a beige solid.

Rf: 0.39 (petroleum ether : AcOEt = 8:2, v/v)

^{1}H NMR (400 MHz, CDCl3): δ 4.76 – 4.74 (m, 1H, H-12a), 4.73 (apparent p, J = 1.5 Hz, 1H, H-12b), 4.49 (dd, *J* = 7.1, 2.9 Hz, 1H, H-9), 3.00 – 2.83 (overlapped signals 3H: 2.94, d, *J* = 20.8 Hz, 1H, H-2a; 2.92-2.85, m, 1H, H-6a; 2.86, d, *J* = 20.8 Hz, 1H, H-2b), 2.78 – 2.69 (m, 1H, H-7), 2.60 (dd, *J* = 16.5, 10.6 Hz, 1H, H-6b), 2.04 (dddd, *J* = 14.1, 7.1, 4.5, 1.3 Hz, 1H, H-8a), 1.92 – 1.84 (overlapped signals 4H: 1.92 – 1.84, m, 1H, H-8b; 1.85, br s, 3H, H-14), 1.76 – 1.74 (m, 3H, H-13), 1.76 (br s, 3H, H-15), 0.91 (s, 9H, H-TBS), 0.09, (br s, 3H, H-TBS), 0.08 (br s, 3H, H-TBS).

^{13}C NMR (100 MHz, $CDCl_3$): δ 204.5 (C-3), 166.2 (C-5), 149.7 (C-11), 139.5 (C-4), 136.9 (C-10), 131.7 (C-1), 110.0 (C-12), 72.7 (C-9), 41.1 (C-2), 41.1 (C-8), 38.2 (C-7), 35.7 (C-6), 26.0 (C-TBS), 20.8 (C-14), 20.3 (C-13), 8.6 (C-15), -4.3 (C-TBS), -4.6 (C-TBS).

ν_{max} (ATR): 2928, 1687, 1252, 1066, 1003, 962, 834, 825, 808, 774 cm^{-1}.

HRMS (ESI+) *m/z*: calculated for $[M+Na]^+$ $C_{21}H_{34}NaO_2Si^+$: 369.2220; found: 369.2224; calculated for $[M+H]^+$ $C_{21}H_{35}O_2Si^+$: 347.2401, found: 347.2399.

$[\alpha]_D^{20}$ = +61.2 (c = 0.22, $CHCl_3$)

M.p. = 72-73°C

Note: The structure of compound **9b** was confirmed by X-ray crystallography (see the crystallographic section). Single crystals suitable for X-ray diffraction were obtained by slow evaporation of a dichloromethane/pentane solution at room temperature.

Deprotection of the diastereomeric mixture 9a/9b en route to oleodaphnone 3

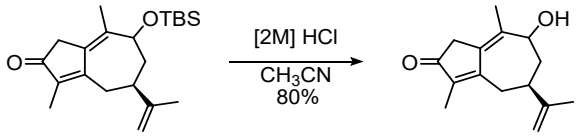

dr 1:1.5 **9a/9b** dr 1:1.5 **10/11**

To a solution of TBS ethers **9a**/**9b** (dr = 1:1.5) (557 mg, 1.60 mmol, 1 equiv) in 23 mL of acetonitrile at 0 °C, $[2M]_{aq}$ hydrochloric acid (8 mL, 10 equiv) was added dropwise. The resulting mixture was allowed to warm at room temperature and was stirred during 1h45. Then, the mixture was quenched with sat. aq. $NaHCO_3$ and extracted three times with AcOEt. The combined organic phases were washed with water, brine, then dried over anhydrous $MgSO_4$ and concentrated under vacuum. The residue was purified by flash chromatography on silica gel (7/3 petroleum ether/AcOEt) to afford 297 mg of a mixture **10**/**11** (80%, dr = 1:1.5).

Data for **10** and **11** are separately described below.

Diathroncha C (10, structure as reported in ref. [5])

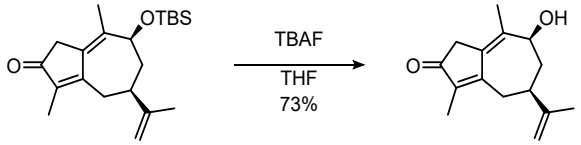

9a **10**

*The deprotection method was modified compared to previously, since we observed epimerization of the C-9 center when diastereomerically pure **9a** was tentatively treated with aq. HCl.*

To a solution of diastereomerically pure TBS ether **9a** (30 mg, 0.087 mmol, 1.0 equiv) in 0.9 mL of THF at 0 °C room temperature, TBAF [1M in THF] (0.17 mL, 2.0 equiv) was added dropwise. The resulting mixture was allowed to warm at room temperature and was stirred during 3h. Then, diethyl ether and water were added to the mixture and the phases were separated. After three extractions diethyl ether, the combined organic phases were washed with water, brine, then dried over anhydrous $MgSO_4$ and concentrated under vacuum. The residue was purified by flash chromatography on silica gel (9/1 dichlorometane/acetone) to afford 14.7 mg of **10** (73%) as a white solid.

Rf: 0.58 (dichlorometane/acetone = 8:2, v/v)

^{1}H NMR (400 MHz, DMSO-d_6): δ 5.08 (d, J = 5.9 Hz, 1H, OH), 4.78 – 4.74 (m, 2H, H-12), 4.21 – 4.12 (m, 1H, H-9), 2.98 (d, J = 20.7 Hz, 1H, H-2a), 2.84 (d, J = 20.7 Hz, 1H, H-2b), 2.81 – 2.73 (m, 1H, H-6a), 2.72

– 2.64 (m, 1H, H-6b), 2.42 – 2.31 (m, 1H, H-7), 2.12 – 2.02 (m, 1H, H-8a), 1.87 (br s, 3H, H-14), 1.76 – 1.69 (overlapped signals 4H: 1.76 – 1.69, m, 1H, H-8b; 1.74 – 1.72, m, 3H, H-13), 1.66 (br s, 3H, H-15).

^{13}C NMR (100 MHz, DMSO-d_6): δ 202.7 (C-3), 165.2 (C-5), 149.5 (C-11), 138.6 (C-10), 138.4 (C-4), 130.0 (C-1), 109.5 (C-12), 71.6 (C-9), 42.2 (C-8), 40.5 (C-2), 39.6 (C-7), 34.7 (C-6), 20.2 (C-14), 19.8 (C-13), 8.2 (C-15).

ν_{max} (ATR): 3343, 1657, 1386, 1376, 1362, 1352,1025, 1002, 892, 633 cm^{-1}.

HRMS (ESI+) *m/z*: calculated for $[M+H]^+$ $C_{15}H_{21}O_2^+$: 233.1536; found: 233.1531.

$[\alpha]_D^{20}$ = +69.0 (c = 0.1, MeOH) [Lit:[5] $[\alpha]_D^{20}$ = +14.2 (c = 0.1, MeOH)]

M.p. = 66-67 °C

Daphnenicillata W (11)

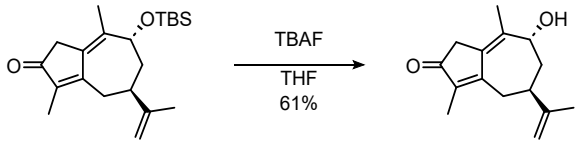

9b **11**

To a solution of diastereomerically pure TBS ether **9b** (30.1 mg, 0.087 mmol, 1.0 equiv) in 0.9 mL of THF at 0 °C room temperature, TBAF [1M in THF] (0.17 mL, 2.0 equiv) was added dropwise. The resulting mixture was allowed to warm at room temperature and was stirred during 3h. Then, diethyl ether and water were added to the mixture and the phases were separated. After three extractions with diethyl ether, the combined organic phases were washed with water, brine, then dried over anhydrous $MgSO_4$ and concentrated under vacuum. The residue was purified by flash chromatography on silica gel (9/1 dichlorometane/acetone) to afford 12.3 mg of natural product **11** (61%) as a colorless oil.

Rf: 0.58 (dichlorometane/acetone = 8:2, v/v)

NMR data in $CDCl_3$

^{1}H NMR (400 MHz, $CDCl_3$): δ 4.80 – 4.79 (m, 1H, H-12a), 4.78 (apparent p, *J* = 1.5 Hz, 1H, H-12b), 4.52 – 4.46 (m, 1H, H-9), 3.02 – 2.88 (overlapped signals 3H: 2.98, d, *J* = 20.8, 1H, H-2a; 2.98 – 2.90, m, 1H, H-6a; 2.92, d, *J* = 20.8, 1H, H-2b), 2.73 – 2.66 (m, 1H, H-7), 2.59 (dd, *J* = 17.0, 11.5 Hz, 1H, H-6b), 2.14 (dddd, *J* = 14.4, 6.2, 3.1, 1.6 Hz, 1H, H-8a), 2.05 – 1.95 (overlapped signals 4H: 2.05 – 1.95, m, 1H, H-8b; 1.97, br s, 3H, H-14), 1.81 – 1.80 (m, 3H, H-13), 1.77 (br s, 3H, H-15).

^{13}C NMR (100 MHz, $CDCl_3$): δ 204.1 (C-3), 165.3 (C-5), 149.5 (C-11), 140.4 (C-4), 135.1 (C-10), 132.5 (C-1), 109.9 (C-12), 72.5 (C-9), 41.5 (C-8), 41.2 (C-2), 37.6 (C-7), 36.5 (C-6), 21.0 (C-14), 20.5 (C-13), 8.7 (C-15).

NMR data in DMSO-d6

^{1}H NMR (400 MHz, DMSO-d_6): δ 5.04 (d, *J* = 5.9 Hz, 1H, OH), 4.77 – 4.75 (m, 1H, H-12a), 4.72 – 4.70 (m, 1H, H-12b), 4.35 – 4.30 (m, 1H, H-9), 2.92 (d, *J* = 21.0 Hz, 1H, H-2a), 2.88 (d, *J* = 21.0 Hz, 1H, H-2b), 2.83 – 2.76 (m, 1H, H-7), 2.69 – 2.64 (m, 1H, H-6a), 2.63 – 2.59 (m, 1H, H-6b), 1.98 – 1.91 (m, 1H, H-8a), 1.90 – 1.85 (overlapped signals 4H: 1.90 – 1.85, m, 1H, H-8b; 1.86, br s, 3H, H-14), 1.76 – 1.74 (m, 3H, H-13), 1.66 (br s, 3H, H-15).

^{13}C NMR (100 MHz, DMSO-d_6): δ 202.8 (C-3), 165.4 (C-5), 149.7 (C-11), 138.2 (C-4), 137.3 (C-10), 130.5 (C-1), 109.3 (C-12), 70.0 (C-9), 41.0 (C-8), 40.4 (C-2), 37.2 (C-6), 35.2 (C-7), 20.4 (C-13), 20.1 (C-14), 8.2 (C-15).

ν_{max} (ATR): 3390, 1666, 1440, 1385, 1277, 1064, 996, 888, 729 cm^{-1}.

HRMS (ESI+) *m/z*: calculated for $[M+H]^+$ $C_{15}H_{21}O_2^+$: 233.1536; found: 233.1531.

$[\alpha]_D^{20}$ = +50.0 (c = 0.1, MeOH); [Lit:[6] $[\alpha]_D^{20}$ = +29.0 (c = 0.1, MeOH)]

Oleodaphnone (3)

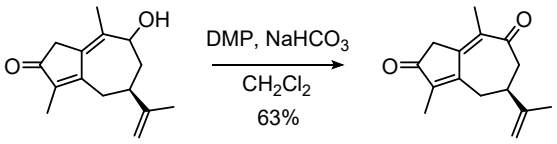

dr 1:1.5
10/11

3

To a solution of diastereomeric mixture **10/11** (dr = 1:1.5) (824 mg, 3.55 mmol, 1 equiv) in 35 mL of CH_2Cl_2 at -18°C, $NaHCO_3$ (1.58 g, 18.8 mmol, 5.3 equiv) and DMP (3.01 g, 7.10 mmol, 2.0 equiv) were added portionwise. After 5 minutes, the mixture was allowed to warm at room temperature. The resulting mixture was additionally stirred for 30 min. Then, the reaction was quenched at 0 °C with a solution of sat. aq. $NaHCO_3$: $Na_2S_2O_3$ (1:1, 30 mL) and extracted three times with CH_2Cl_2. The combined organic phases were washed with water, brine, then dried over anhydrous $MgSO_4$ and concentrated under vacuum. The residue was purified by flash chromatography on silica gel (8/2 petroleum ether/AcOEt) to afford 523 mg of oleodaphnone **3** (63%) as a green solid.

Rf: 0. 51 (petroleum ether : AcOEt = 7:3, v/v)

^{1}H NMR (400 MHz, $CDCl_3$): δ 4.80 (apparent p, J = 1.4 Hz, 1H, H-12a), 4.79 – 4.77 (m, 1H, H-12b), 3.13 (d, *J* = 21.1 Hz, 1H, H-2a), 3.06 (d, *J* = 21.1 Hz, 1H, H-2b), 3.02 – 2.93 (m, 1H, H-6a), 2.90 – 2.88 (m, 1H, H-8a), 2.88 – 2.86 (m, 1H, H-8b), 2.79 – 2.74 (m, 1H, H-6b), 2.74 – 2.70 (m, 1H, H-7), 1.97 (s, 3H, H-14), 1.87 (s, 3H, H-15), 1.78 (s, 3H, H-13).

^{13}C NMR (100 MHz, $CDCl_3$): δ 201.9 (C-3), 200.7 (C-9), 162.8 (C-5), 147.2 (C-11), 145.0 (C-4), 144.3 (C-1), 131.7 (C-10), 111.3 (C-12), 49.9 (C-8), 41.3 (C-2), 39.2 (C-7), 35.6 (C-6), 20.3 (C-13), 17.6 (C-14), 9.1 (C-15).

ν_{max} (ATR): 2920, 1690, 1643, 1600, 1436, 1384, 1305, 1231, 1196 1074, 908, 894 cm-[1].

HRMS (ESI+) *m/z*: calculated for $[M+H^+]$ $C_{15}H_{19}O_2^+$: 231.1380; found: 231.1388.

$[\alpha]_D^{25}$ = +14.1 (c = 0.11, $CHCl_3$) [Lit:[4] $[\alpha]_D^{25}$ = +4.1, c = 0.93, $CHCl_3$]

M.p. = 37-38 °C

Note: The structure of compound **3** was confirmed by X-ray crystallography (see the crystallographic section). Single crystals suitable for X-ray diffraction were obtained by evaporation of petroleum ether/AcOEt after the purification at room temperature.

(1*S*,7*R*,11*S*)-4,10,11-Trimethyl-7,12dihydro-2*H*-1,7,10-(epiethane[1,1,2]triyl)azulene-3,9(1*H*,8*H*)-dione (2)

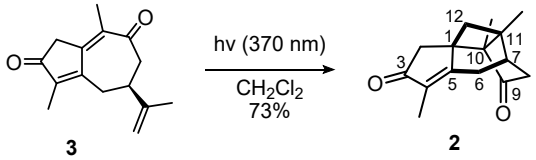

3

2

A degassed (Ar) solution of oleodaphnone **3** (462 mg, 2 mmol, 1 equiv) in 100 mL of CH_2Cl_2 at room temperature was irradiated at 370 nm (Kessil lamp) for 56 hours, maintaining an Ar atmosphere throughout the irradiation period. The reaction mixture was concentrated and the residue was purified by flash chromatography on silica (7/3 petroleum ether/AcOEt) to afford 339 mg of **2** (73%) as a white solid.

Rf: 0. 40 (petroleum ether : AcOEt = 6:4, v/v)

^{1}H NMR (400 MHz, CD_3OD): δ 3.05 (d, *J* = 17.8 Hz, 1H, H-6a), 2.74 – 2.61 (overlapped signals 3H: 2.70 d, J = 17.8 Hz, 1H, H-6b; 2.69 – 2.65, m, 1H, H-8a; 2.65 – 2.61, m, 1H, H-7), 2.39 (apparent dt, *J* = 19.3, 1.3 Hz, 1H, H-2a), 2.32 (d, *J* = 9.8 Hz, 1H, H-12a), 2.21 – 2.09 (overlapped signals 3H: 2.21 – 2.13, m, 1H, H-8b; 2.17, d, J = 9.8 Hz, 1H, H-12b; 2.12, dd, *J* = 19.3, 1.3 Hz, 1H, H-2b), 1.63 – 1.61 (m, 3H, H-15), 1.16 (br s, 3H, H-13), 1.13 (br s, 3H, H-14).

^{13}C NMR (75 MHz, CD_3OD): δ 221.5 (C-9), 209.1 (C-3), 177.9 (C-5), 134.8 (C-4), 62.7 (C-10), 58.8 (C-1), 49.3 (C-8), 46.2 (C-11), 39.8 (C-2), 39.7 (C-7), 37.0 (C-12), 31.0 (C-6), 18.5 (C-13), 10.8 (C-14), 7.6 (C-15).

ν_{max} (ATR): 2956, 2919, 1720, 1690, 1649, 1452, 1352, 1302, 1070, 1052, 926 cm-^{1}.

HRMS (ESI+) *m/z*: calculated for [M+H$^+$] $C_{15}H_{19}O_2^+$: 231.1380; found: 231.1389.

$[\alpha]_D^{20}$ = +94.5 (c = 0.27, $CHCl_3$)

M.p. = 124-125°C

Note: The structure of compound **2** was confirmed by X-ray crystallography (see the crystallographic section). Single crystals suitable for X-ray diffraction were obtained by slow evaporation of a dichloromethane/pentane solution at room temperature.

(4*R*,5*R*,7*R*,11*S*)-4,10,11-Trimethyl-7,8,11,12-tetrahydro-5,7-methanocyclopenta[a]pentalene-3,9(4*H*,10*H*)-dione (13)

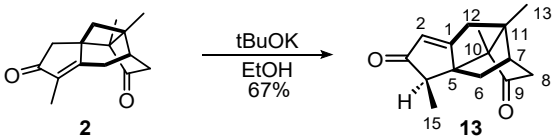

To a solution of enone **2** (6.4 mg, 0.028 mmol, 1 equiv) in 0.5 mL of EtOH was added tBuOK (6.1 mg, 0.055 mmol, 2 equiv) at room temperature under argon. The resulting mixture was stirred during 16h, and the reaction was quenched with aq. sat. NH_4Cl, and extracted three times with AcOEt. The combined organic phases were washed with water, brine and dried over anhydrous $MgSO_4$ and concentrated under vacuum. The residue was purified by flash chromatography on silica gel (95/5 CH_2Cl_2/Et_2O) to afford 4.3 mg of **13** (67%, dr 15:1) as a white solid.

Rf: 0. 63 (CH_2Cl_2:Et_2O = 9:1, v/v)

^{1}H NMR (400 MHz, $CDCl_3$): δ 5.73 (apparent t, *J* = 1.7 Hz, 1H, H-2), 2.73 (dd, *J* = 19.0, 1.7 Hz, 1H, H-12a), 2.49 (dddd, *J* = 17.6, 4.0, 2.9, 1.1 Hz, 1H, H-8a), 2.44 – 2.33 (overlapped signals 2H: 2.40, d, *J* = 19.0 Hz, 1H, H-12b; 2.38 – 2.34, m, 1H, H-7), 2.19 (q, *J* = 7.5 Hz, 1H, H-4), 2.04 (d, *J* = 17.6 Hz, 1H, H-8b), 1.58 (ddd, *J* = 12.7, 5.8, 2.9 Hz, 1H, H-6a), 1.47 (d, *J* = 12.7 Hz, 1H, H-6b), 1.10 (br s, 3H, H-13), 0.99 (d, *J* = 7.5 Hz, 3H, H-15), 0.74 (br s, 3H, H-14).

^{13}C NMR (100 MHz, $CDCl_3$): δ 215.9 (C-9), 212.0 (C-3), 188.4 (C-1), 120.0 (C-2), 64.2 (C-5), 64.0 (C-10), 57.5 (C-11), 46.5 (C-8), 41.5 (C-4), 39.9 (C-7), 34.8 (C-12), 33.1 (C-6), 14.9 (C-13), 12.0 (C-15), 5.7 (C-14).

ν_{max} (ATR): 2921, 1738, 1694, 1632, 1456, 1385, 1156, 1031, 991, 850 cm^{-1}.

HRMS (ESI+) *m/z*: calculated for $[M+H]^+$ $C_{15}H_{19}O_2^+$: 231.1380; found 231.1378.

$[\alpha]_D^{20}$ = +122.0 (c 0.2, $CHCl_3$)

M.p. = 68-69 °C

Note: The structure of compound **13** was confirmed by X-ray crystallography (see the crystallographic section). Single crystals suitable for X-ray diffraction were obtained by slow evaporation of a dichloromethane/pentane solution at room temperature.

6-*epi*-Daphnepapytone A (*epi*-1)

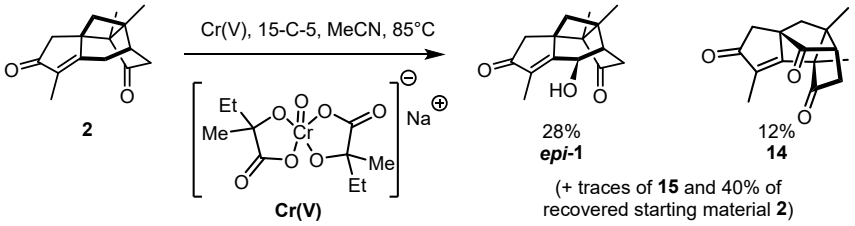

According to a known procedure,[13] into a flame-dried Schlenk flask equipped with a magnetic stir bar, the **Cr(V)** complex (315 mg, 0.97 mmol, 10 equiv) and 0.4 mL of MeCN were added. While vigorously stirring the reaction mixture, a solution of enone **2** (22.4 mg, 0.097 mmol, 1.0 equiv) in 2 mL of MeCN was added, followed by 15-crown-5 ether (9 µL, 0.5 equiv). The mixture was placed in a sonication bath at room temperature for 5 minutes before being transferred into a preheated oil bath at 85 °C. After stirring for 19 hours, the reaction vessel was removed from the oil bath and allowed to cool to room temperature. The reaction mixture was then filtered through a pad of Celite®, which was washed twice with EtOAc (2 × 10 mL). The filtrate was diluted with brine and extracted three times with EtOAc. The combined organic phase was washed with saturated aqueous $NaHCO_3$ until it became clear, then with brine, dried over anhydrous $MgSO_4$, and concentrated under vacuum. The residue was purified by flash chromatography on silica gel (9/1 to 7/3 CH_2Cl_2/diethyl ether) to afford 6.7 mg of ***epi*-1** (28%, or 46% b.r.s.m.) and 8.9 mg of **2** (40%) as white solids. Compounds **14** and **15** were purified by a second flash chromatography on silica gel (6/4 petroleum ether/ethyl acetate) to afford 3 mg of **14** (12%) and traces of **15** (<0.5 mg)**.**

Data for compound *epi*-1

Rf: 0.20 (CH_2Cl_2 : diethyl ether = 7:3, v/v)

^{1}H NMR (400 MHz, $CDCl_3$): δ 4.69 (s, 1H, H-6), 2.66 (d, *J* = 9.6 Hz, 1H, H-12), 2.62 (dd, *J* = 8.1, 1.1 Hz, 1H, H-7), 2.56 (dd, *J* = 17.4, 8.1 Hz, 1H, H-8), 2.46 (d, *J* = 19.5 Hz, 1H, H-2), 2.29 (d, *J* = 9.6 Hz, 1H, H-12), 2.19 – 2.11 (overlapped signals 2H: 2.16, d, *J* = 17.4 Hz, 1H, H-8; 2.14, d, *J* = 19.5 Hz, H-2), 1.75 (br s, 3H, H-15), 1.15 (br s, 3H, H-13 or H-14), 1.14 (br s, 3H, H-13 or H-14).

^{13}C NMR (100 MHz, $CDCl_3$): δ 217.6 (C-9), 207.2 (C-3), 170.9 (C-5), 137.5 (C-4), 68.8 (C-6), 62.0 (C-10), 56.9 (C-1), 46.8 (C-7), 44.6 (C-11), 44.6 (C-8), 40.0 (C-2), 36.6 (C-12), 18.9 (C-13 or C-14), 10.7 (C-13 or C-14), 8.0 (C-15).

ν_{max} (ATR): 3403, 2954, 1692, 1656, 1294, 1044, 927, 880, 731, 629 cm^{-1}.

HRMS (ESI+) *m/z*: calculated for $[M+H]^+$ $C_{15}H_{19}O_3^+$: 247.1329; found: 247.1325.

$[\alpha]_D^{20}$ = +72.0 (c 0.17, $CHCl_3$)

Data of compound 14

Rf: 0.75 (CH_2Cl_2 : diethyl ether = 9:1, v/v)

Rf: 0.25 (petroleum ether : ethyl acetate = 6:4, v/v)

^{1}H NMR (400 MHz, $CDCl_3$): δ 2.96 (d, *J* = 18.7 Hz, 1H, H-2), 2.72 – 2.57 (overlapped signals 3H, m, 3H, H-7+H-6), 2.28 (d, *J* = 18.7 Hz, 1H, H-2), 2.15 (d, *J* = 10.8 Hz, 1H, H-12), 1.98 (d, *J* = 10.8 Hz, 1H, H-12), 1.74 (br s, 3H, H-15), 1.35 (br s, 3H, H-14), 1.30 (br s, 3H, H-13).

^{13}C NMR (100 MHz, $CDCl_3$): δ 211.1 (C-8), 209.6 (C-9), 207.6 (C-3), 170.8 (C-5), 135.9 (C-4), 65.3 (C-1), 60.7 (C-10), 54.6 (C-11), 51.9 (C-7), 42.7 (C-12), 41.1 (C-6), 34.8 (C-2), 15.4 (C-13), 12.9 (C-14), 8.2 (C-15).

ν_{max} (ATR): 2919, 1733, 1703, 1652, 1377, 1230, 1074, 1030, 932, 732 cm^{-1}.

HRMS (ESI+) *m/z*: calculated for $[M+H]^+$ $C_{15}H_{17}O_3^+$: 247.1172; found: 247.1170.

$[\alpha]_D^{20}$ = +131.1 (c 0.09, $CHCl_3$)

(1*S*,7*R*,11*S*)-4,10,11-Trimethyl-7,8-dihydro-2*H*-1,7,10-(epiethane[1,1,2]triyl)azulene-3,6,9(10*H*)-trione (15)

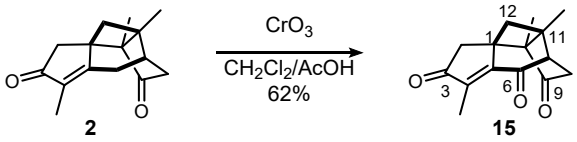

2 **15**

To a solution of enone **2** (7.6 mg, 0.033 mmol, 1 equiv) in 0.66 mL of CH_2Cl_2 and 0.33 mL of glacial AcOH, dry CrO_3 (17.2 mg, 0.17 mmol, 5.2 equiv) was added portion-wise at room temperature. After the addition, the suspension was stirred at the same temperature during 38h. Then, the reaction was quenched with isopropanol (0.5 mL), and extracted three times with CH_2Cl_2. The combined organic phases were washed with water, brine and dried over anhydrous $MgSO_4$ and concentrated under vacuum. The residue was purified by flash chromatography on silica gel (9/1 CH_2Cl_2/Et_2O) to afford 5 mg of ketone **15** (62%) as a slightly beige solid.

Rf: 0. 69 (CH_2Cl_2/Et_2O = 8:2, v/v)

^{1}H NMR (400 MHz, $CDCl_3$): δ 3.09 (d, *J* = 8.1 Hz, 1H, H-7), 2.81 (dd, *J* = 18.2, 8.1 Hz, 1H, H-8a), 2.57 (d, *J* = 20.0 Hz, 1H, H-2a), 2.48 (d, *J* = 10.4 Hz, 1H, H-12a), 2.39 (d, *J* = 18.2 Hz, 1H, H-8b), 2.26 (d, *J* = 20.0 Hz, 1H, H-2b), 2.03 – 1.98 (overlapped signals 4H: 2.00, d, *J* = 10.4 Hz, 1H, H-12b; 1.99, br s, 3H, H-15) 1.25 (br s, 3H, H-14), 1.16 (br s, 3H, H-13).

^{13}C NMR (100 MHz, $CDCl_3$): δ 215.1 (C-9), 206.5 (C-3), 199.2 (C-6), 160.1 (C-5), 142.7 (C-4), 61.9 (C-10), 56.0 (C-7), 53.1 (C-1), 45.1 (C-8), 44.7 (C-11), 39.8 (C-2), 39.4 (C-12), 17.6 (C-13), 11.0, 9.2 (C-4).

ν_{max} (ATR): 2919, 1728, 1699, 1650, 1390, 1265, 1213, 1121, 1030, 928 cm^{-1}.

HRMS (ESI+) *m/z*: calculated for $[M+H]^+$ $C_{15}H_{17}O_3^+$: 247.1172; found: 247.1168.

$[\alpha]_D^{20}$ = +90.1 (c = 0.21, $CHCl_3$)

M.p. = 113-114 °C

Note: The structure of compound **15** was confirmed by X-ray crystallography (see the crystallographic section). Single crystals suitable for X-ray diffraction were obtained by slow evaporation of a dichloromethane/pentane solution at room temperature.

Daphnepapytone A (1)

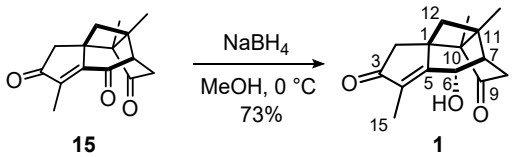

To a solution of triketone **15** (5.8 mg, 0.0237 mmol, 1 equiv) in 0.2 mL of MeOH, $NaBH_4$ (0.7 mg, 0.0184 mmol, 0.77 equiv) was added at 0 °C. The mixture was stirred for 5 min, and then quenched with aq. sat. NH_4Cl, and extracted three times with AcOEt. The combined organic phases were washed with water and brine, dried over anhydrous $MgSO_4$ and concentrated under vacuum. The residue was purified by flash chromatography on silica (CH_2Cl_2/Et_2O 8:2) to afford 4.3 mg of **1** (73%) as a white solid.

Rf: 0.21 (petroleum ether: AcOEt 8:2)

^{1}H NMR (400 MHz, CD_3OD): δ 5.29 (d, *J* = 6.5 Hz, 1H, H-6), 2.77 (d, *J* = 18.1 Hz, 1H, H-8a), 2.58 (apparent t, *J* = 6.8 Hz, 1H, H-7), 2.42 – 2.33 (overlapped signals 2H: 2.39, ddd, *J* = 18.1, 7.2, 1.4 Hz, 1H, H-8b; 2.35, d, *J* = 19.4, 1H, H-2a), 2.22 (d, *J* = 10.0 Hz, 1H, H-12a), 2.18 (d, *J* = 10.0 Hz, 1H, H-12b), 2.13 (dd, *J* = 19.4, 1.4 Hz, 1H, H-2b), 1.82 (d, *J* = 1.9 Hz, 3H, H-15), 1.15 (br s, 3H, H-13), 1.12 (br s, 3H, H-14).

^{13}C NMR (100 MHz, CD_3OD): δ 221.3 (C-9), 209.7 (C-3), 176.2 (C-5), 136.7 (C-4), 69.3 (C-6), 62.2 (C-10), 55.7 (C-1), 46.9 (C-7), 45.8 (C-11), 41.2 (C-8), 40.2 (C-2), 36.1 (C-12), 18.5 (C-13), 10.7 (C-14), 8.1 (C-15).

ν_{max} (ATR): 3367, 1722, 1678, 1633, 1372, 1292, 1272, 1088, 1050, 922 cm^{-1}.

HRMS (ESI+) *m/z*: calculated for $[M+H]^+$ $C_{15}H_{19}O_3^+$: 247.1329; found: 247.1326.

$[\alpha]_D^{25}$ = +42.0 (c = 0.1, MeOH) [Lit:[9] $[\alpha]_D^{26}$ = +29.0 (c = 0.11, MeOH)]

M.p. = 140-141 °C

Note: The structure of compound **1** was confirmed by X-ray crystallography (see the crystallographic section). Single crystals suitable for X-ray diffraction were obtained by slow evaporation of a dichloromethane/pentane solution at room temperature.

(1*S*,6*S*,7*R*,9*S*,11*S*)-4,10,11-Trimethyl-7,8-dihydro-6,9-dihydroxy-2*H*-1,7,10-(epiethane[1,1,2]triyl)azulene-3(10*H*)-one (19)

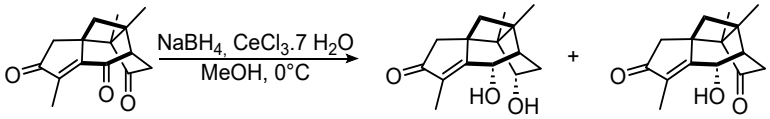

To a solution of triketone **15** (7.6 mg, 0.031 mmol, 1 equiv.) in 0.26 mL of MeOH, $CeCl_3.7H_2O$ (11.6 mg, 0.031 mmol, 1 equiv.) was added at 0 °C. The mixture was stirred for 6 min, and then $NaBH_4$ (0.9 mg, 0.023 mmol, 0.75 equiv.) was added at 0 °C. The mixture was stirred for 5 min, and then quenched with aq. sat. NH_4Cl, and extracted three times with AcOEt. The combined organic phases were washed with water, brine and dried over anhydrous $MgSO_4$ and concentrated under vacuum. The residue was purified by flash chromatography on silica (CH_2Cl_2/diethyl ether 8:2 to CH_2Cl_2/diethyl ether/acetone 2:2:0.5) to afford 1.2 mg of daphnepapytone A (**1,** 16%) and 1.5 mg of **19** (19%) as a white solid.

Rf: 0.22 (CH_2Cl_2 : diethyl ether : acetone = 2:2:0.5, v/v)

^{1}H NMR (400 MHz, $CDCl_3$): δ 5.07 (s, 1H, H-6), 3.72 (apparent t, *J* = 7.5 Hz, 1H, H-9), 2.70 (dd, *J* = 13.7, 7.2 Hz, 1H, H-8), 2.39 – 2.33 (overlapped signals 2H: 2.39-2.34, m, 1H, H-2; 2.37-2.33, m, 1H, H-7), 2.08 (dd, *J* = 19.2, 1.3 Hz, 1H, H-2), 1.91 (d, *J* = 10.0 Hz, 1H, H-12), 1.90 (d, *J* = 1.8 Hz, 3H, H-15), 1.86 (d, *J* = 10.0 Hz, 1H, H-12), 1.70-1.65, m, 1H, H-8, 1.10 (br s, 6H, H-13+H-14).

^{13}C NMR (100 MHz, $CDCl_3$): δ 208.7 (C-3), 175.5 (C-5), 135.3 (C-4), 74.9 (C-9), 69.0 (C-6), 57.9 (C-10), 53.2(C-1), 49.6 (C-7), 48.2 (C-11), 39.5 (C-2), 37.8 (C-8), 34.9 (C-12), 19.8 (C-13 or C-14), 11.5 (C-13 or C-14), 8.3 (C-15).

ν_{max} (ATR): 3369, 2923, 2851, 1686, 1642, 1254, 1088, 1058, 1024, 773 cm^{-1}.

HRMS (ESI+) *m/z*: calculated for $[M+H]^+$ $C_{15}H_{21}O_3^+$: 249.1485; found: 249.1483.

$[\alpha]_D^{20}$ = +39.3 (c 0.08, $CHCl_3$)

Note: The structure of compound **19** was confirmed by X-ray crystallography. Single crystals suitable for X-ray diffraction were obtained by slow evaporation of a $CDCl_3$/pentane solution at room temperature.

4 Computational details

Calculations were performed using the Gaussian 16 software package.[14] All structures were fully optimized without symmetry constraints at the DFT level using the B3LYP functional.[15–17] This functional has been previously employed to study the reduction of ketones by $NaBH_4$.[18,19] Grimme's D3 dispersion correction[20] was included as implemented in Gaussian 16. The 6-311++G(d,p) basis set[21–23] was applied to all atoms. Implicit solvent effects were incorporated using the SMD continuum solvation model for methanol.[24] Additionally, based on prior studies demonstrating their critical influence on transition state energies and geometries,[25–27] three explicit solvent molecules were included in the system under investigation. Each stationary point was characterized by frequency analysis, confirming the correct number of negative eigenvalues (zero for a local minimum and one for a transition state). All transition states were validated by intrinsic reaction coordinate (IRC) calculations, ensuring they connected the corresponding reactants and products. Final energy calculations were performed at the M06-2X level with the aug-cc-pVTZ basis set, incorporating both implicit and explicit solvation effect, using geometries optimized at the SMD(methanol)-B3LYP-D3/6-311++G(d,p) level.

To get accurate geometries and energies, the SCF convergence criterion was systematically tightened to 10^{-8} atomic units (au), and the force minimizations were carried out until the rms force became smaller that (at least) 1 x 10^{-5} au (using the "tight" optimisation keyword in Gaussian 16). The "UltraFine" grid (99 radial shells and 590 angular points per shell) was used throughout the calculations. Thermal corrections to free energy were calculated at 0°C (273.15 K) and the condensed-phase standard state (1 M)[26] using Grimme's quasi-rigid rotor-harmonic oscillator approximation,[28] as implemented in the Goodvibes program.[29] A lower frequency cut-off (50 cm^{-1}) was applied instead of the standard 100 cm^{-1}, in line with recent recommendations.[30] Vibrational scale factor of 1.0 has been used in all cases.

Geometry optimisation

To ensure that the choice of the selected computational level does not affect the conclusions, the transition states $\mathbf{TS_{ax}}$ and $\mathbf{TS_{eq}}$ were re-optimized using the M06-2X functional, while keeping all other optimisation parameters unchanged. The resulting structures were found to be equivalent to those obtained with B3LYP-D3. However, a stronger interaction was observed between BH_3 and the H-C-O moiety (shorter B···H and B···O bonds) (Figure S4).

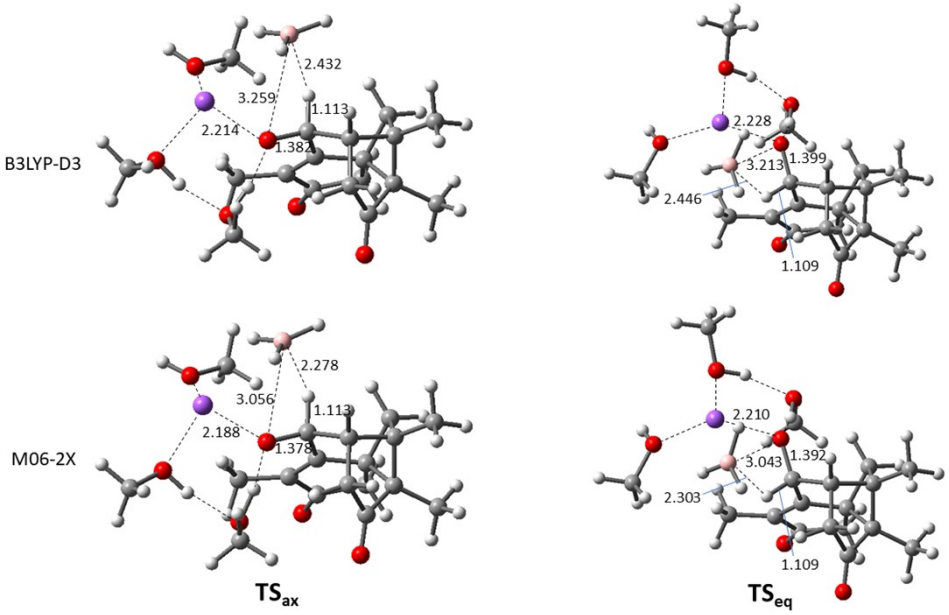

Figure S4. Optimised structures of $\mathbf{TS_{ax}}$ and $\mathbf{TS_{eq}}$ at the B3LYP-D3 and M06-2X level with the 6-311++G(d,p) basis set.

Final energy calculation

Furthermore, final energies were recalculated using different functionals, always with the aug-cc-pVTZ basis set, to assess the influence of the method on the energy gap between $\mathbf{TS_{ax}}$ and $\mathbf{TS_{eq}}$. The results (Table S11) indicate that, in all cases, $\mathbf{TS_{ax}}$ is either equal or lower in energy than $\mathbf{TS_{eq}}$, showing that the energy gap varies depending on the method employed. Specifically, the MP2 method yields the largest energy difference between the two transition states, whereas B3LYP-D3, B3LYP-D3BJ, and PBE result in a nearly negligible energy gap, contradicting the experimental findings. Other functionals tested, including M06-2X, which was selected for this study, provide intermediate results. Notably, the final outcome is independent of the method used for geometry optimisation.

Table S12. Computed relative Gibbs free energy (in kJ/mol) between TS_{ax} and TS_{eq} at various level of calculations.

Method[a]	$\Delta\Delta G^{\ddagger}$ [b]
B3LYP-D3	0.4
B3LYP-D3BJ	-0.3
M06-2X	6.6
M06-2X[c]	5.7
M06	7.4
M06-L	7.9
ωB97X-D	2.6
PBE0[d]	1.7
PBE[e]	-0.3
MP2[f]	16.8

[a] Final energy calculation at the SMD(methanol)-method/aug-cc-pVTZ level on the SMD(methanol)-B3LYP-D3/6-311++G(d,p) optimised geometry, unless otherwise noted ; [b] $\Delta\Delta G^{\ddagger} = \Delta G(TS_{eq}) - \Delta G(TS_{ax})$; [c] Final energy calculation on the SMD(methanol)-M06-2X/6-311++G(d,p) optimised geometry ; [d] PBE1PBE keyword in G16 ; [e] PBEPBE keyword in G16 ; [f] all electrons (MP2=Full option) MP2 calculation.

Reaction mechanism

Starting from the structure **15**, transition states corresponding to the reduction of each of the three ketones by $NaBH_4$ were investigated for both faces of the ketones. To facilitate the search for these transition states, which include microsolvation with three methanol molecules, we drew inspiration from the transition states reported by Tomeda et al. for 4-methylcyclohexanone.[3] Due to the lack of symmetry around each ketone group, two transition states, equivalent to those previously obtained for 4-methylcyclohexanone, are possible for each face of each ketone in **15**. This led us to identify and characterize 12 transition states. Among these, only 6 were retained—specifically, the lowest-energy transition state for each face of each ketone. These are illustrated in Figure S5.

For the two transition states involving the C-9 ketone, $\mathbf{TS^1_{C\text{-}9}}$ and $\mathbf{TS^2_{C\text{-}9}}$, the IRC calculations led to the separated reactants and the product of BH_3 addition to the oxygen atom of the reduced ketone, consistent with structures reported in prior studies, as illustrated in Figure S6A for $\mathbf{TS^1_{C\text{-}9}}$.[3,8] In other cases, however, the mechanism is more complex. Although the product type remains the same (formation of a O-BH_3 bond, but on a different oxygen atom), the pathway to the separated reactants involves a second, lower-energy transition state. This transition state corresponds to **24** in Figure S6B, which illustrates this pathway for $\mathbf{TS_{ax}}$. A detailed investigation of this specific reaction pathway, which features two transition states and was also obtained using the M06-2X functional, falls outside the scope of this work and will be presented in due course.

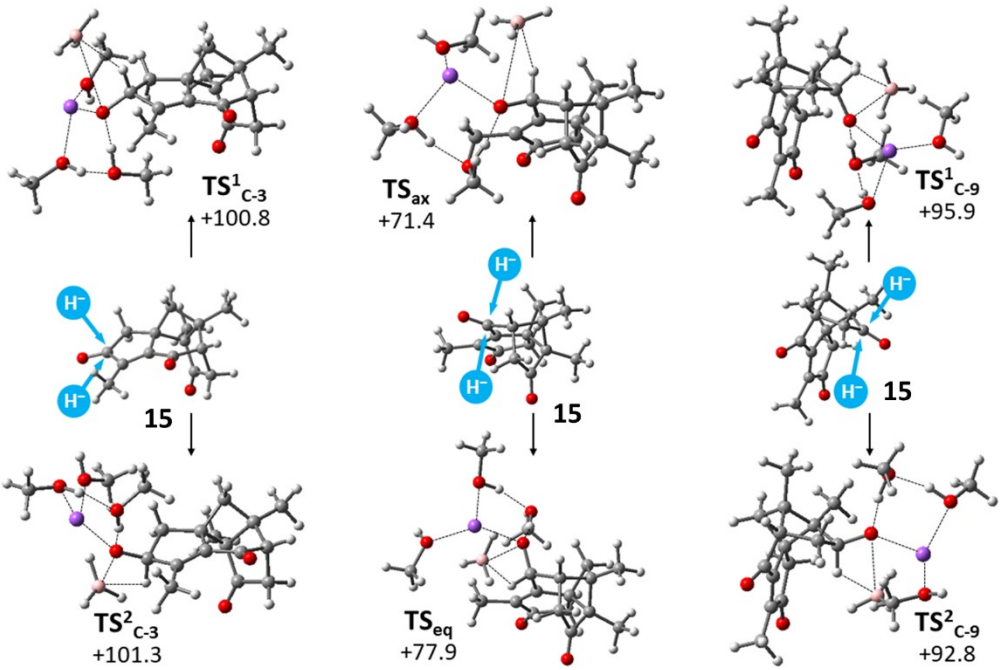

Figure S5. Optimised transition state structures for the reduction of **15** by $NaBH_4$ for the three different CO groups and their two faces. Relative free energies with respect to the separated fragments (**15** and $NaBH_4(MeOH)_3$) computed at the SMD(methanol)-M06-2X/aug-cc-pVTZ//SMD(methanol)-B3LYP-D3/6-311++G(d,p) level.

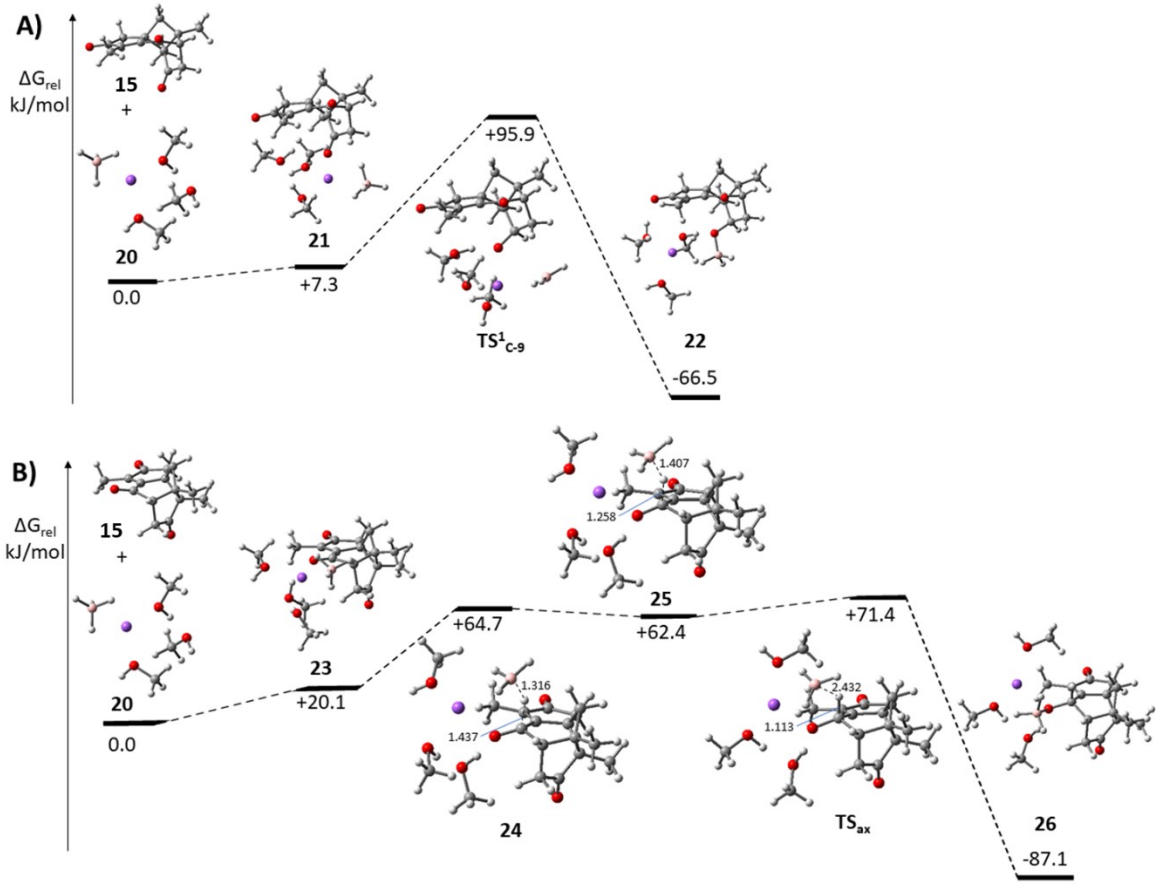

Figure S6. Reaction mechanism for the $NaBH_4$ reduction of **15**, including three explicit solvent molecules, computed at the SMD(methanol)-M06-2X/aug-cc-pVTZ//SMD(methanol)-B3LYP-D3/6-311++G(d,p) level through A) transition state $\mathbf{TS^1_{C\text{-}9}}$ and B) transition state $\mathbf{TS_{ax}}$.

Energies

Table S13. Absolute electronic energies and thermal corrections (in a.u.) for all molecules (B3LYP-D3 geometry optimisation).

	E SMD(methanol)-B3LYP-D3/6-311++G(d,p)	Thermal correction to Gibbs Free Energy[a]	E SMD(methanol)-M06-2X/aug-cc-pVTZ[b]
15	-807.157374	0.241721	-806.870487
20	-536.979277	0.156531	-536.767506
21	-1344.158147	0.418175	-1343.655134
$TS^1_{C\text{-}9}$	-1344.119938	0.421311	-1343.624537
22	-1344.188979	0.427403	-1343.692484
$TS^2_{C\text{-}9}$	-1344.119740	0.420094	-1343.624479
$TS^1_{C\text{-}3}$	-1344.117352	0.418608	-1343.619975
$TS^2_{C\text{-}3}$	-1344.117191	0.419077	-1343.620242
23	-1344.157829	0.420920	-1343.653019
24	-1344.135212	0.419611	-1343.634714
25	-1344.135795	0.420606	-1343.636580
TS_{ax}	-1344.128579	0.420707	-1343.633272
26	-1344.193260	0.428786	-1343.701687
TS_{eq}	-1344.129061	0.421326	-1343.631388

[a] Calculated at 273.15 K, a vibrational scale factor of 1.0 and the condensed-phase standard state (1 M) using Grimme's quasi-rigid rotor-harmonic oscillator approximation for low-frequency vibration (cut-off at 50 cm^{-1}). [b] Energies computed at the SMD(methanol)-B3LYP-D3/6-311++G(d,p) geometries.

Table S14. Absolute electronic energies and thermal corrections (in a.u.) for TS_{ax} and TS_{eq} (M06-2X geometry optimisation).

	E SMD(methanol)-M06-2X/ 6-311++G(d,p)	Thermal correction to Gibbs Free Energy[a]	E SMD(methanol)-M06-2X/aug-cc-pVTZ[b]
TS_{ax}	-1343.509730	0.429105	-1343.637048
TS_{eq}	-1343.507119	0.428409	-1343.634196

[a] Calculated at 273.15 K, a vibrational scale factor of 1.0 and the condensed-phase standard state (1 M) using Grimme's quasi-rigid rotor-harmonic oscillator approximation for low-frequency vibration (cut-off at 50 cm^{-1}). [b] Energies computed at the SMD(methanol)-M06-2X/6-311++G(d,p) geometries.

Table S15. Absolute electronic energies (in a.u.) of TS_{ax} and TS_{eq} computed at various level.

method	E(**TS_{ax}**)[a]	E(**TS_{eq}**)[a]
B3LYP-D3	-1344.238151	-1344.238628
B3LYP-D3BJ	-1344.286706	-1344.287459
M06-2X	-1343.633272	-1343.631388
M06	-1343.341918	-1343.339700
M06-L	-1343.955147	-1343.952767
ωB97X-D	-1343.788473	-1343.788110
PBE0	-1342.653377	-1342.653352
PBE	-1342.537050	-1342.537764
MP2	-1341.625723	-1341.619937

[a] Energies computed at the SMD(methanol)-method/aug-cc-pVTZ level at the SMD(methanol)-B3LYP-D3/6-311++G(d,p) geometries.

The Cartesian coordinates of the optimised structures are provided in an attached .xyz file.

5 X-Ray crystallographic data

A suitable crystal was selected (see the crystallisation method in the synthetic part) and mounted on a STOE STADIVARI diffractometer. The crystal was kept at 150 K during data collection. Using Olex2,[31] the structure was solved with the SHELXT[32] structure solution program using Intrinsic Phasing and refined with the SHELXL[33] refinement package using Least Squares minimisation.

Table S16. Crystal data and structure refinement for compound 1 (CCDC 2418571)

Identification code	CCDC 2418571
Empirical formula	$C_{15}H_{18}O_3$
Formula weight	246.29
Temperature/K	150
Crystal system	trigonal
Space group	$P3_2$
a/Å	7.6126(5)
b/Å	7.6126(5)
c/Å	18.9125(15)
α/°	90
β/°	90
γ/°	120
Volume/Å^3	949.17(15)
Z	3
ρ_{calc}g/cm^3	1.293
μ/mm^{-1}	0.089
F(000)	396.0
Crystal size/mm^3	? × ? × ?
Radiation	Mo Kα (λ = 0.71073)
2Θ range for data collection/°	6.18 to 58.316
Index ranges	-9 ≤ h ≤ 10, -9 ≤ k ≤ 10, -25 ≤ l ≤ 25
Reflections collected	16816
Independent reflections	3196 [R_{int} = 0.0320, R_{sigma} = 0.0414]
Data/restraints/parameters	3196/1/168
Goodness-of-fit on F^2	0.985
Final R indexes [I>=2σ (I)]	R_1 = 0.0335, wR_2 = 0.0718
Final R indexes [all data]	R_1 = 0.0406, wR_2 = 0.0727
Largest diff. peak/hole / e Å^{-3}	0.23/-0.20
Flack parameter	-0.5(4)

Table S17. Crystal data and structure refinement for compound 2 (CCDC 2419407)	
Identification code	CCDC 2419407
Empirical formula	$C_{15}H_{18}O_2$
Formula weight	230.29
Temperature/K	150
Crystal system	orthorhombic
Space group	$P2_12_12_1$
a/Å	9.7955(10)
b/Å	10.5156(16)
c/Å	12.1712(12)
α/°	90
β/°	90
γ/°	90
Volume/Å^3	1253.7(3)
Z	4
ρ_{calc}g/cm^3	1.220
μ/mm^{-1}	0.079
F(000)	496.0
Crystal size/mm^3	? × ? × ?
Radiation	Mo Kα (λ = 0.71073)
2Θ range for data collection/°	5.12 to 58.048
Index ranges	-13 ≤ h ≤ 12, -13 ≤ k ≤ 14, -16 ≤ l ≤ 16
Reflections collected	14022
Independent reflections	3108 [R_{int} = 0.0376, R_{sigma} = 0.0420]
Data/restraints/parameters	3108/0/157
Goodness-of-fit on F^2	0.969
Final R indexes [I>=2σ (I)]	R_1 = 0.0376, wR_2 = 0.0831
Final R indexes [all data]	R_1 = 0.0493, wR_2 = 0.0857
Largest diff. peak/hole / e Å^{-3}	0.17/-0.16
Flack parameter	-0.3(7)

Table S18. Crystal data and structure refinement for compound 3 (CCDC 2418579)	
Identification code	CCDC 2418579
Empirical formula	$C_{15}H_{18}O_2$
Formula weight	230.29
Temperature/K	150
Crystal system	monoclinic
Space group	$P2_1$
a/Å	9.4319(3)
b/Å	5.7056(2)
c/Å	23.0001(6)
α/°	90
β/°	95.478(2)
γ/°	90
Volume/Å^3	1232.09(7)
Z	4
ρ_{calc}g/cm^3	1.242
μ/mm^{-1}	0.081
F(000)	496.0
Crystal size/mm^3	? × ? × ?
Radiation	Mo Kα (λ = 0.71073)
2Θ range for data collection/°	4.338 to 58.452
Index ranges	-12 ≤ h ≤ 11, -7 ≤ k ≤ 7, -31 ≤ l ≤ 29
Reflections collected	21331
Independent reflections	6063 [R_{int} = 0.0186, R_{sigma} = 0.0210]
Data/restraints/parameters	6063/1/313
Goodness-of-fit on F^2	1.067
Final R indexes [I>=2σ (I)]	R_1 = 0.0350, wR_2 = 0.0963
Final R indexes [all data]	R_1 = 0.0397, wR_2 = 0.0981
Largest diff. peak/hole / e Å^{-3}	0.24/-0.14
Flack parameter	-0.1(3)

Table S19. Crystal data and structure refinement for compound 9b (CCDC 2419409)	
Identification code	CCDC 2419409
Empirical formula	$C_{21}H_{34}O_2Si$
Formula weight	346.57
Temperature/K	150
Crystal system	triclinic
Space group	P1
a/Å	7.4300(6)
b/Å	10.0076(8)
c/Å	14.9814(12)
α/°	96.641(6)
β/°	101.339(6)
γ/°	99.843(7)
Volume/Å^3	1063.22(15)
Z	2
ρ_{calc}g/cm^3	1.083
μ/mm^{-1}	0.120
F(000)	380.0
Crystal size/mm^3	? × ? × ?
Radiation	Mo Kα (λ = 0.71073)
2Θ range for data collection/°	4.662 to 50.048
Index ranges	-8 ≤ h ≤ 8, -11 ≤ k ≤ 11, -17 ≤ l ≤ 15
Reflections collected	8759
Independent reflections	5325 [R_{int} = 0.0649, R_{sigma} = 0.0786]
Data/restraints/parameters	5325/33/451
Goodness-of-fit on F^2	1.046
Final R indexes [I>=2σ (I)]	R_1 = 0.0946, wR_2 = 0.2532
Final R indexes [all data]	R_1 = 0.1213, wR_2 = 0.2739
Largest diff. peak/hole / e Å^{-3}	0.82/-0.70
Flack parameter	0.1(3)

Table S20. Crystal data and structure refinement for Compound 13 (CCDC 2419408)	
Identification code	CCDC 2419408
Empirical formula	$C_{15}H_{18}O_2$
Formula weight	230.29
Temperature/K	150
Crystal system	orthorhombic
Space group	$P2_12_12$
a/Å	17.7579(18)
b/Å	19.141(3)
c/Å	7.3717(8)
α/°	90
β/°	90
γ/°	90
Volume/Å^3	2505.6(5)
Z	8
ρ_{calc}g/cm^3	1.221
μ/mm^{-1}	0.079
F(000)	992.0
Crystal size/mm^3	? × ? × ?
Radiation	Mo Kα (λ = 0.71073)
2Θ range for data collection/°	4.588 to 50.048
Index ranges	-21 ≤ h ≤ 21, -22 ≤ k ≤ 21, -8 ≤ l ≤ 8
Reflections collected	10888
Independent reflections	4053 [R_{int} = 0.1266, R_{sigma} = 0.1510]
Data/restraints/parameters	4053/0/313
Goodness-of-fit on F^2	0.900
Final R indexes [I>=2σ (I)]	R_1 = 0.0810, wR_2 = 0.1864
Final R indexes [all data]	R_1 = 0.1761, wR_2 = 0.2285
Largest diff. peak/hole / e Å^{-3}	0.25/-0.34
Flack parameter	-2.7(10)

Table S21. Crystal data and structure refinement for compound 14 (CCDC 2428644)	
Identification code	JP472-2-F1
Empirical formula	$C_{15}H_{16}O_3$
Formula weight	244.28
Temperature/K	150
Crystal system	orthorhombic
Space group	$P2_12_12_1$
a/Å	8.8918(3)
b/Å	10.0340(4)
c/Å	13.7443(6)
α/°	90
β/°	90
γ/°	90
Volume/Å^3	1226.27(8)
Z	4
ρ_{calc}g/cm^3	1.323
μ/mm^{-1}	0.091
F(000)	520.0
Crystal size/mm^3	? × ? × ?
Radiation	Mo Kα (λ = 0.71073)
2Θ range for data collection/°	5.026 to 58.088
Index ranges	-11 ≤ h ≤ 12, -13 ≤ k ≤ 13, -18 ≤ l ≤ 18
Reflections collected	13303
Independent reflections	3002 [R_{int} = 0.0194, R_{sigma} = 0.0168]
Data/restraints/parameters	3002/0/167
Goodness-of-fit on F^2	1.095
Final R indexes [I>=2σ (I)]	R_1 = 0.0355, wR_2 = 0.0976
Final R indexes [all data]	R_1 = 0.0388, wR_2 = 0.0988
Largest diff. peak/hole / e Å^{-3}	0.28/-0.16
Flack parameter	0.5(12)

Table S22. Crystal data and structure refinement for compound 15 (CCDC 2418568)	
Identification code	CCDC 2418568
Empirical formula	$C_{15}H_{16}O_3$
Formula weight	244.28
Temperature/K	220
Crystal system	monoclinic
Space group	C2
a/Å	22.8543(11)
b/Å	7.3211(3)
c/Å	19.0970(10)
α/°	90
β/°	126.949(3)
γ/°	90
Volume/Å^3	2553.6(2)
Z	8
ρ_{calc}g/cm^3	1.271
μ/mm^{-1}	0.088
F(000)	1040.0
Crystal size/mm^3	? × ? × ?
Radiation	Mo Kα (λ = 0.71073)
2Θ range for data collection/°	4.446 to 58.516
Index ranges	-30 ≤ h ≤ 30, -9 ≤ k ≤ 9, -24 ≤ l ≤ 25
Reflections collected	22701
Independent reflections	6166 [R_{int} = 0.0212, R_{sigma} = 0.0283]
Data/restraints/parameters	6166/1/331
Goodness-of-fit on F^2	0.988
Final R indexes [I>=2σ (I)]	R_1 = 0.0357, wR_2 = 0.0858
Final R indexes [all data]	R_1 = 0.0450, wR_2 = 0.0882
Largest diff. peak/hole / e Å^{-3}	0.20/-0.16
Flack parameter	0.4(3)

Table S23. Crystal data and structure refinement for compound 19 (CCDC 2423044)	
Identification code	CCDC 2423044
Empirical formula	$C_{15}H_{20}O_3$
Formula weight	248.31
Temperature/K	150
Crystal system	monoclinic
Space group	$P2_1$
a/Å	7.2282(8)
b/Å	14.1294(13)
c/Å	13.1197(16)
α/°	90
β/°	90.972(9)
γ/°	90
Volume/Å^3	1339.7(3)
Z	4
ρ_{calc}g/cm^3	1.231
μ/mm^{-1}	0.084
F(000)	536.0
Crystal size/mm^3	? × ? × ?
Radiation	Mo Kα (λ = 0.71073)
2Θ range for data collection/°	5.636 to 50.052
Index ranges	-8 ≤ h ≤ 8, -16 ≤ k ≤ 16, -15 ≤ l ≤ 15
Reflections collected	8893
Independent reflections	4410 [R_{int} = 0.1143, R_{sigma} = 0.1038]
Data/restraints/parameters	4410/811/335
Goodness-of-fit on F^2	1.169
Final R indexes [I>=2σ (I)]	R_1 = 0.1276, wR_2 = 0.3007
Final R indexes [all data]	R_1 = 0.1498, wR_2 = 0.3180
Largest diff. peak/hole / e Å^{-3}	0.78/-0.65
Flack parameter	5.4(10)

6 Copies of spectra

Compound S1

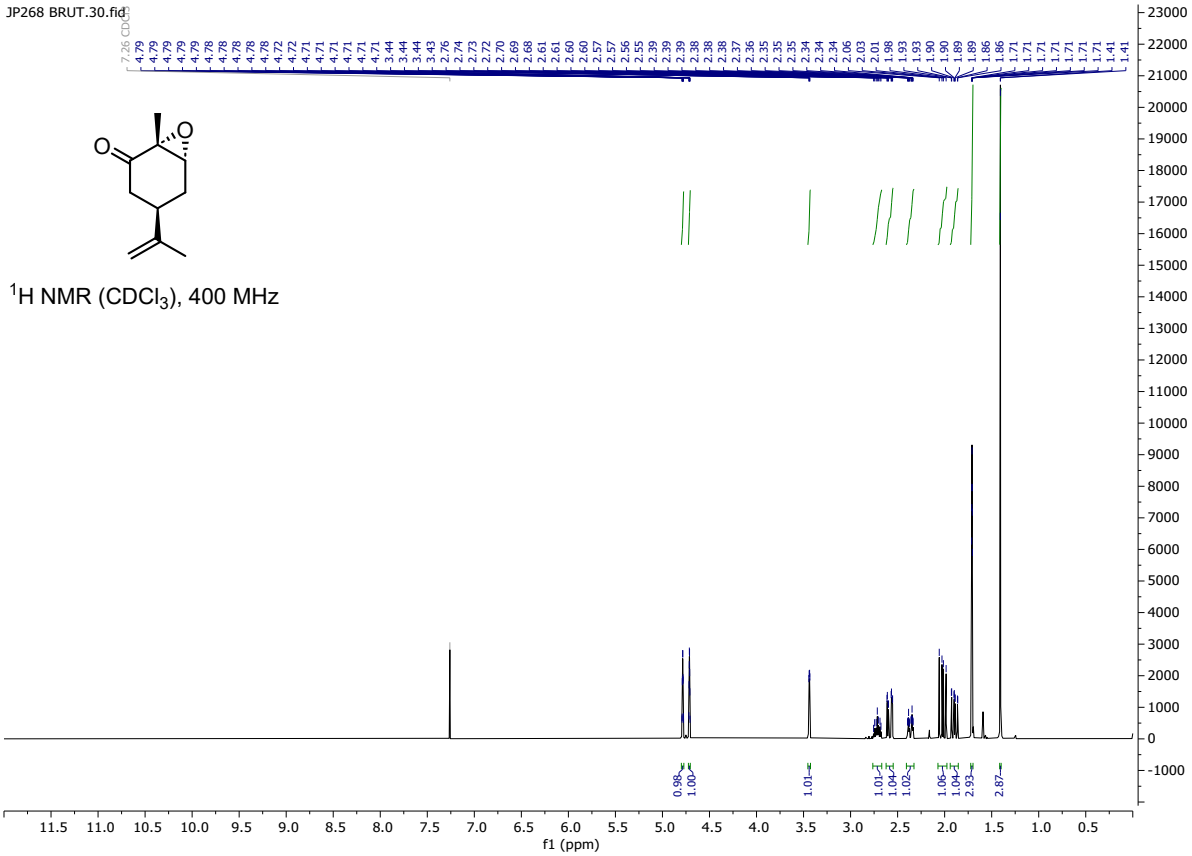

^{1}H NMR ($CDCl_3$), 400 MHz

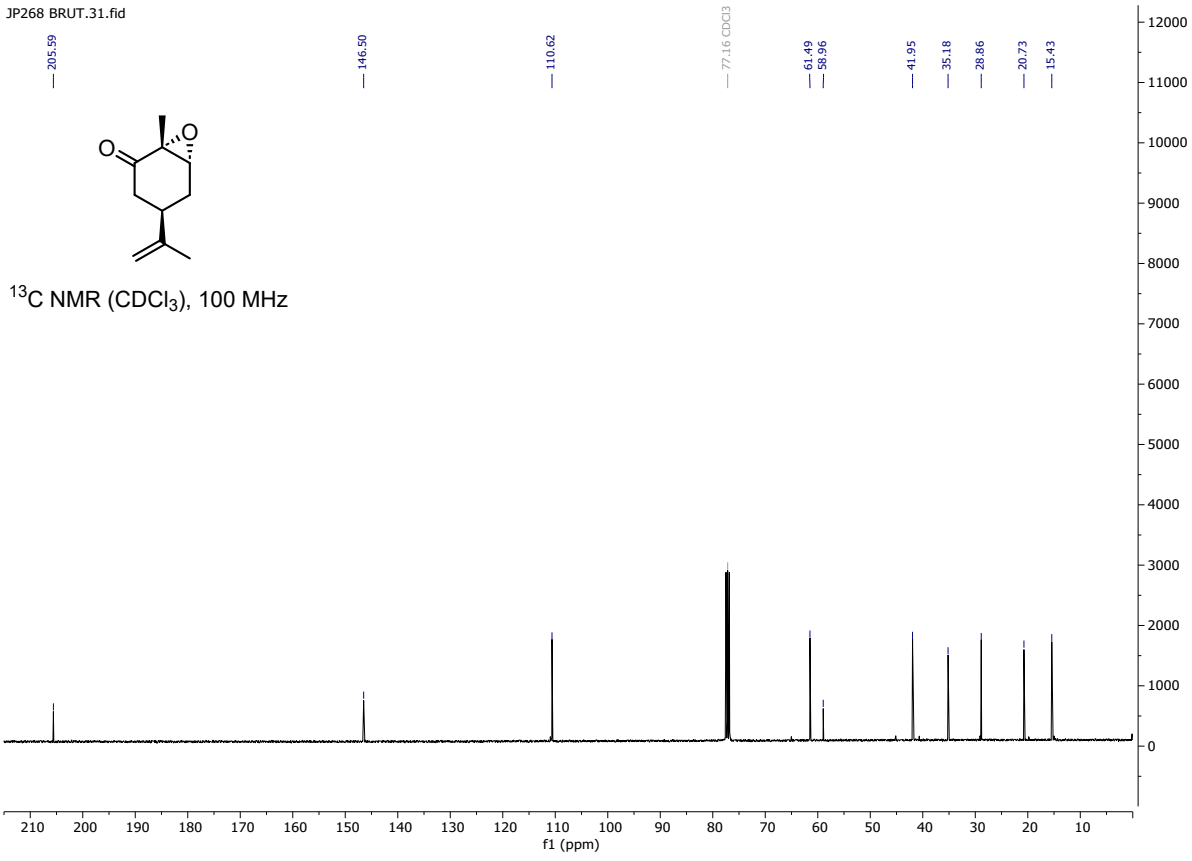

^{13}C NMR ($CDCl_3$), 100 MHz

Compound 5

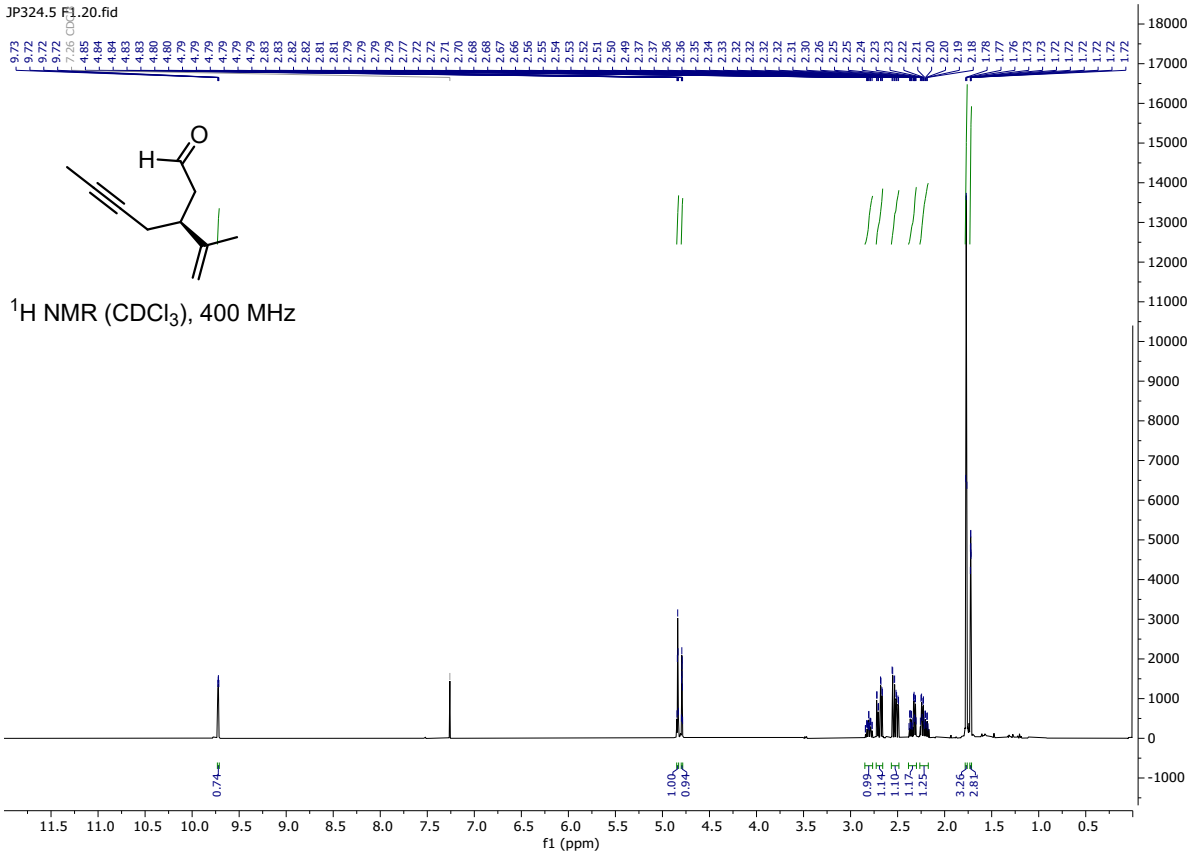

^{1}H NMR ($CDCl_3$), 400 MHz

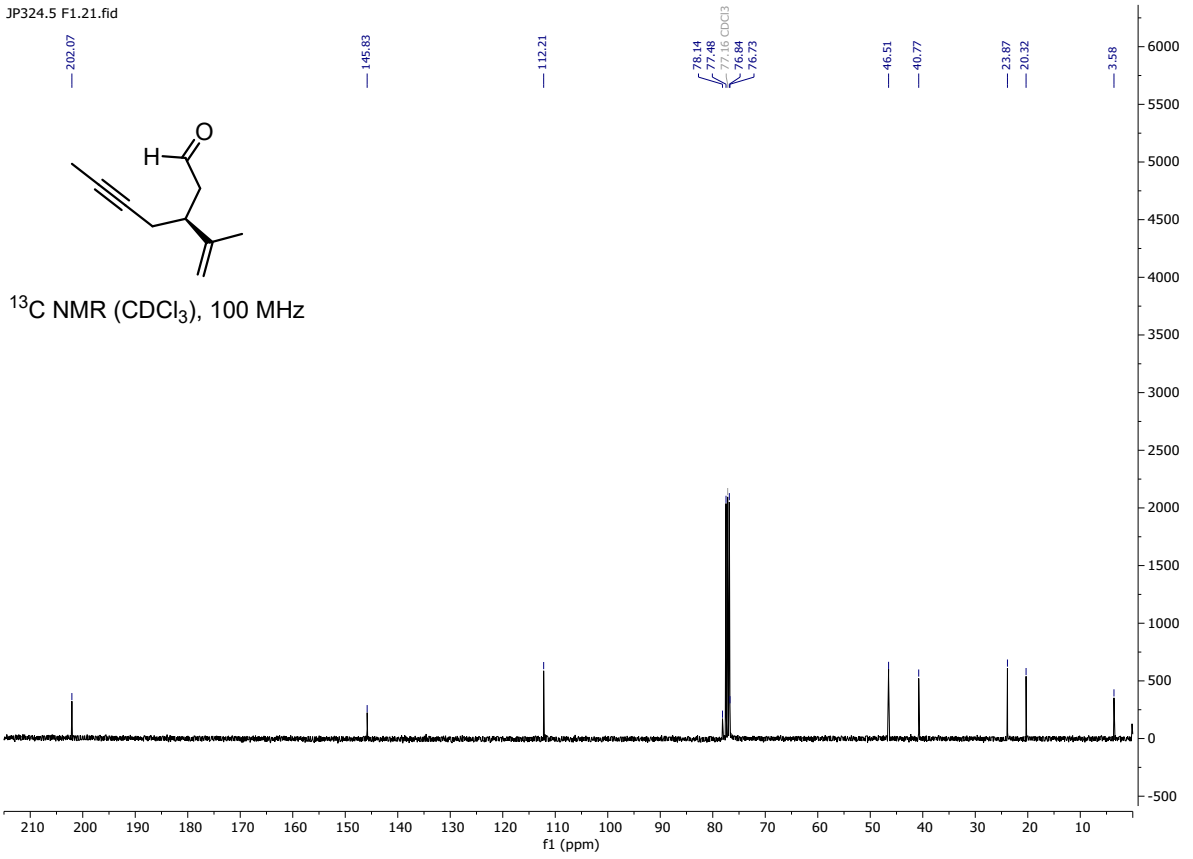

^{13}C NMR ($CDCl_3$), 100 MHz

Compound 7a

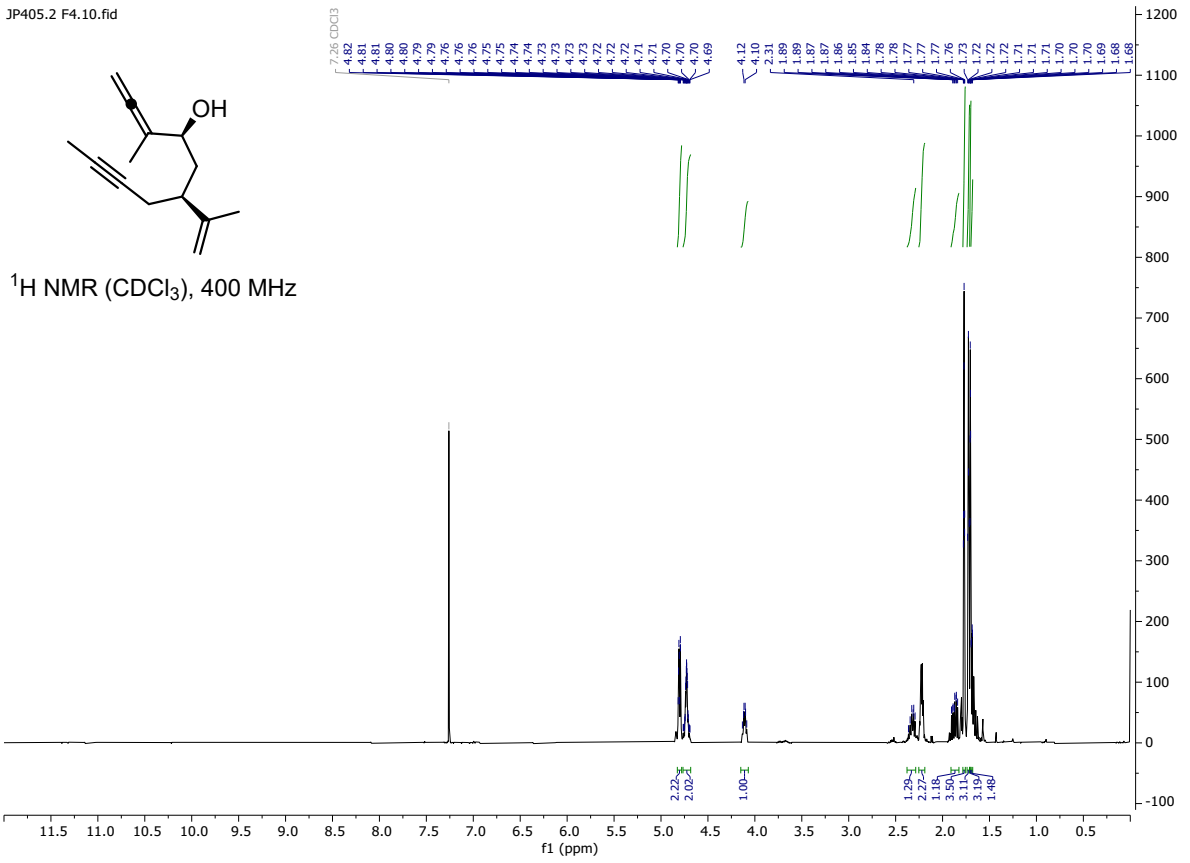

^{1}H NMR ($CDCl_3$), 400 MHz

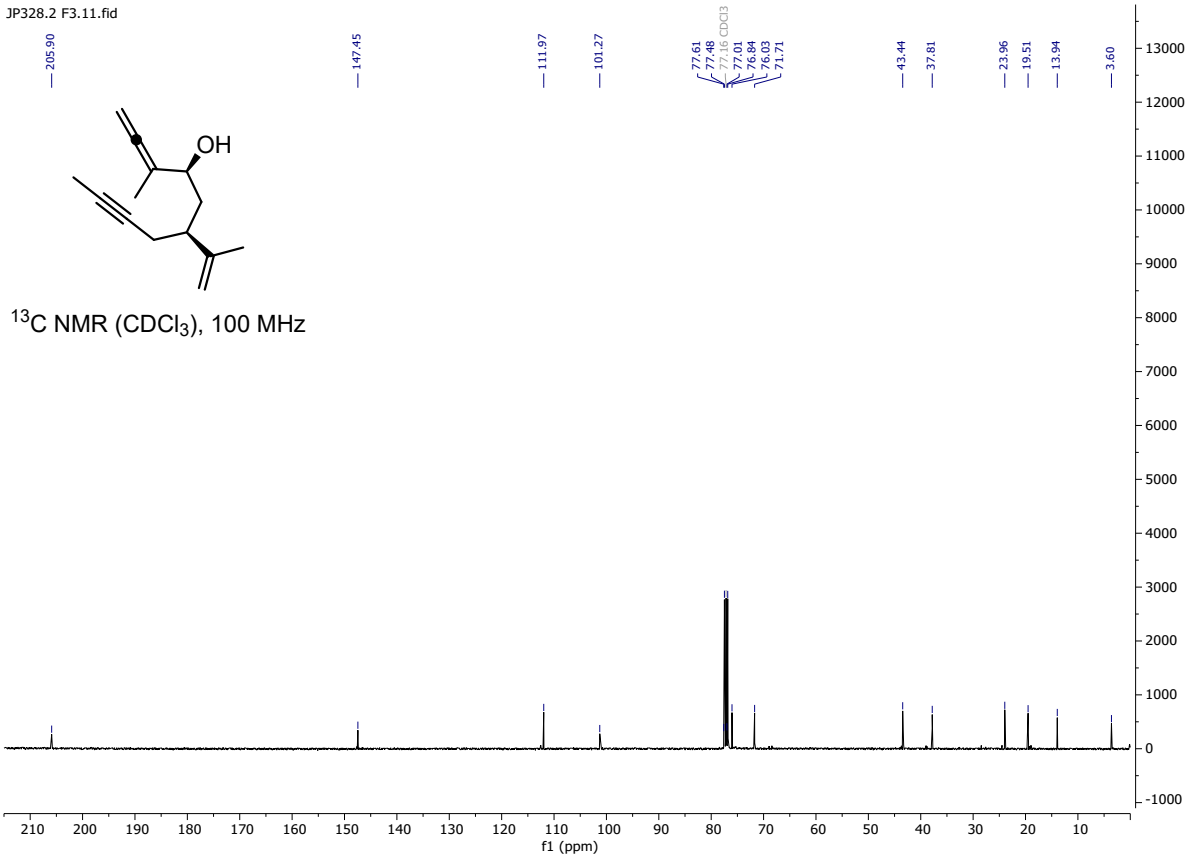

^{13}C NMR ($CDCl_3$), 100 MHz

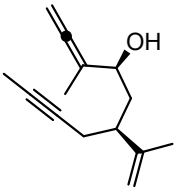

JP328-2-F3

m/z mesured	Ion formula	Theoretical m/z	Error (ppm)	Score
205.1581	$C_{14}H_{21}O^+$	205.1587	3.1	100

Analysed on Sept 5th 2024

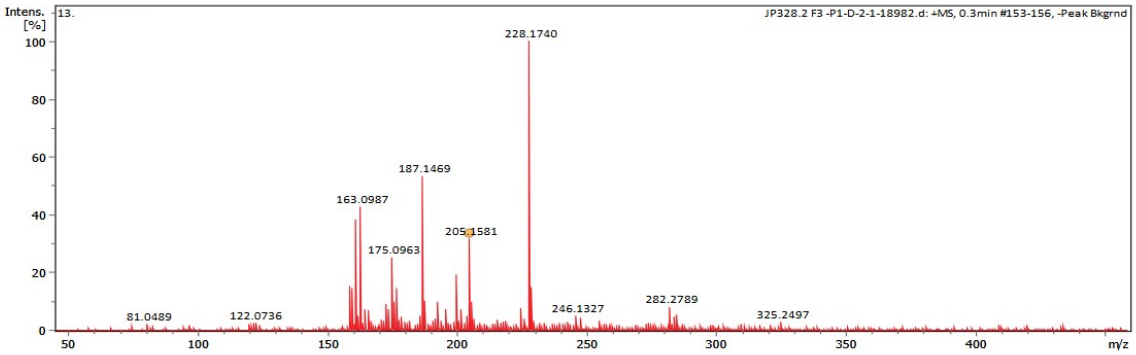

Mass spectrometry experiments was performed on a tims-TOF mass spectrometer (Bruker) in Laboratoire de Chimie Moléculaire (Ecole polytechnique, CNRS, Palaiseau, France). Electrospray source has been used in positive mode. Samples was prepared in acetonitrile with 0.1% of formic acid, introduced at a 5 µL/min flow rate into the interface of the instrument. Capillary and end plate voltages were set at 4.5 kV and 0.7 kV . Nitrogen was used as the nebulizer and drying gas at 2.5 bar and 3 L/min, respectively, with a drying temperature of 180°C. Tuning mix (Agilent) was used for calibration. The elemental compositions of all ions were determined with the instrument software Data Analysis, the precision of mass measurement was less than 3 ppm.

Compound 7b

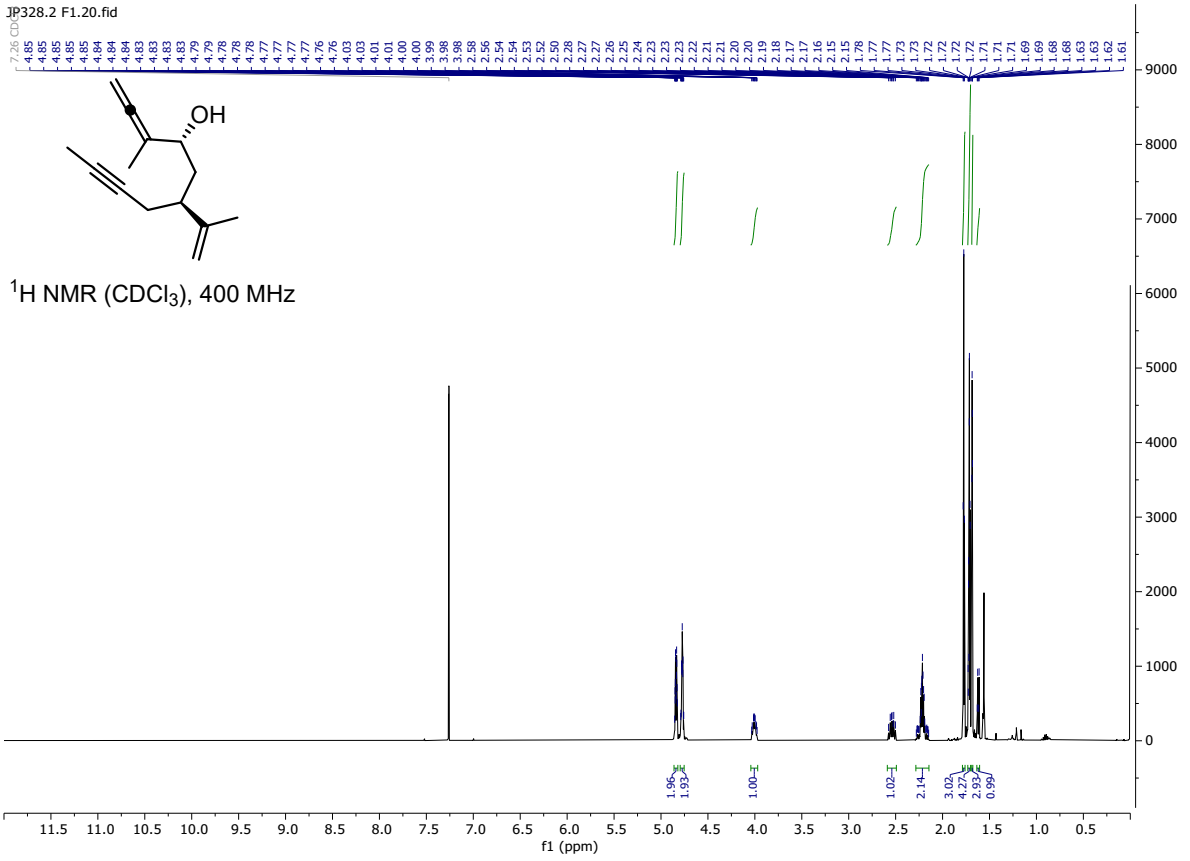

^{1}H NMR ($CDCl_3$), 400 MHz

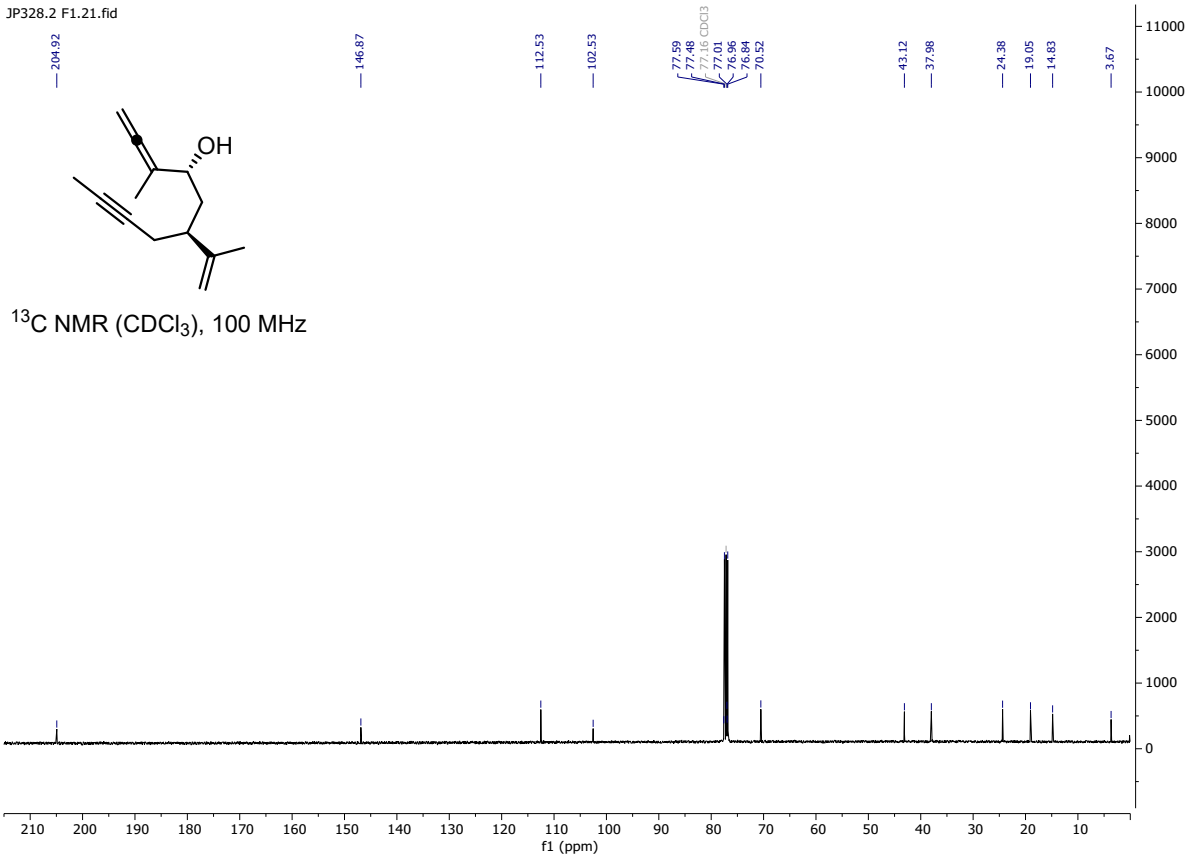

^{13}C NMR ($CDCl_3$), 100 MHz

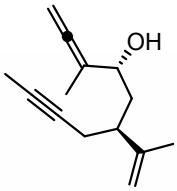

JP328-2-F1

m/z mesured	Ion formula	Theoretical m/z	Error (ppm)	Score
205.158	$C_{14}H_{21}O^+$	205.1587	3.3	100

Analysed on Sept 5th 2024

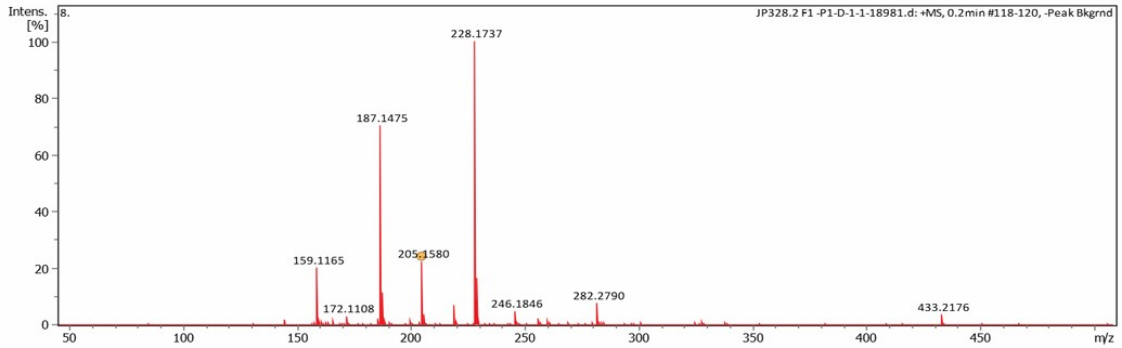

Mass spectrometry experiments was performed on a tims-TOF mass spectrometer (Bruker) in Laboratoire de Chimie Moléculaire (Ecole polytechnique, CNRS, Palaiseau, France). Electrospray source has been used in positive mode. Samples was prepared in acetonitrile with 0.1% of formic acid, introduced at a 5 µL/min flow rate into the interface of the instrument. Capillary and end plate voltages were set at 4.5 kV and 0.7 kV . Nitrogen was used as the nebulizer and drying gas at 2.5 bar and 3 L/min, respectively, with a drying temperature of 180°C. Tuning mix (Agilent) was used for calibration. The elemental compositions of all ions were determined with the instrument software Data Analysis, the precision of mass measurement was less than 3 ppm.

Compound 8a

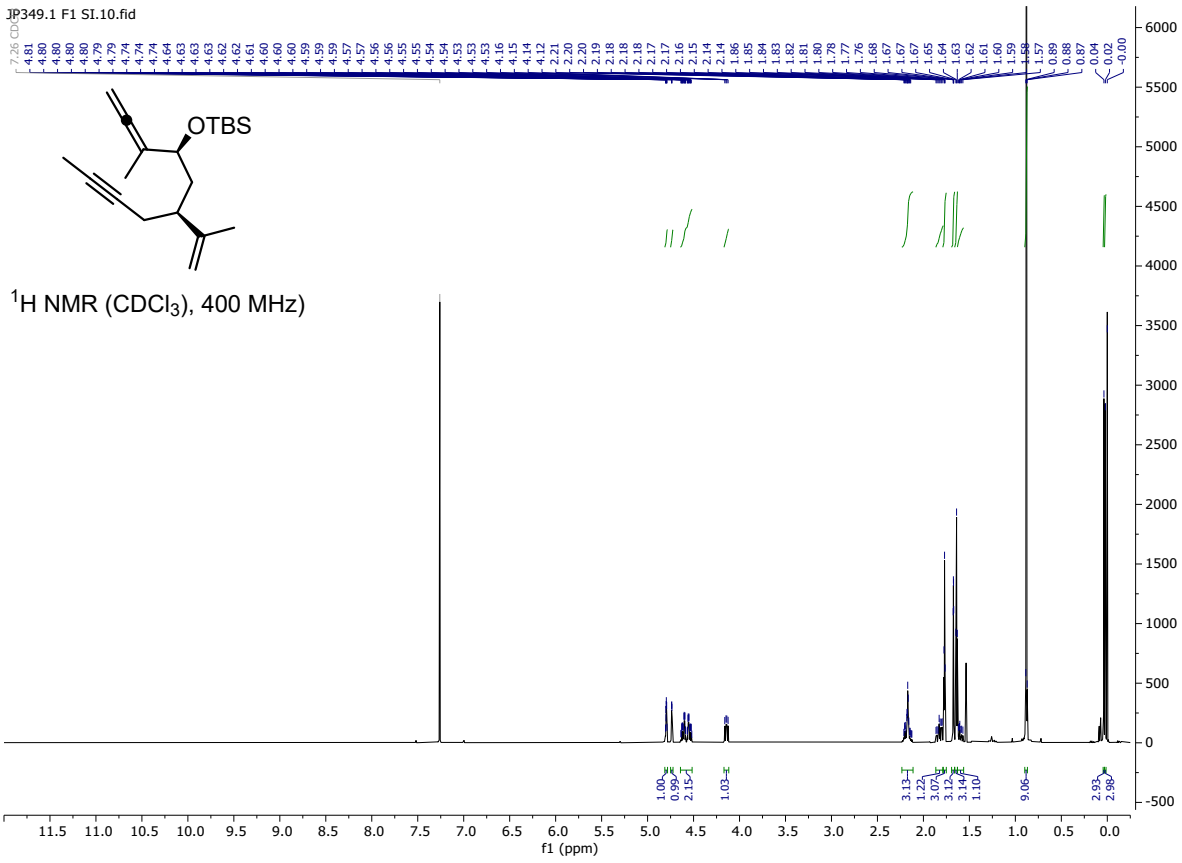

^{1}H NMR ($CDCl_3$), 400 MHz)

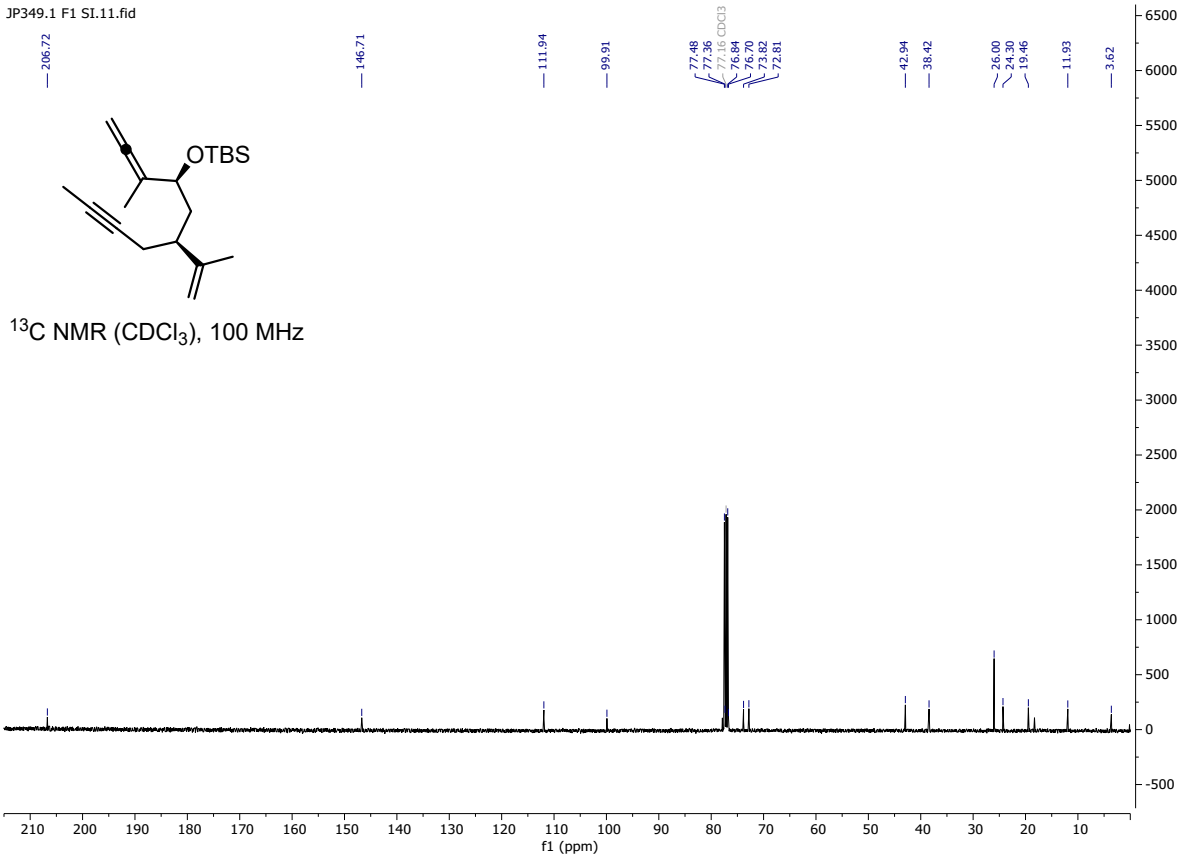

^{13}C NMR ($CDCl_3$), 100 MHz

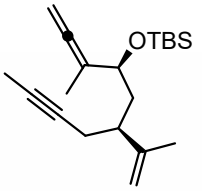

JP3349.1 F1

m/z mesured	Ion formula	Theoretical m/z	Error (ppm)	Score
319.2452	$C_{20}H_{35}OSi^+$	319.2452	-0.2	100

Analysed on 13/12/2024

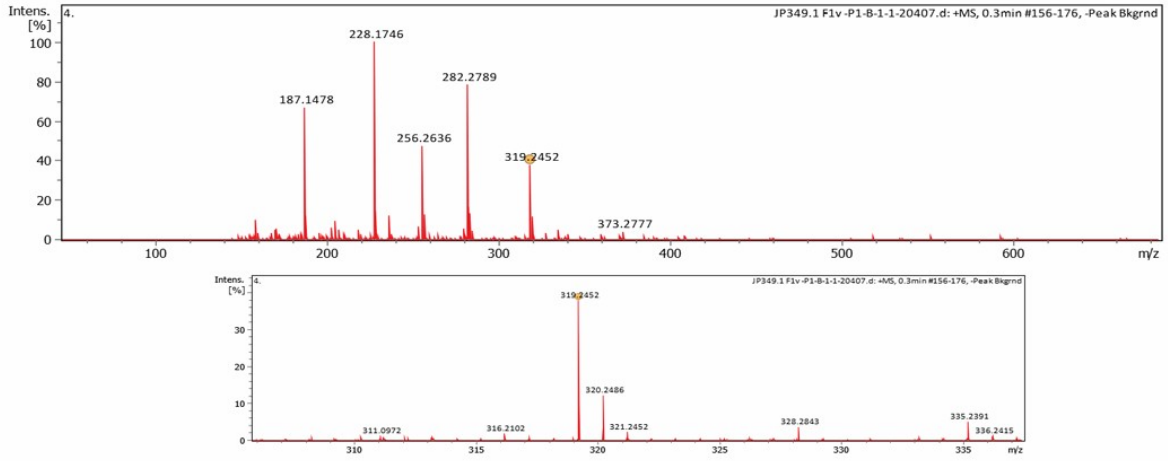

Mass spectrometry experiments was performed on a tims-TOF mass spectrometer (Bruker) in Laboratoire de Chimie Moléculaire (Ecole polytechnique, CNRS, Palaiseau, France). Electrospray source has been used in positive mode. Samples was prepared in acetonitrile with 0.1% of formic acid, introduced at a 5 µL/min flow rate into the interface of the instrument. Capillary and end plate voltages were set at 4.5 kV and 0.7 kV . Nitrogen was used as the nebulizer and drying gas at 2.5 bar and 3 L/min, respectively, with a drying temperature of 180°C. Tuning mix (Agilent) was used for calibration. The elemental compositions of all ions were determined with the instrument software Data Analysis, the precision of mass measurement was less than 3 ppm.

Compound 8b

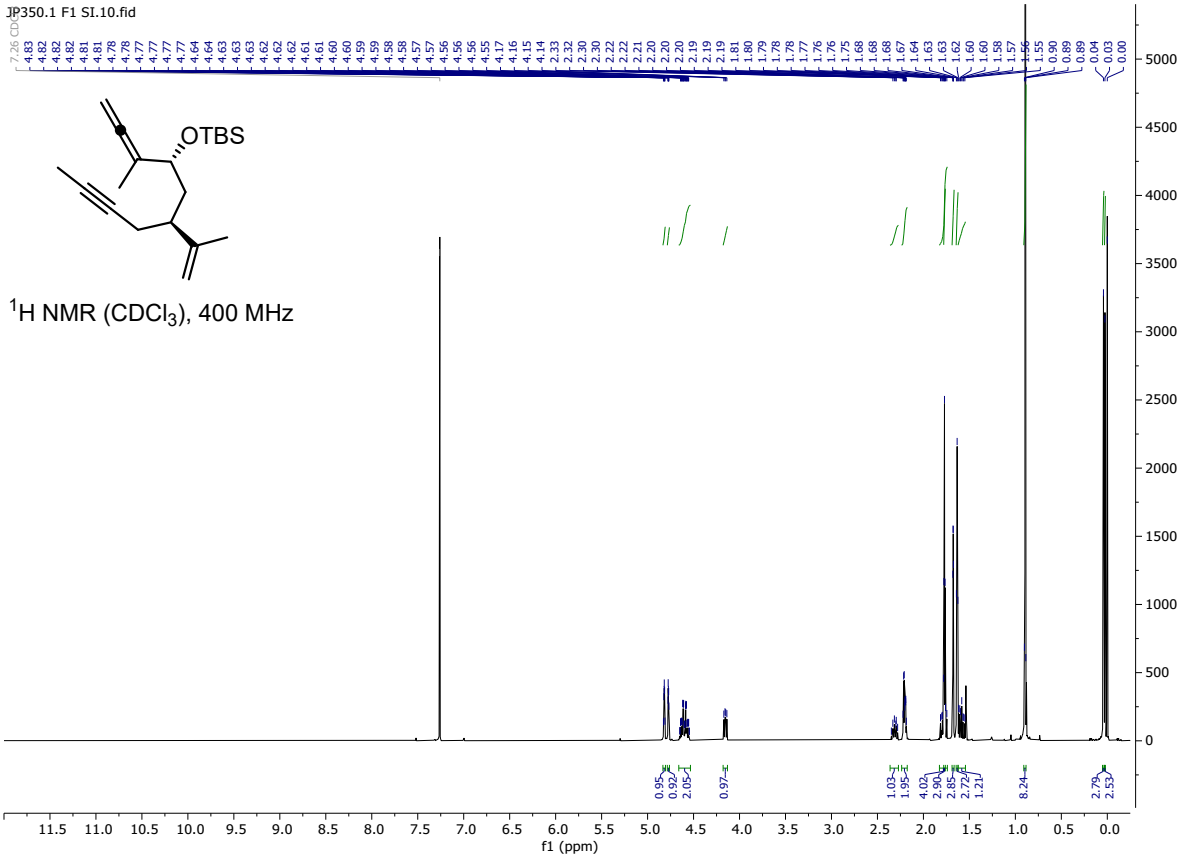

^{1}H NMR ($CDCl_3$), 400 MHz

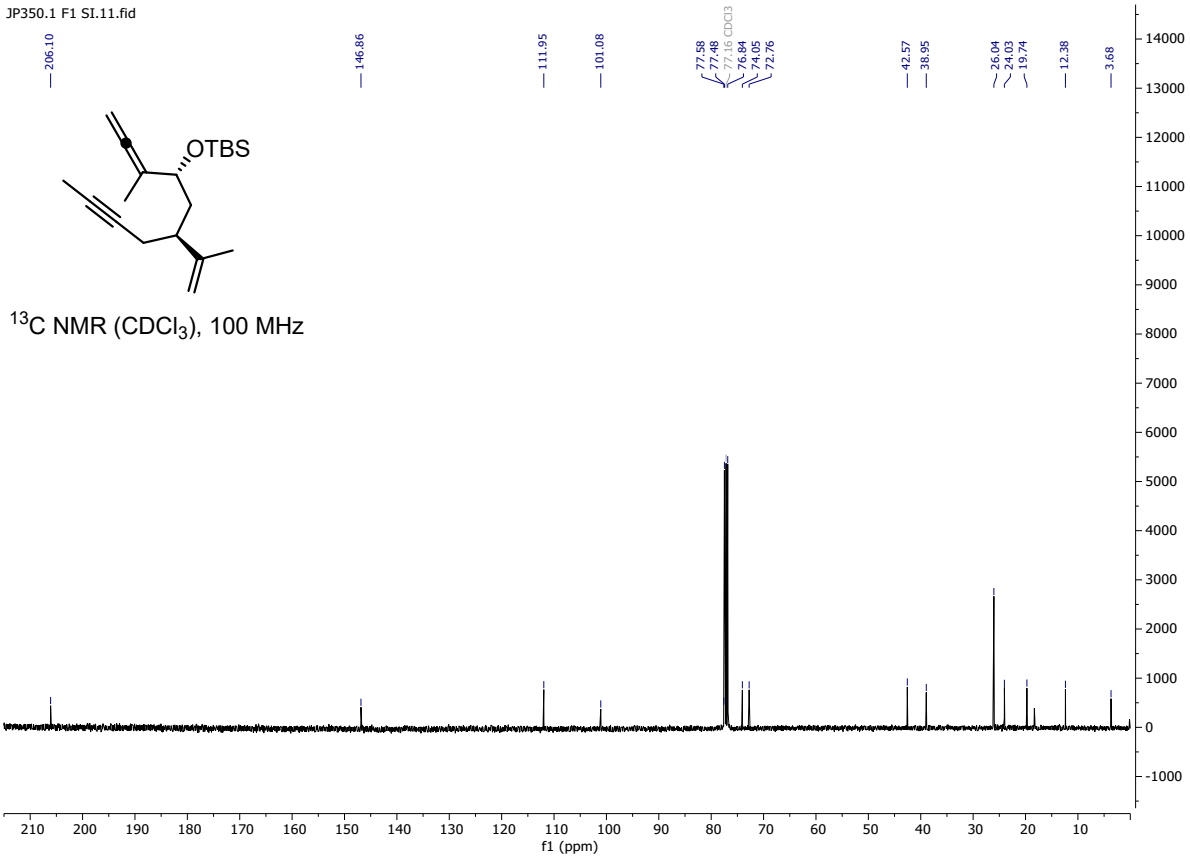

^{13}C NMR ($CDCl_3$), 100 MHz

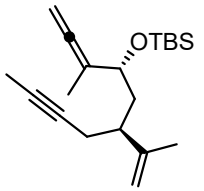

JP196-1F1

Analysed on March1st, 2024

m/z mesured	Ion formula	Theoretical m/z	Error (ppm)	Score
319.2443	$C_{20}H_{35}OSi^+$	319.2452	2.9	100

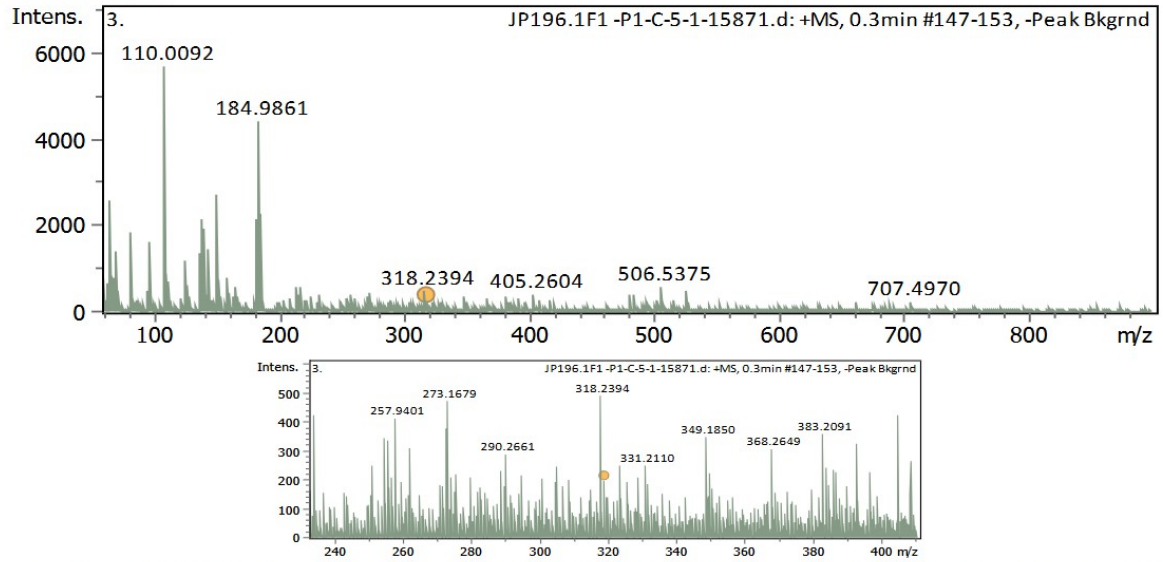

Mass spectrometry experiments was performed on a tims-TOF mass spectrometer (Bruker) in Laboratoire de Chimie Moléculaire (Ecole polytechnique, CNRS, Palaiseau, France). Electrospray source has been used in positive mode. Samples was prepared in acetonitrile with 0.1% of formic acid, introduced at a 5 µL/min flow rate into the interface of the instrument. Capillary and end plate voltages were set at 4.5 kV and 0.7 kV . Nitrogen was used as the nebulizer and drying gas at 2.5 bar and 3 L/min, respectively, with a drying temperature of 180°C. Tuning mix (Agilent) was used for calibration. The elemental compositions of all ions were determined with the instrument software Data Analysis, the precision of mass measurement was less than 3 ppm.

Compound 9a

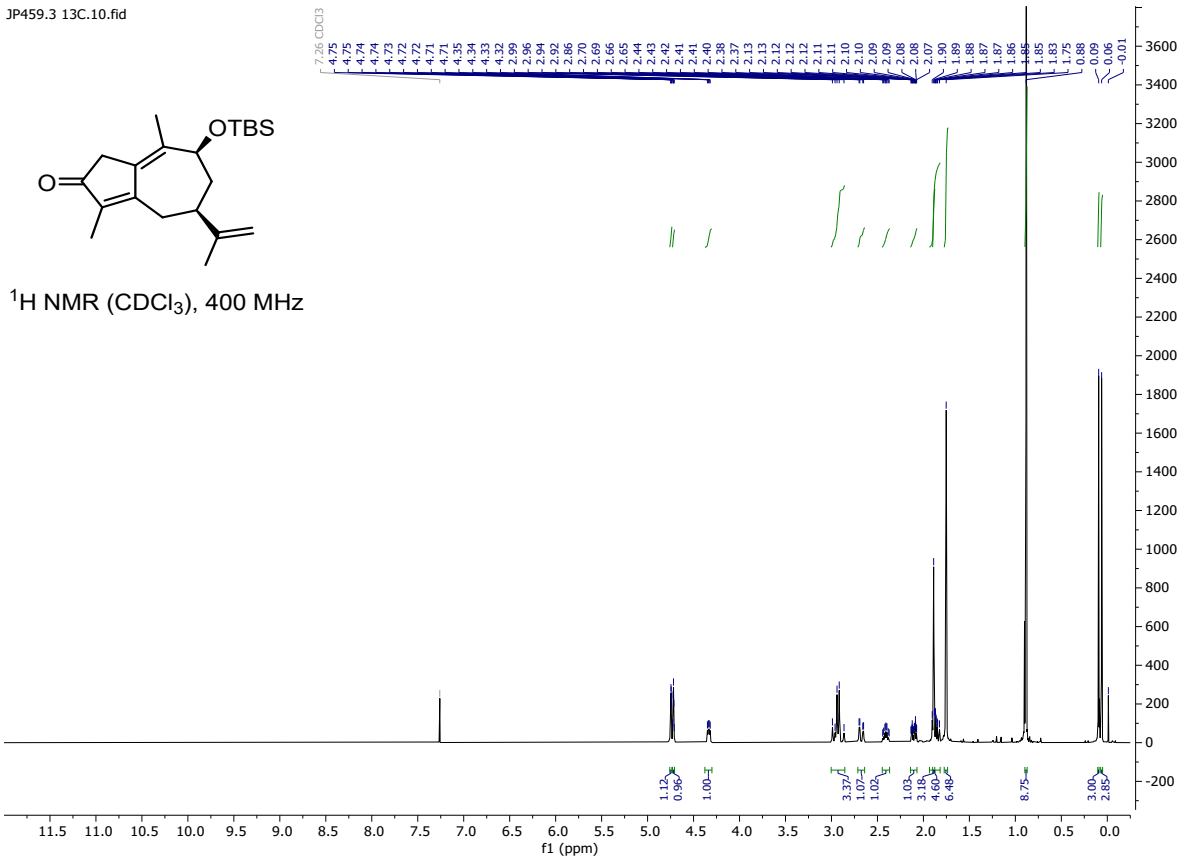

^{1}H NMR ($CDCl_3$), 400 MHz

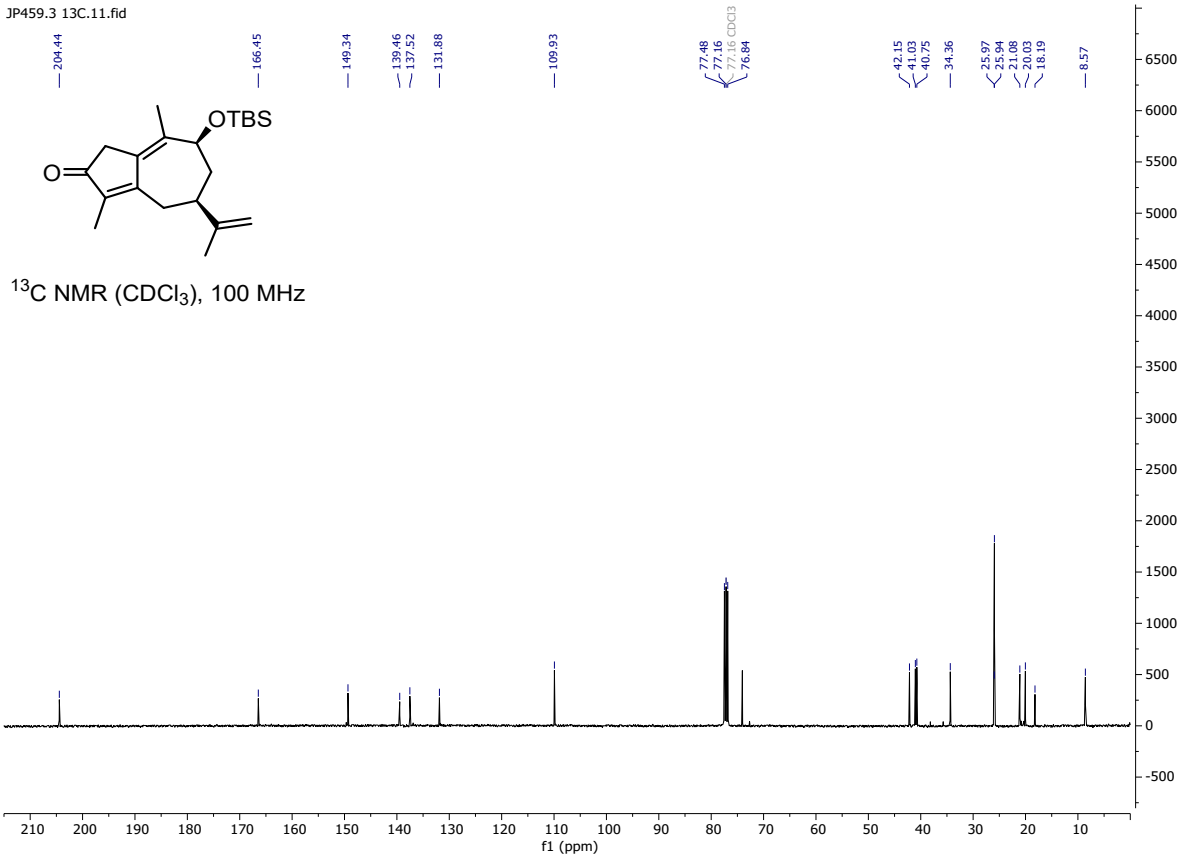

^{13}C NMR ($CDCl_3$), 100 MHz

JP453.1 F1

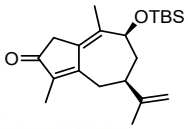

m/z mesured	Ion formula	Theoretical m/z	Error (ppm)	Score
347.2392	$C_{21}H_{35}O_2Si^+$	347.2401	2.6	100

Analysed on 26/02/2025

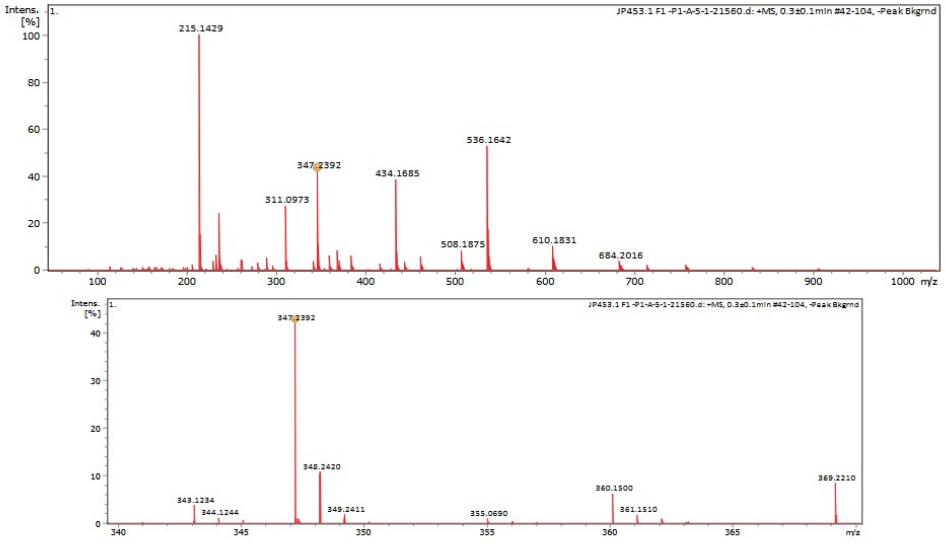

Mass spectrometry experiments was performed on a timsTOF mass spectrometer (Bruker) in Laboratoire de Chimie Moléculaire (Ecole polytechnique, CNRS, Palaiseau, France). Electrospray source has been used in positive mode. Samples was prepared in acetonitri acid, introduced at a 5 µL/min flow rate into the interface of the instrument. Capillary and end plate voltages were set at 4.5 kV and 0.7 kV . Nitrogen was used as the nebulizer and drying gas at 2.5 bar and 3 L/min, respectively, with a drying temperature of 180°C. Tu used for calibration. The elemental compositions of all ions were determined with the instrument software Data Analysis, the precision of mass measurement was less than 3 ppm.

Compound 9b

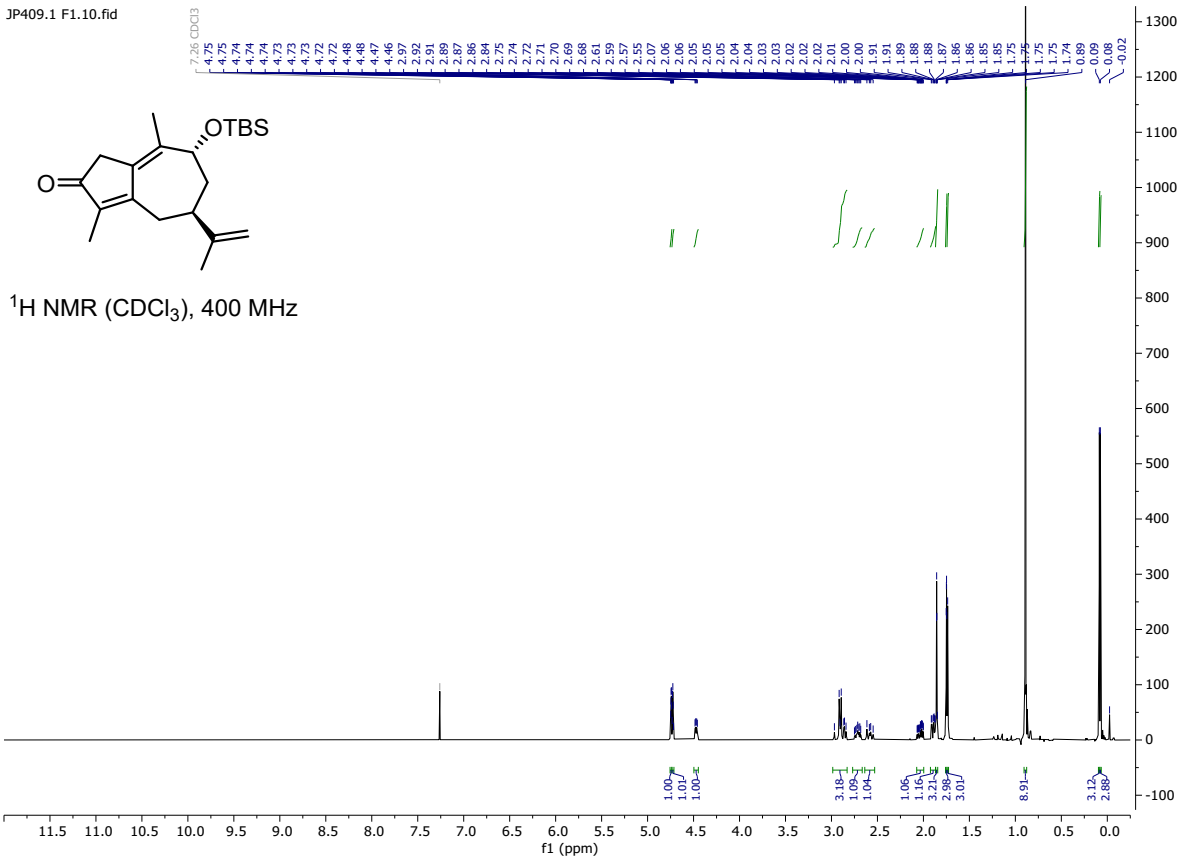

^{1}H NMR ($CDCl_3$), 400 MHz

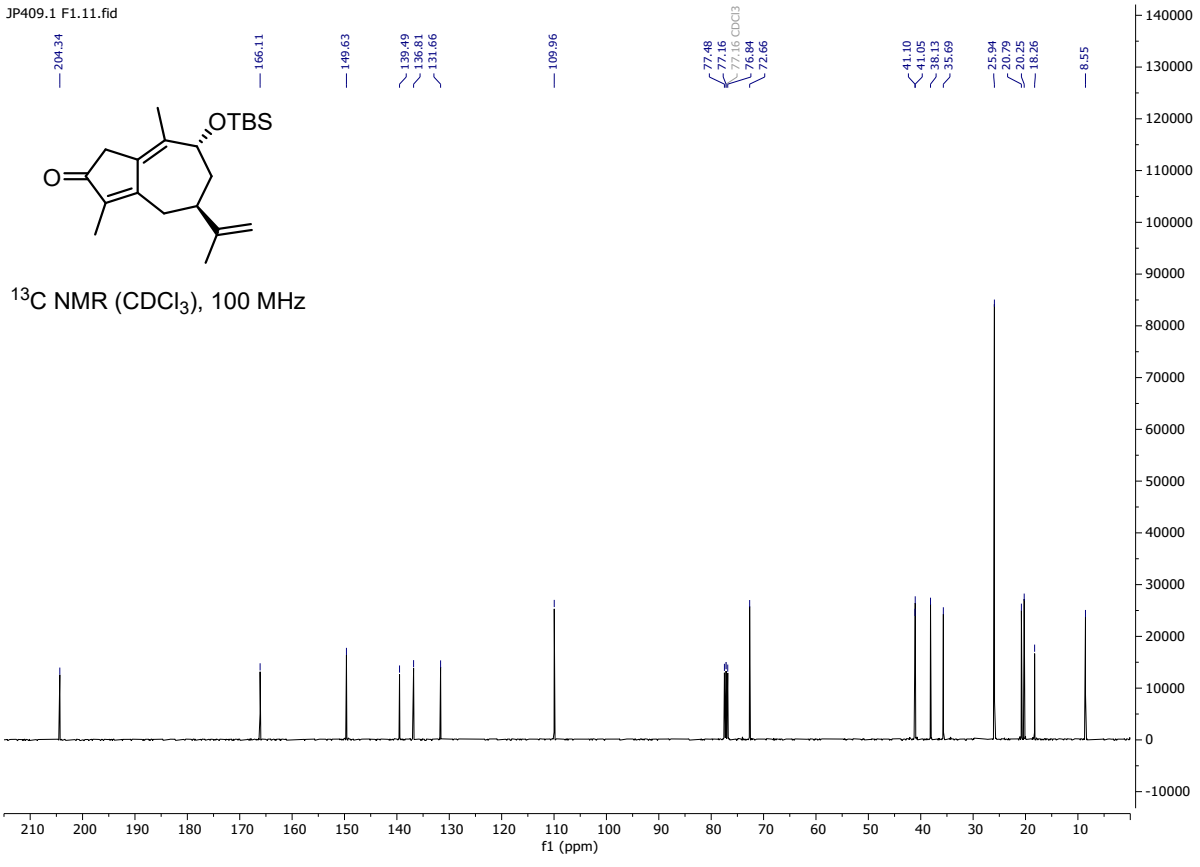

^{13}C NMR ($CDCl_3$), 100 MHz

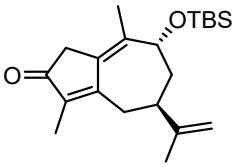

JP208-1F1

Analysed on March 1st, 2024

m/z mesured	Ion formula	Theoretical m/z	Error (ppm)	Score
369.2224	$C_{21}H_{34}NaO_2Si^+$	369.222	-0.9	100
347.2399	$C_{21}H_{35}O_2Si$	347.2401	0.5	100

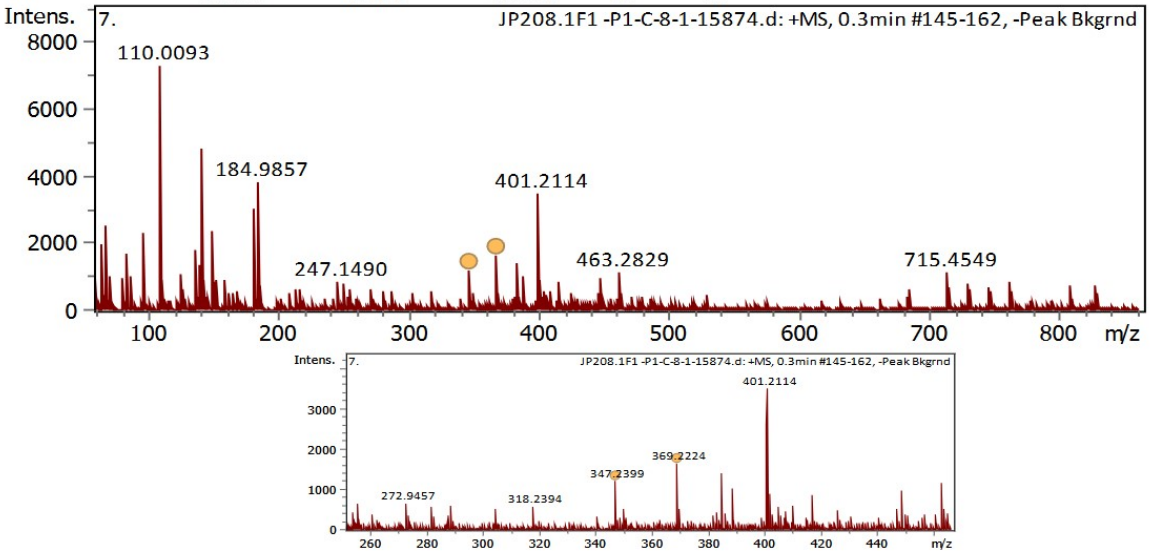

Mass spectrometry experiments was performed on a tims-TOF mass spectrometer (Bruker) in Laboratoire de Chimie Moléculaire (Ecole polytechnique, CNRS, Palaiseau, France). Electrospray source has been used in positive mode. Samples was prepared in acetonitrile with 0.1% of formic acid, introduced at a 5 µL/min flow rate into the interface of the instrument. Capillary and end plate voltages were set at 4.5 kV and 0.7 kV . Nitrogen was used as the nebulizer and drying gas at 2.5 bar and 3 L/min, respectively, with a drying temperature of 180°C. Tuning mix (Agilent) was used for calibration. The elemental compositions of all ions were determined with the instrument software Data Analysis, the precision of mass measurement was less than 3 ppm.

Compound 10 (reported structure of diarthroncha C, in $CDCl_3$)

^{1}H NMR ($CDCl_3$), 400 MHz

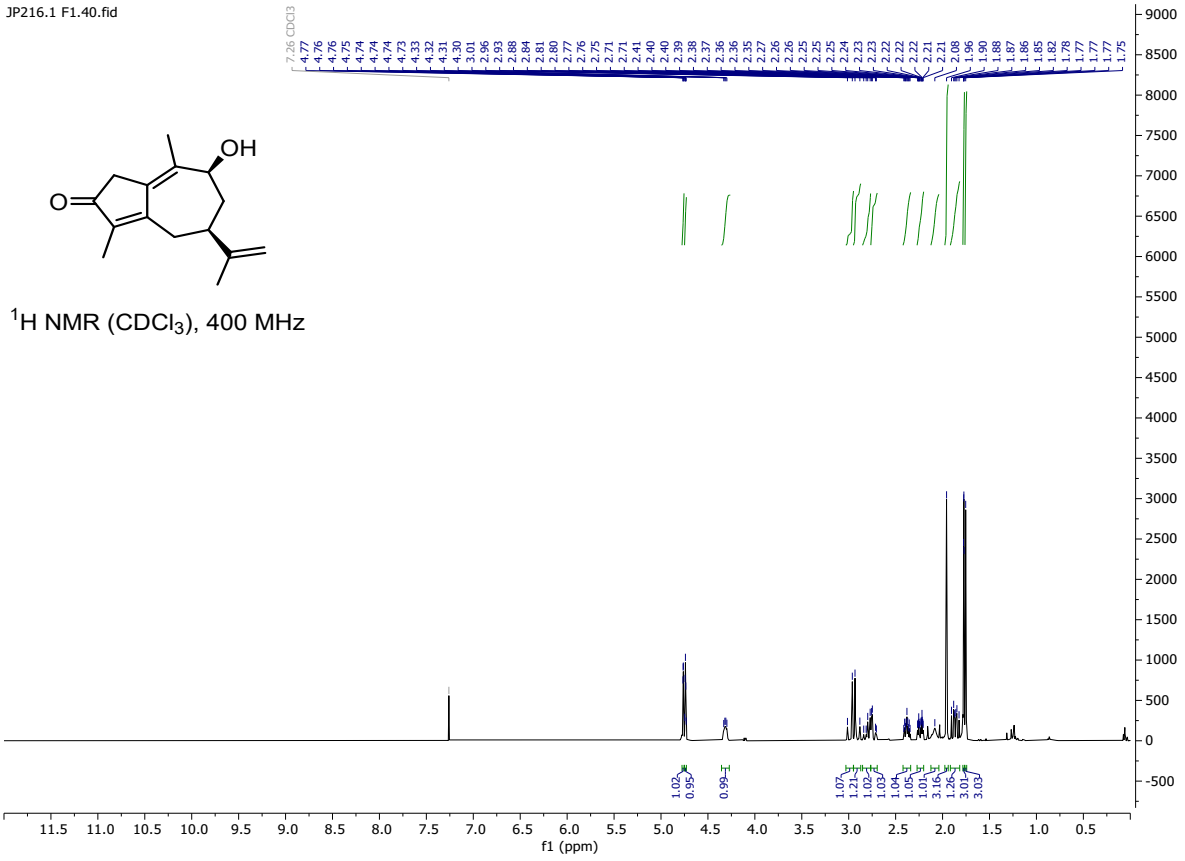

^{13}C NMR ($CDCl_3$), 100 MHz

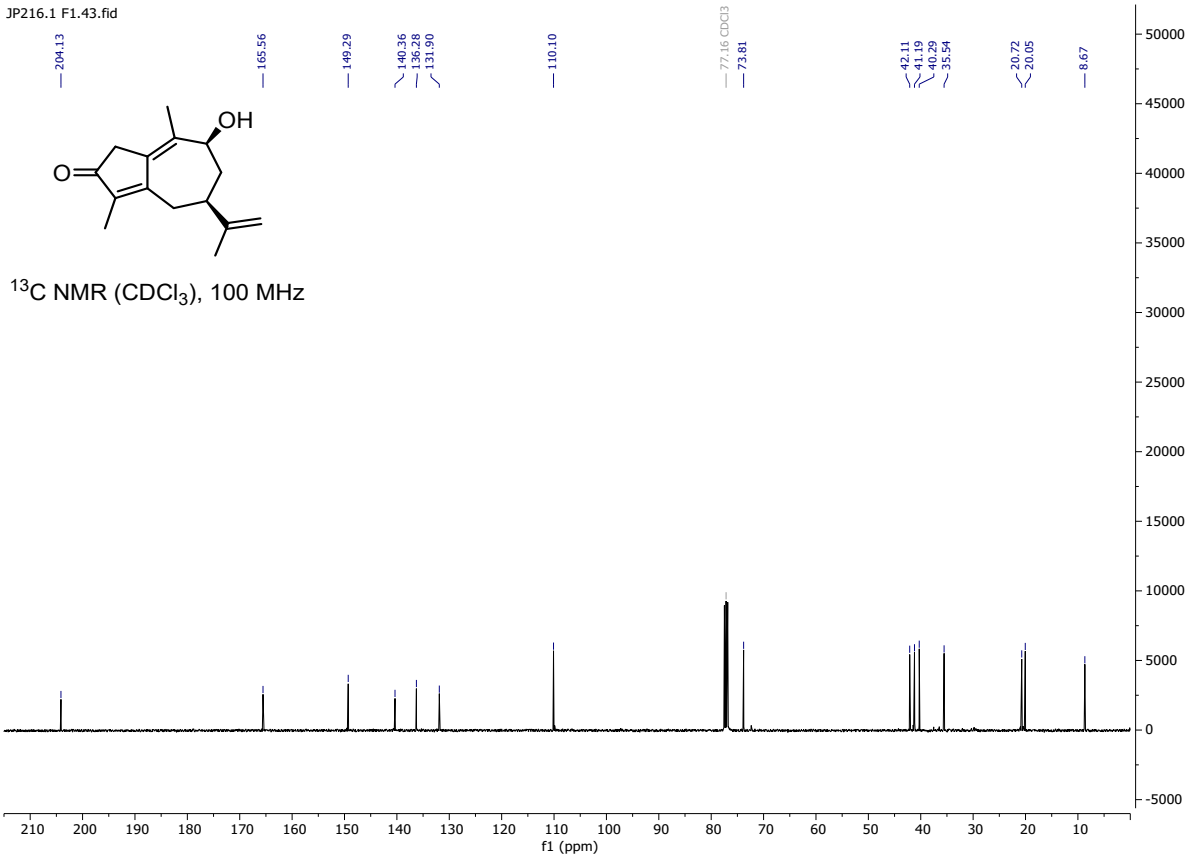

Compound 10 (reported structure of diarthroncha C, in DMSO-d6)

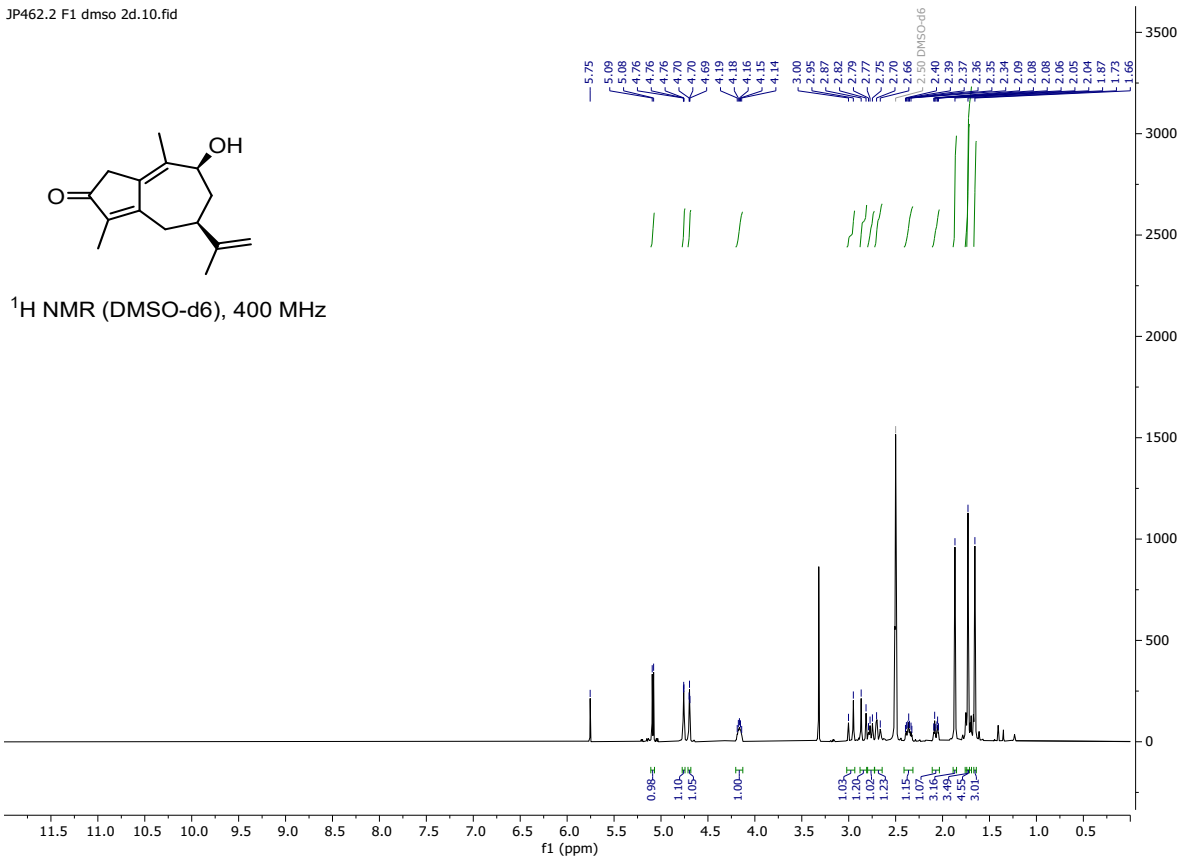

^{1}H NMR (DMSO-d6), 400 MHz

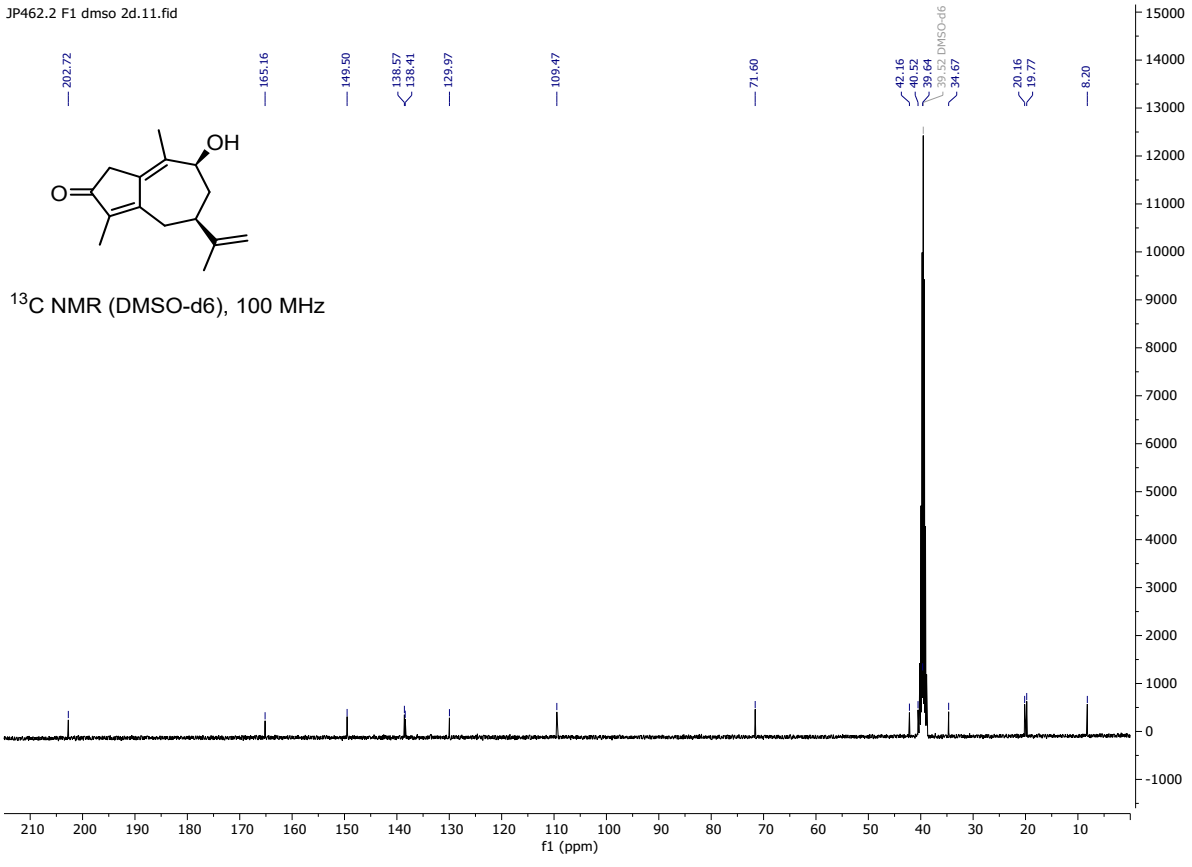

^{13}C NMR (DMSO-d6), 100 MHz

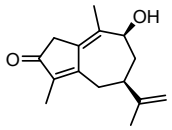

JP462.2 F1

m/z mesured	Ion formula	Theoretical m/z	Error (ppm)	Score
233.1533	$C_{15}H_{21}O_2^+$	233.1536	1.3	100

Analysed on 26/02/2025

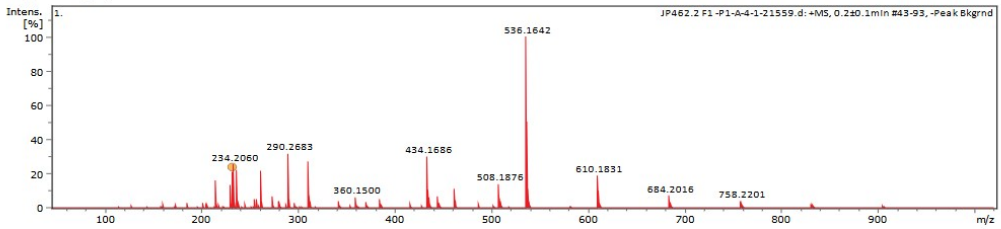

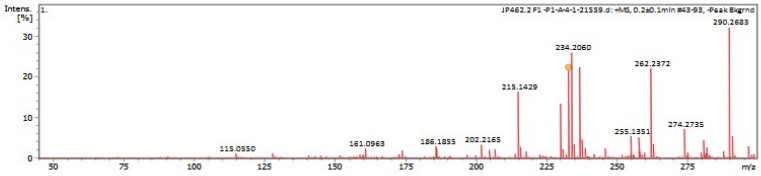

Mass spectrometry experiments was performed on a tims-TOF mass spectrometer (Bruker) in Laboratoire de Chimie Moléculaire (Ecole polytechnique, CNRS, Palaiseau, France). Electrospray source has been used in positive mode. Samples was prepared in acetonitri acid, introduced at a 5 µL/min flow rate into the interface of the instrument. Capillary and end plate voltages were set at 4.5 kV and 0.7 kV . Nitrogen was used as the nebulizer and drying gas at 2.5 bar and 3 L/min, respectively, with a drying temperature of 180°C. Tu used for calibration. The elemental compositions of all ions were determined with the instrument software Data Analysis, the precision of mass measurement was less than 3 ppm.

Compound 11 (daphnenicillata W, in $CDCl_3$)

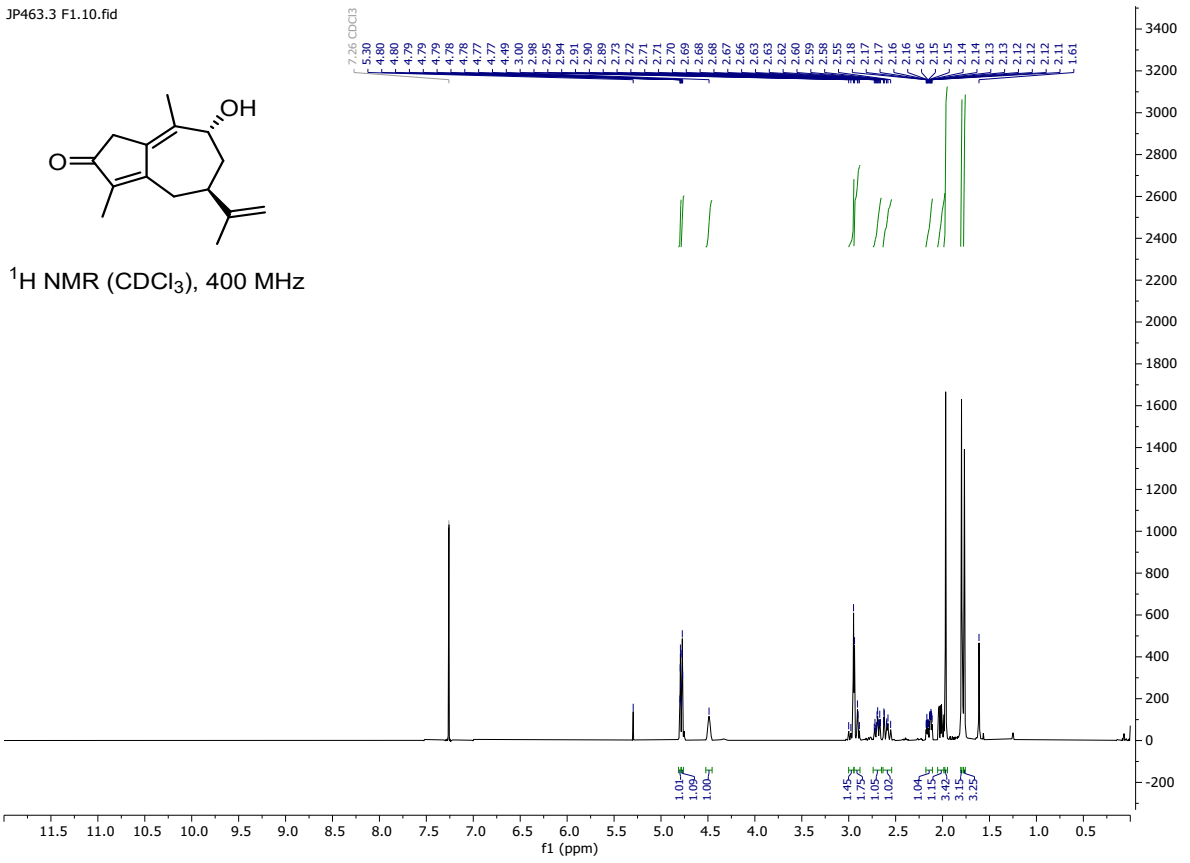

^{1}H NMR ($CDCl_3$), 400 MHz

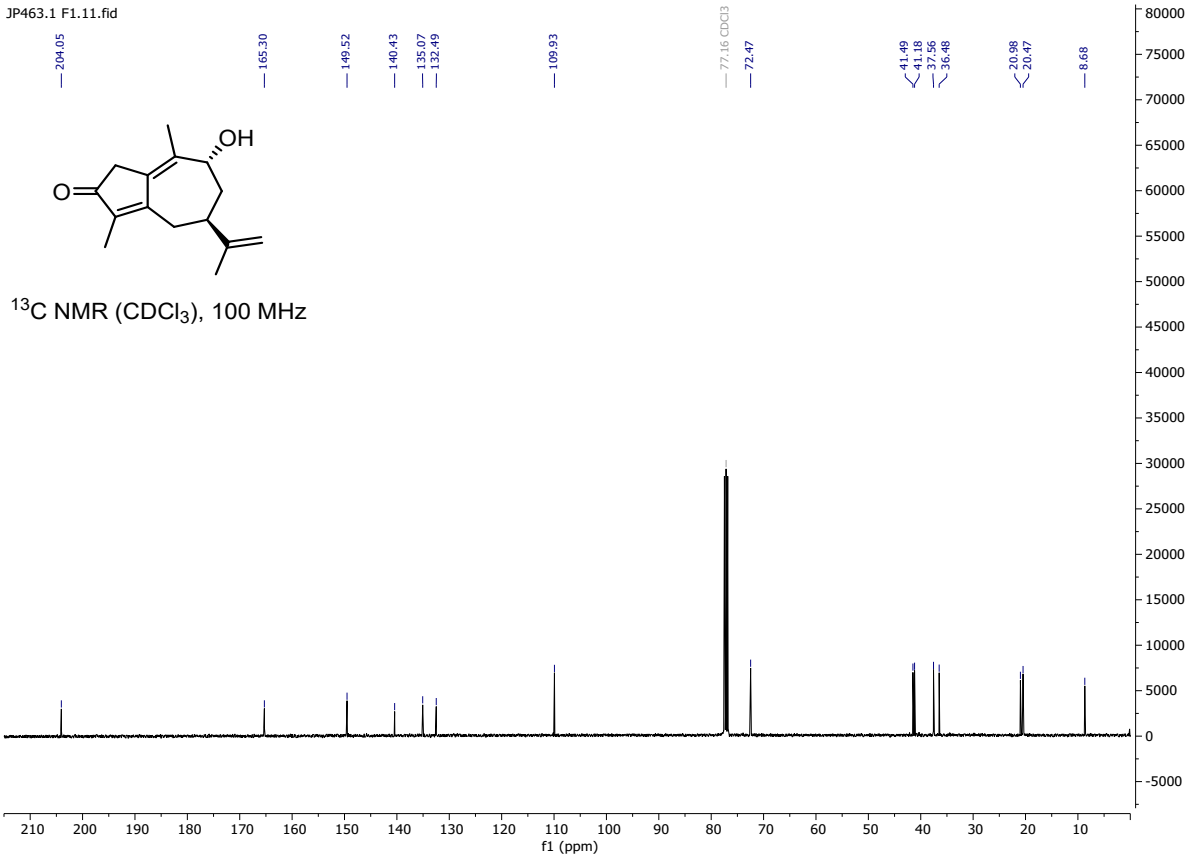

^{13}C NMR ($CDCl_3$), 100 MHz

Compound 11 (daphnenicillata W, in DMSO-d6)

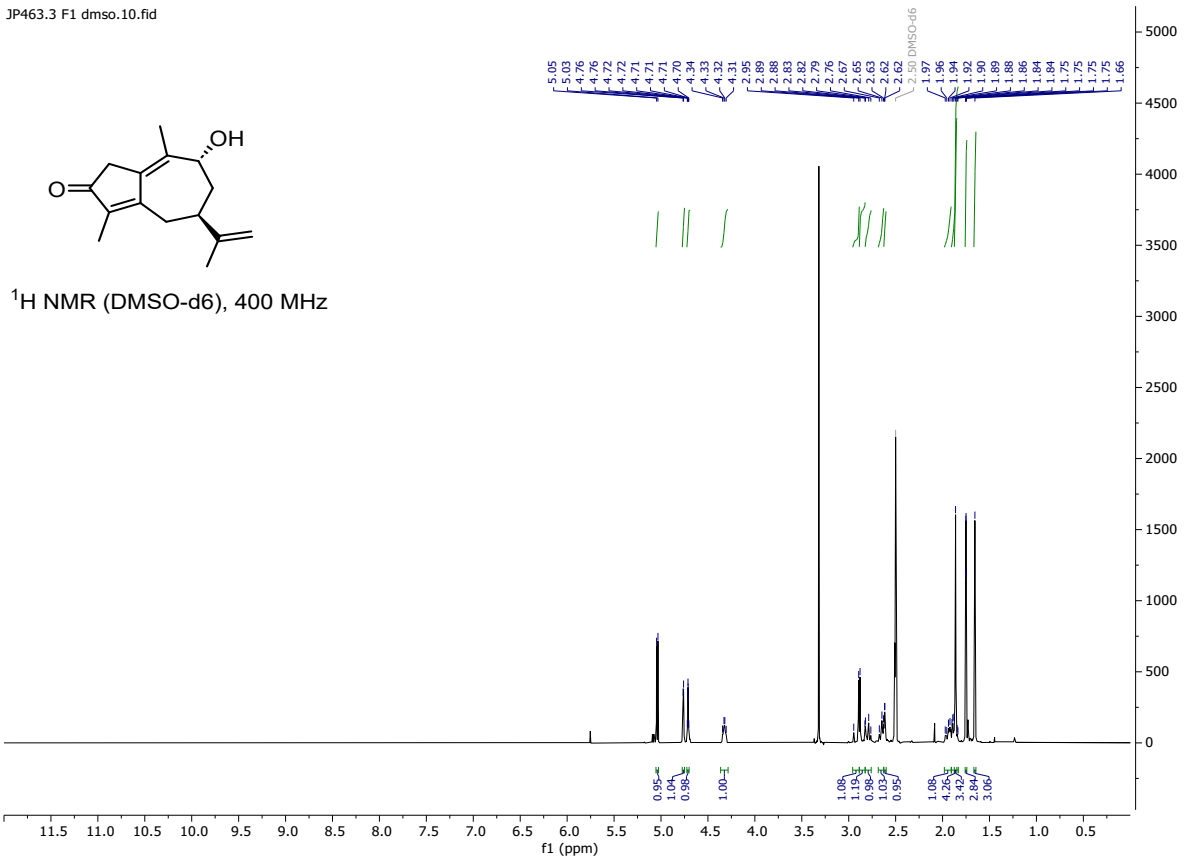

^{1}H NMR (DMSO-d6), 400 MHz

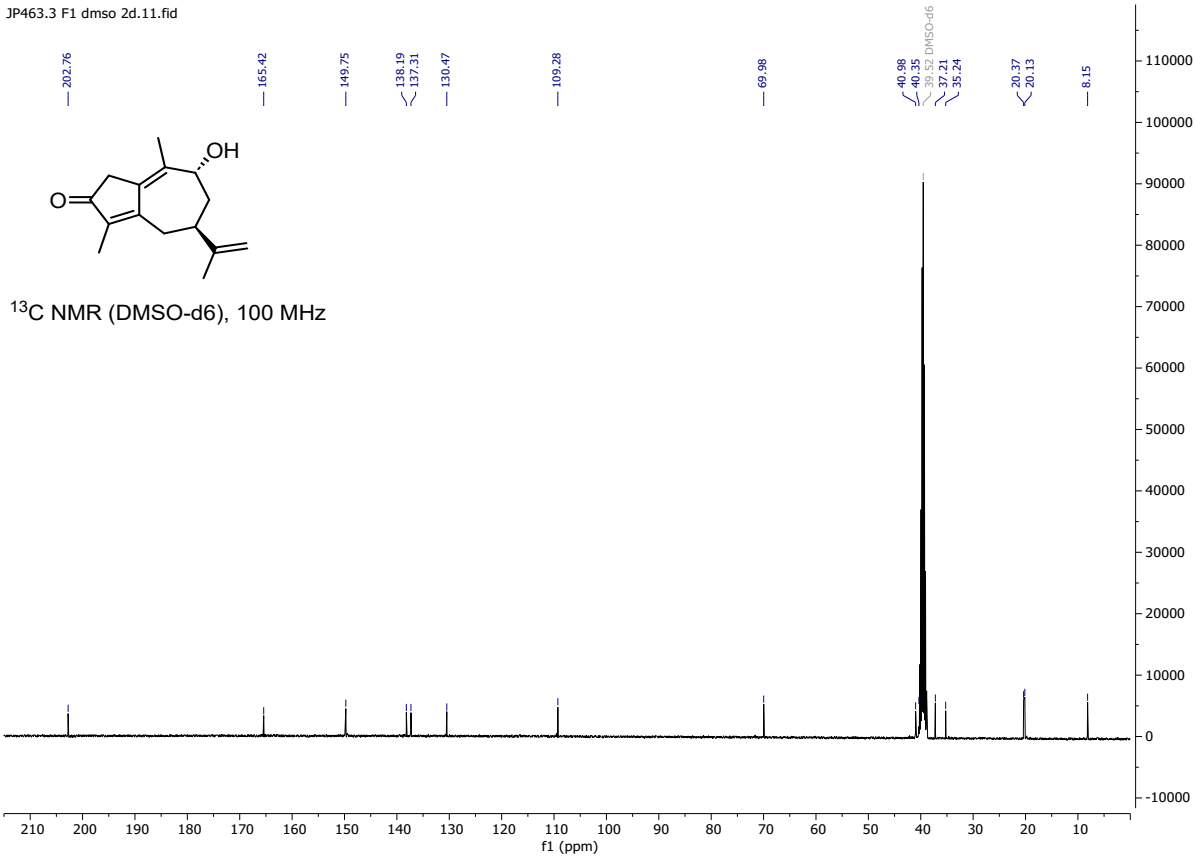

^{13}C NMR (DMSO-d6), 100 MHz

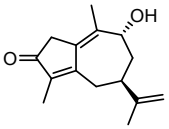

JP463.1 F1

m/z mesured	Ion formula	Theoretical m/z	Error (ppm)	Score
233.1531	$C_{15}H_{21}O_2^+$	233.1536	2.2	100

Analysed on 26/02/2025

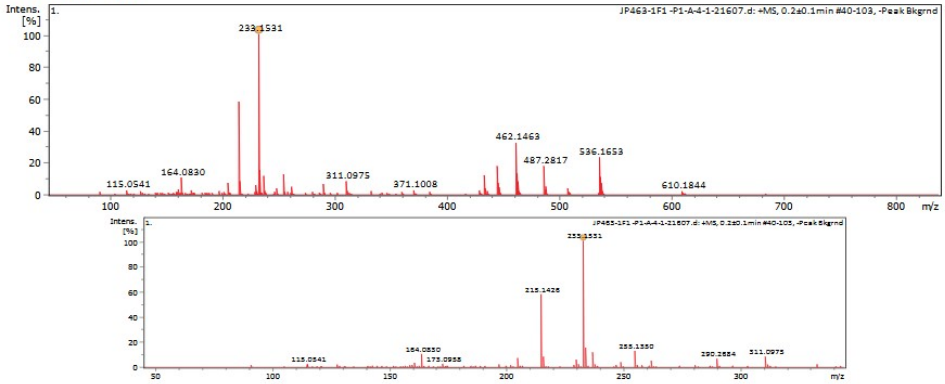

Mass spectrometry experiments was performed on a tims-TOF mass spectrometer (Bruker) in Laboratoire de Chimie Moléculaire (Ecole polytechnique, CNRS, Palaiseau, France). Electrospray source has been used in positive mode. Samples was prepared in acetonitri acid, introduced at a 5 µL/min flow rate into the interface of the instrument. Capillary and end plate voltages were set at 4.5 kV and 0.7 kV . Nitrogen was used as the nebulizer and drying gas at 2.5 bar and 3 L/min, respectively, with a drying temperature of 180°C. Tu used for calibration. The elemental compositions of all ions were determined with the instrument software Data Analysis, the precision of mass measurement was less than 3 ppm.

Compound 3 (oleodaphnone)

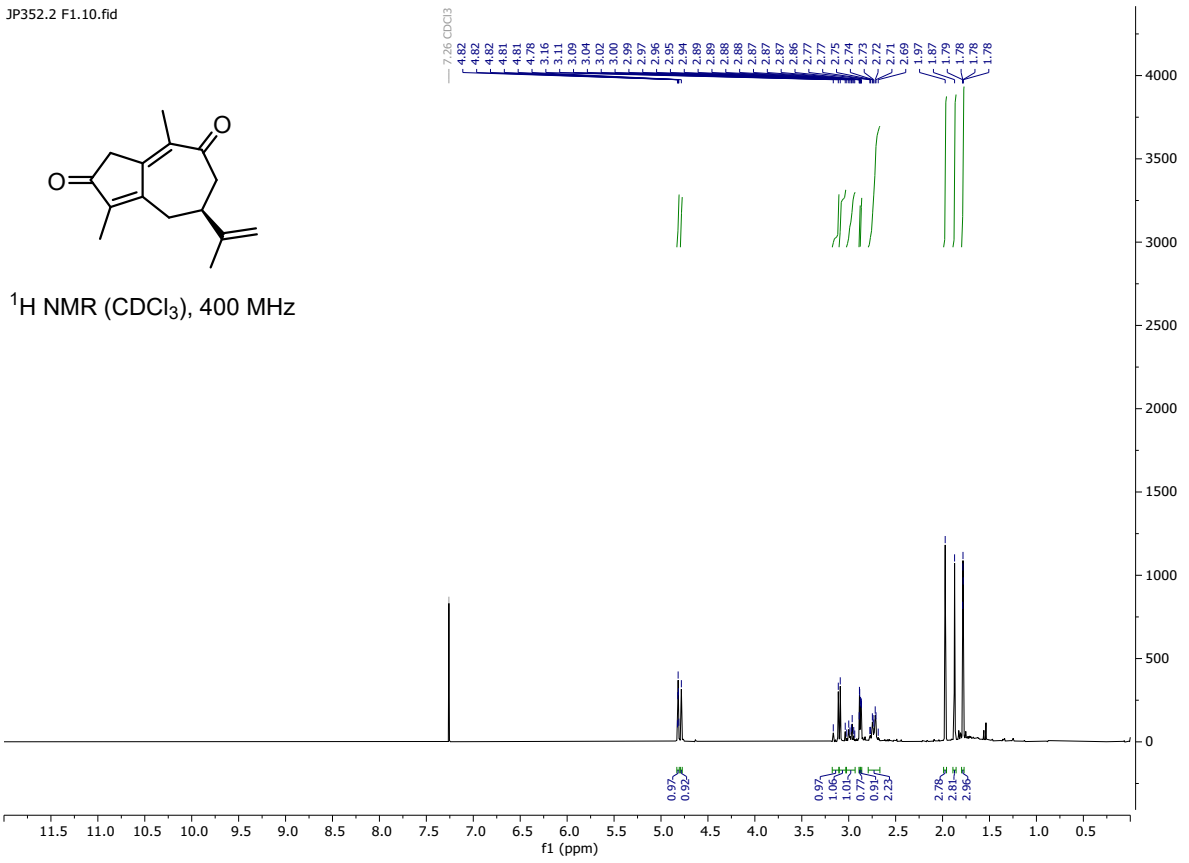

^{1}H NMR ($CDCl_3$), 400 MHz

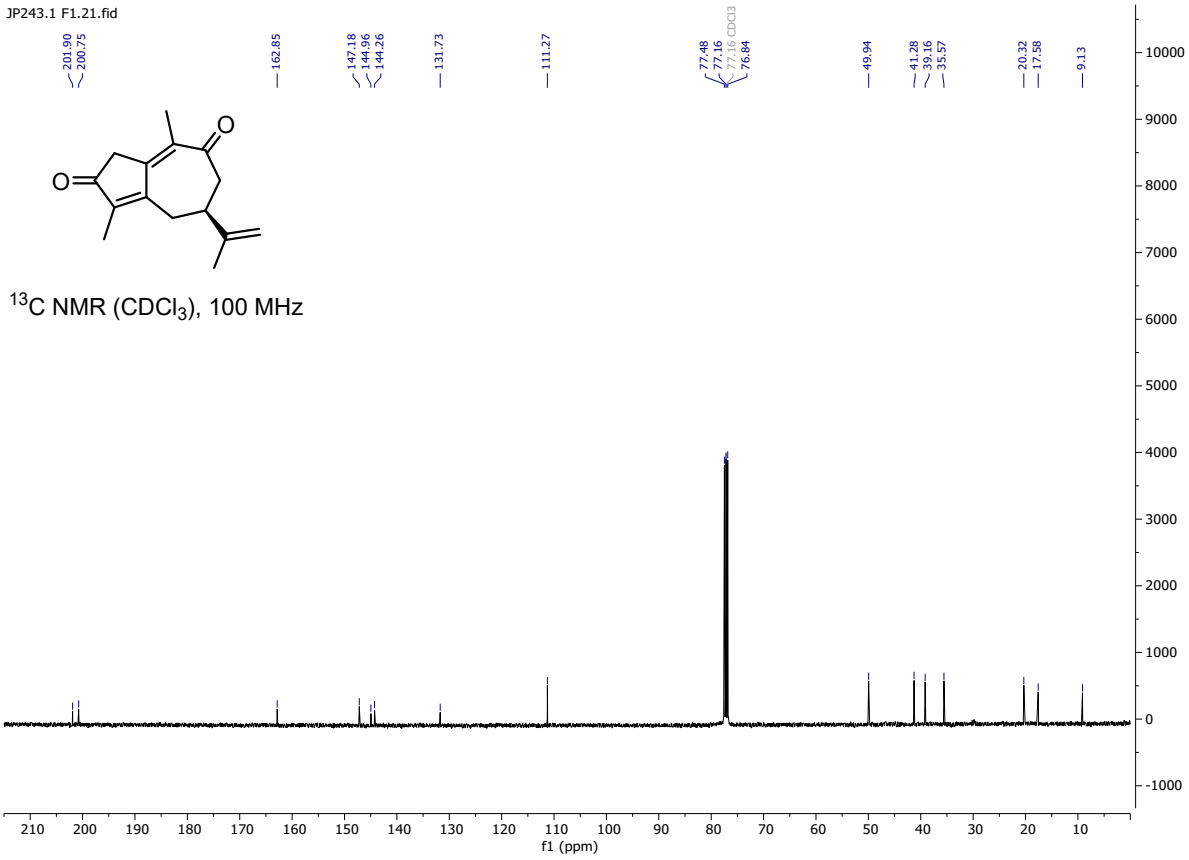

^{13}C NMR ($CDCl_3$), 100 MHz

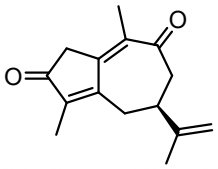

JP389.1 F1

m/z mesured	Ion formula	Theoretical m/z	Error (ppm)	Score
231.1388	$C_{15}H_{19}O_2^+$	231.138	-3.7	100

Analysed on 14/11/2024

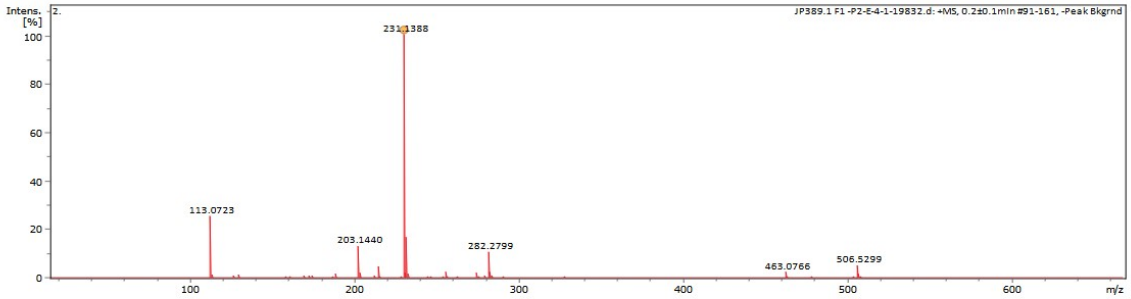

Mass spectrometry experiments was performed on a tims-TOF mass spectrometer (Bruker) in Laboratoire de Chimie Moléculaire (Ecole polytechnique, CNRS, Palaiseau, France). Electrospray source has been used in positive mode. Samples was prepared in acetonitrile with 0.1% of formic acid, introduced at a 5 µL/min flow rate into the interface of the instrument. Capillary and end plate voltages were set at 4.5 kV and 0.7 kV . Nitrogen was used as the nebulizer and drying gas at 2.5 bar and 3 L/min, respectively, with a drying temperature of 180°C. Tuning mix (Agilent) was used for calibration. The elemental compositions of all ions were determined with the instrument software Data Analysis, the precision of mass measurement was less than 3 ppm.

Compound 2

JP393.1 F1.10.fid

^{1}H NMR (CD3OD), 400 MHz

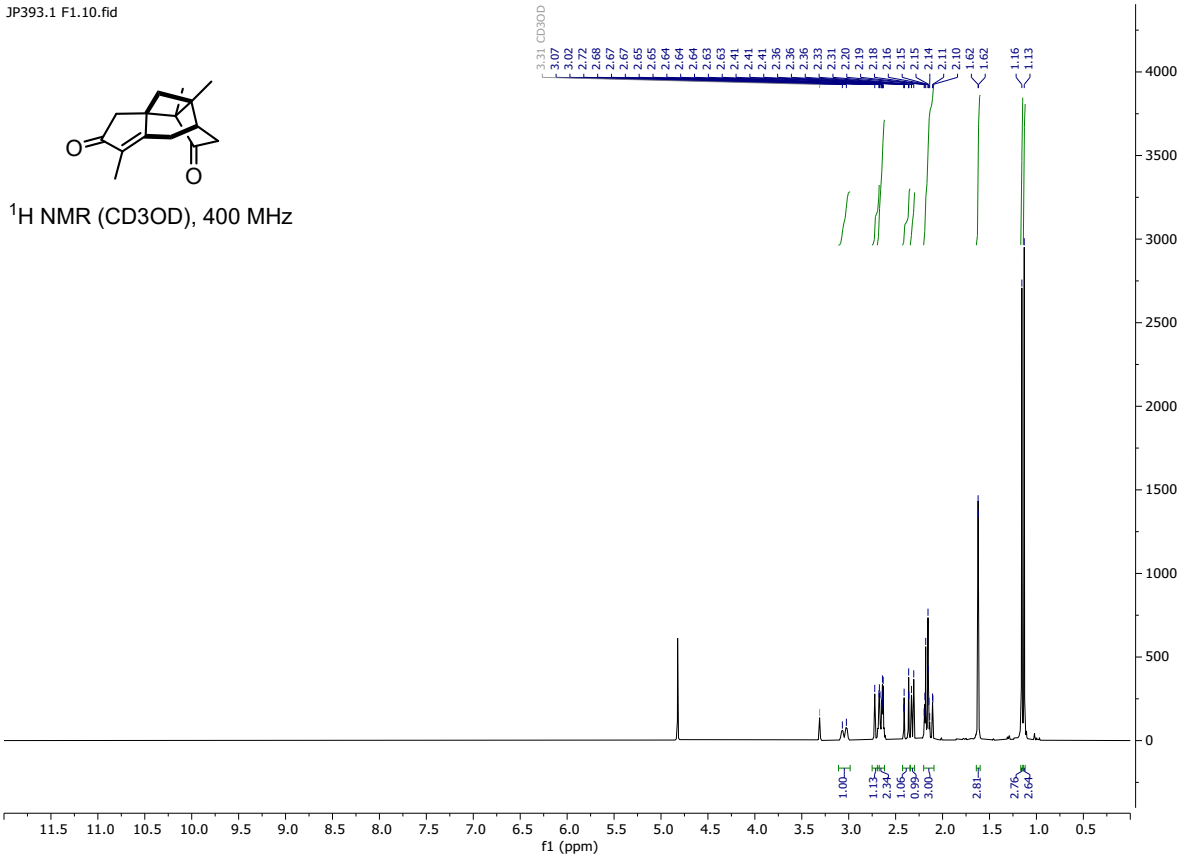

JP393.1 F1.1.fid

13C

^{13}C NMR (CD3OD), 75 MHz

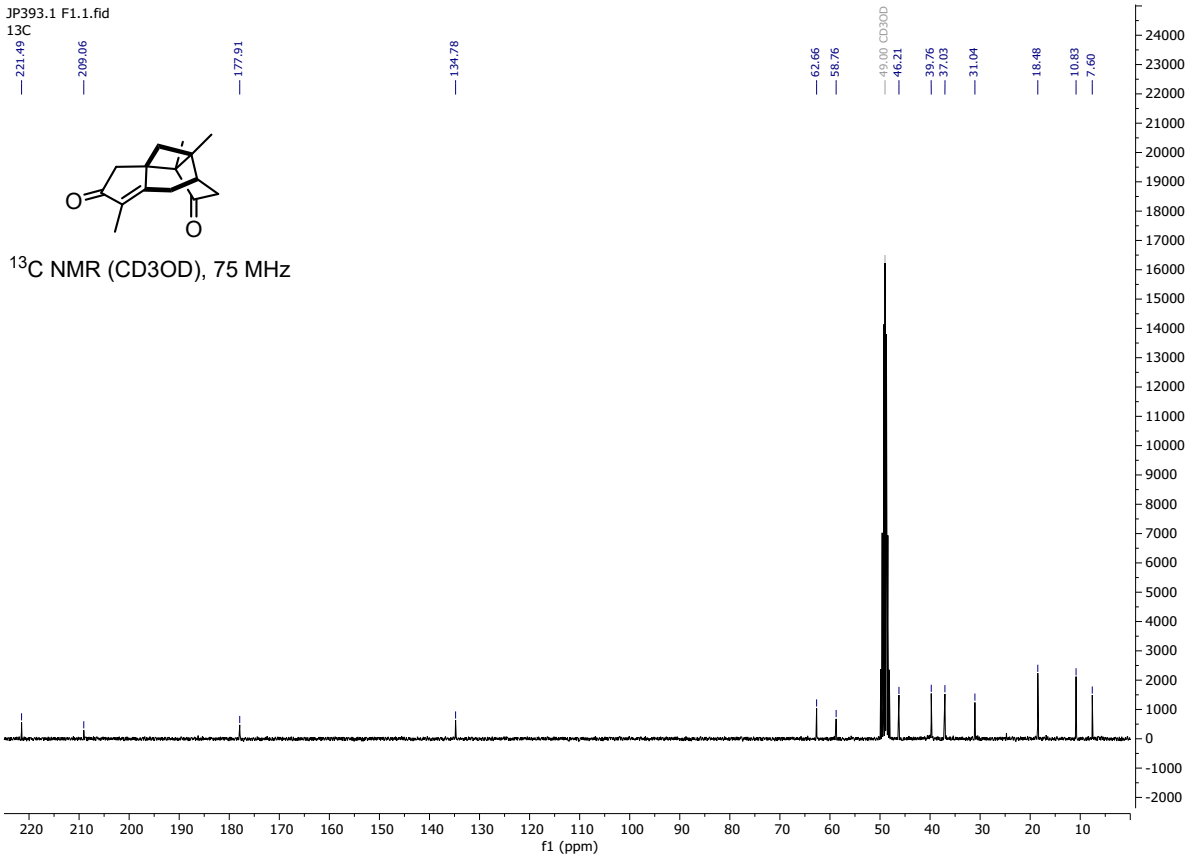

JP393.1 F1

m/z mesured	Ion formula	Theoretical m/z	Error (ppm)	Score
231.1389	$C_{15}H_{19}O_2^+$	231.138	-4.1	100

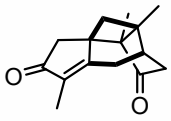

Analysed on 14/11/2024

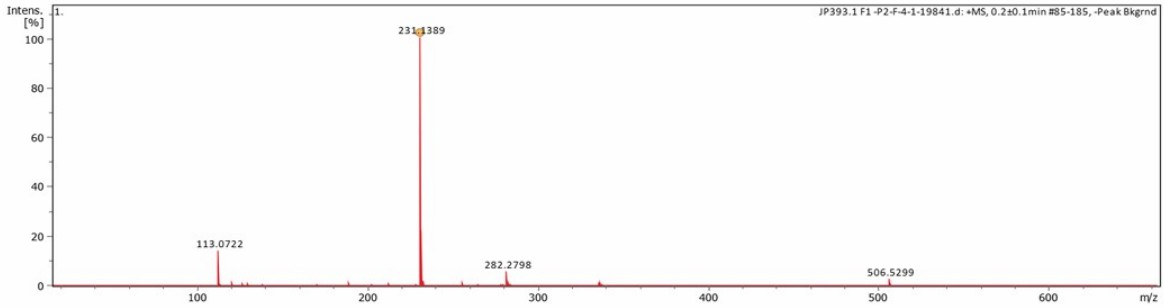

Mass spectrometry experiments was performed on a tims-TOF mass spectrometer (Bruker) in Laboratoire de Chimie Moléculaire (Ecole polytechnique, CNRS, Palaiseau, France). Electrospray source has been used in positive mode. Samples was prepared in acetonitrile with 0.1% of formic acid, introduced at a 5 µL/min flow rate into the interface of the instrument. Capillary and end plate voltages were set at 4.5 kV and 0.7 kV . Nitrogen was used as the nebulizer and drying gas at 2.5 bar and 3 L/min, respectively, with a drying temperature of 180°C. Tuning mix (Agilent) was used for calibration. The elemental compositions of all ions were determined with the instrument software Data Analysis, the precision of mass measurement was less than 3 ppm.

Compound *epi*-1

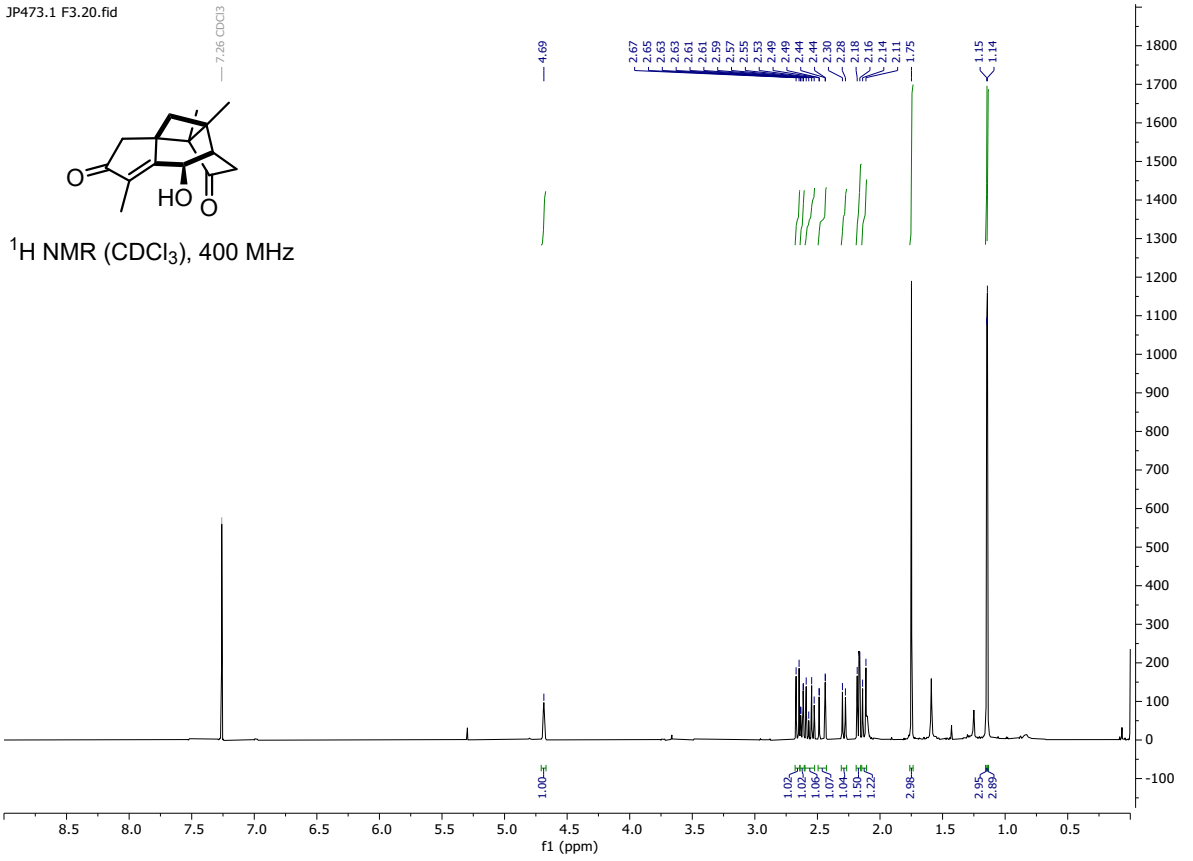

^{1}H NMR ($CDCl_3$), 400 MHz

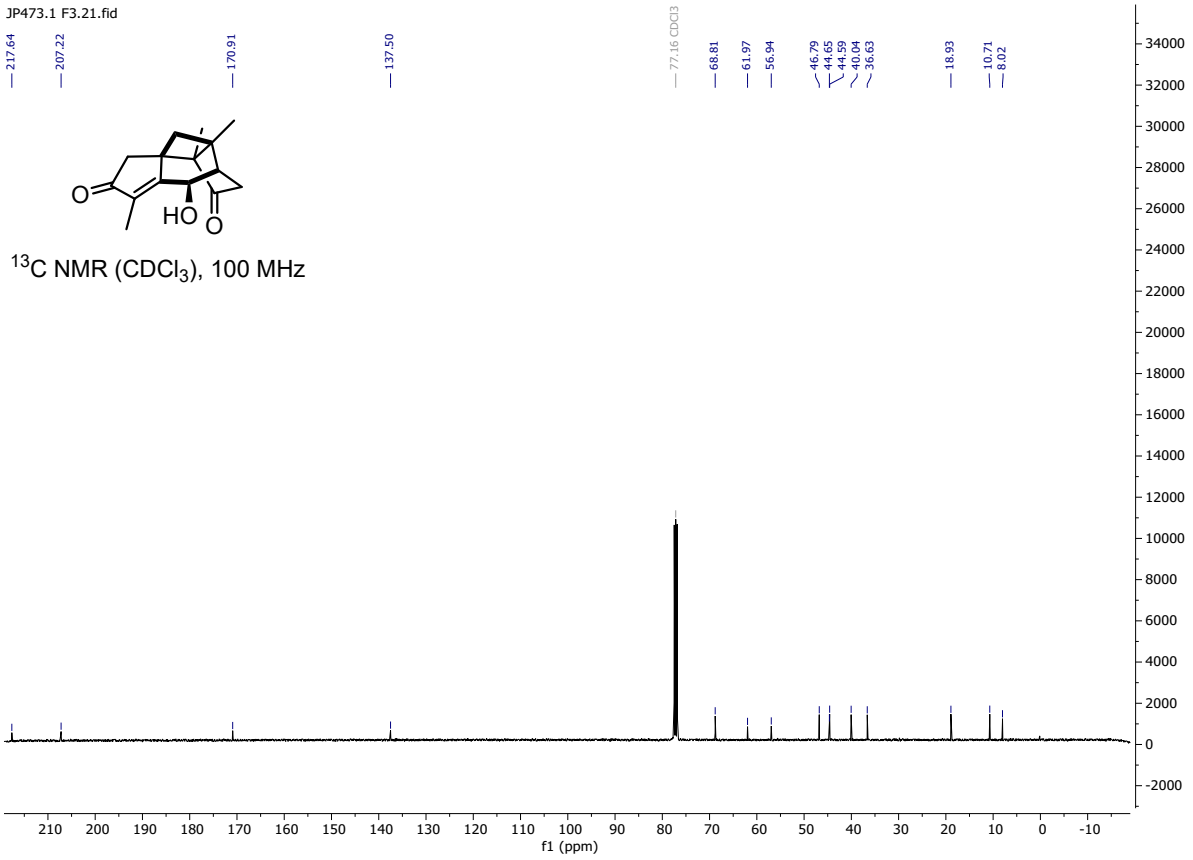

^{13}C NMR ($CDCl_3$), 100 MHz

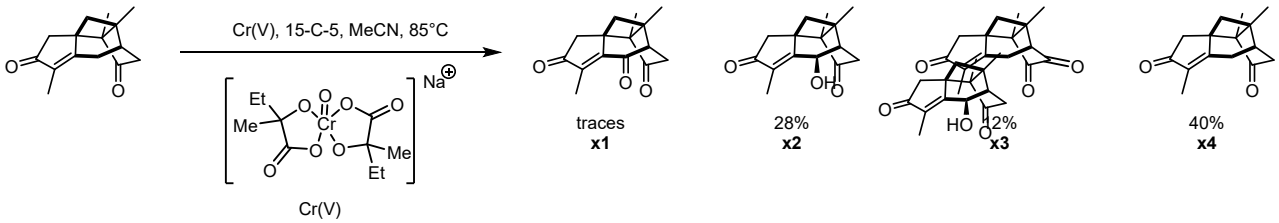

JP472.1 F3

m/z mesured	Ion formula	Theoretical m/z	Error (ppm)	Score
247.1325	$C_{15}H_{19}O_3^+$	247.1329	1.4	100

Analysed on 26/02/2025

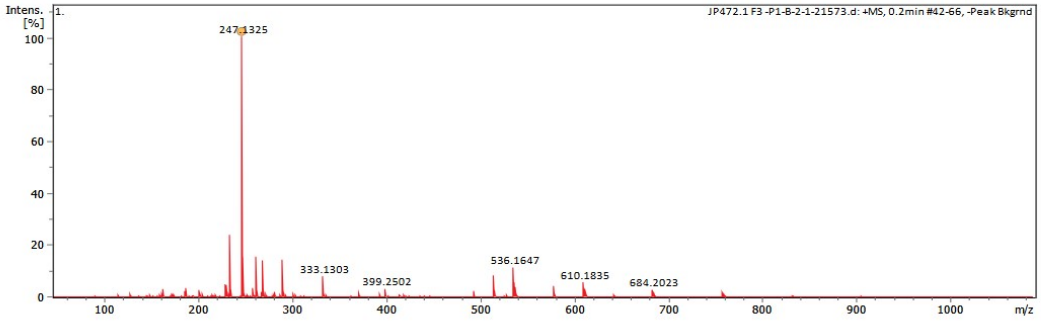

Mass spectrometry experiments was performed on a tims-TOF mass spectrometer (Bruker) in Laboratoire de Chimie Moléculaire (Ecole polytechnique, CNRS, Palaiseau, France). Electrospray source has been used in positive mode. Samples was prepared in acetonitri acid, introduced at a 5 µL/min flow rate into the interface of the instrument. Capillary and end plate voltages were set at 4.5 kV and 0.7 kV . Nitrogen was used as the nebulizer and drying gas at 2.5 bar and 3 L/min, respectively, with a drying temperature of 180°C. Tu used for calibration. The elemental compositions of all ions were determined with the instrument software Data Analysis, the precision of mass measurement was less than 3 ppm.

Compound 14

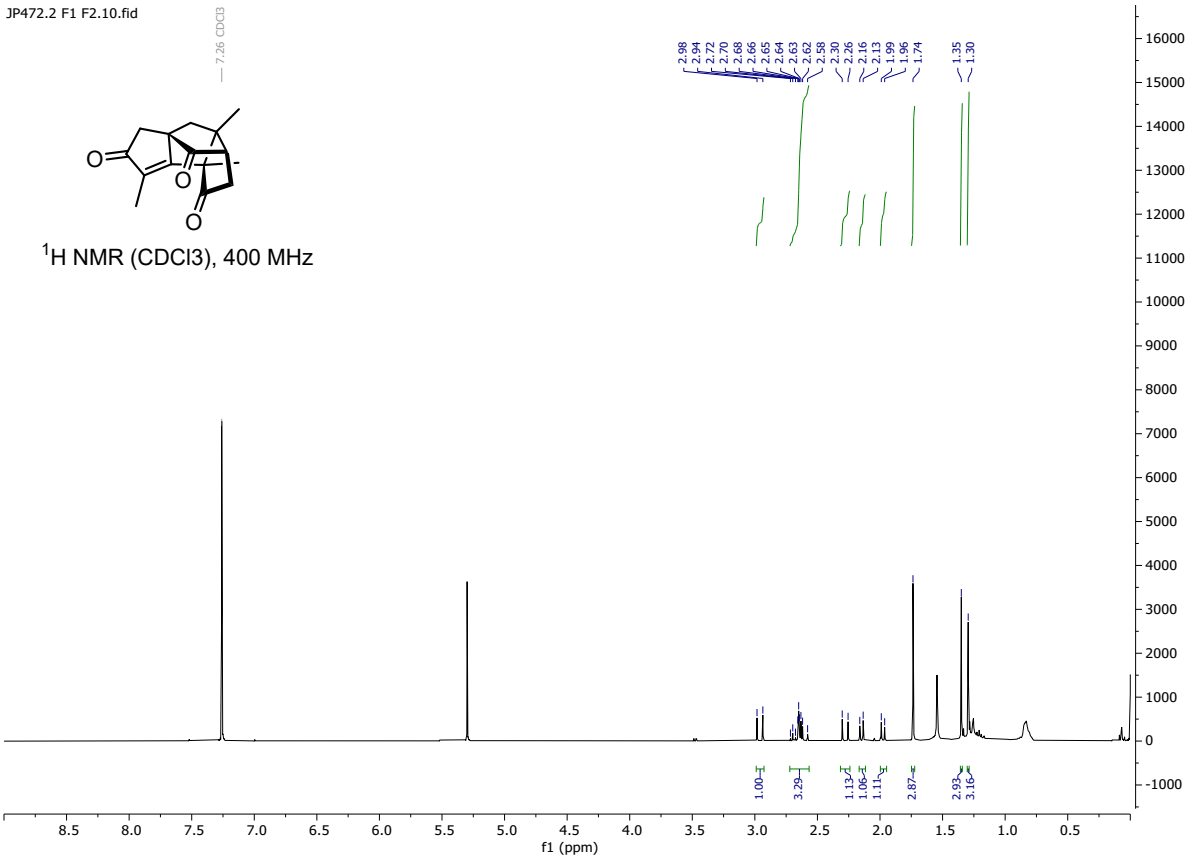

^{1}H NMR (CDCl3), 400 MHz

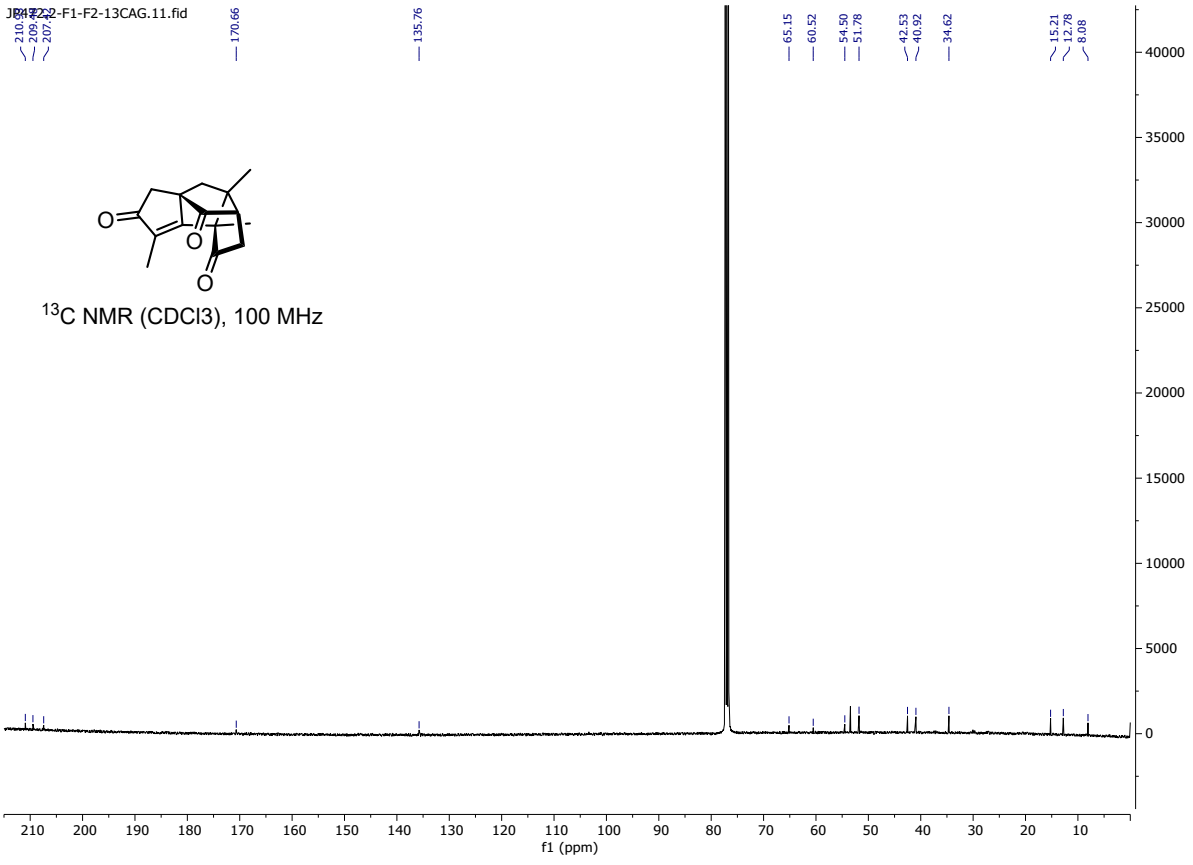

^{13}C NMR (CDCl3), 100 MHz

JP472.2 F1(F2)

m/z mesured	Ion formula	Theoretical m/z	Error (ppm)	Score
245.117	$C_{15}H_{17}O_3^+$	245.1172	0.9	100

Analysed on 26/02/2025

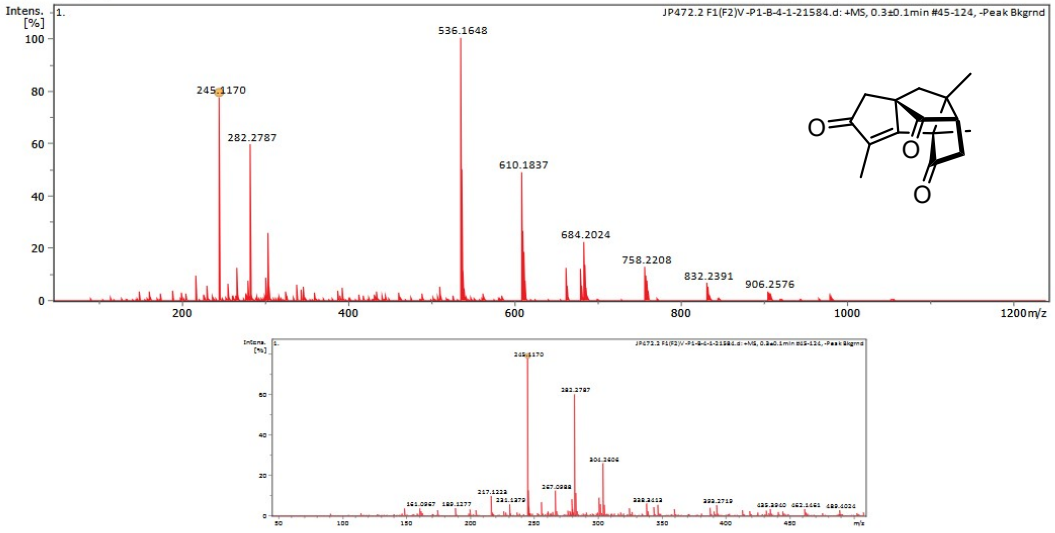

Mass spectrometry experiments was performed on a tims-TOF mass spectrometer (Bruker) in Laboratoire de Chimie Moléculaire (Ecole polytechnique, CNRS, Palaiseau, France). Electrospray source has been used in positive mode. Samples was prepared in acetonitri acid, introduced at a 5 µL/min flow rate into the interface of the instrument. Capillary and end plate voltages were set at 4.5 kV and 0.7 kV . Nitrogen was used as the nebulizer and drying gas at 2.5 bar and 3 L/min, respectively, with a drying temperature of 180°C. Tu used for calibration. The elemental compositions of all ions were determined with the instrument software Data Analysis, the precision of mass measurement was less than 3 ppm.

Compound 15

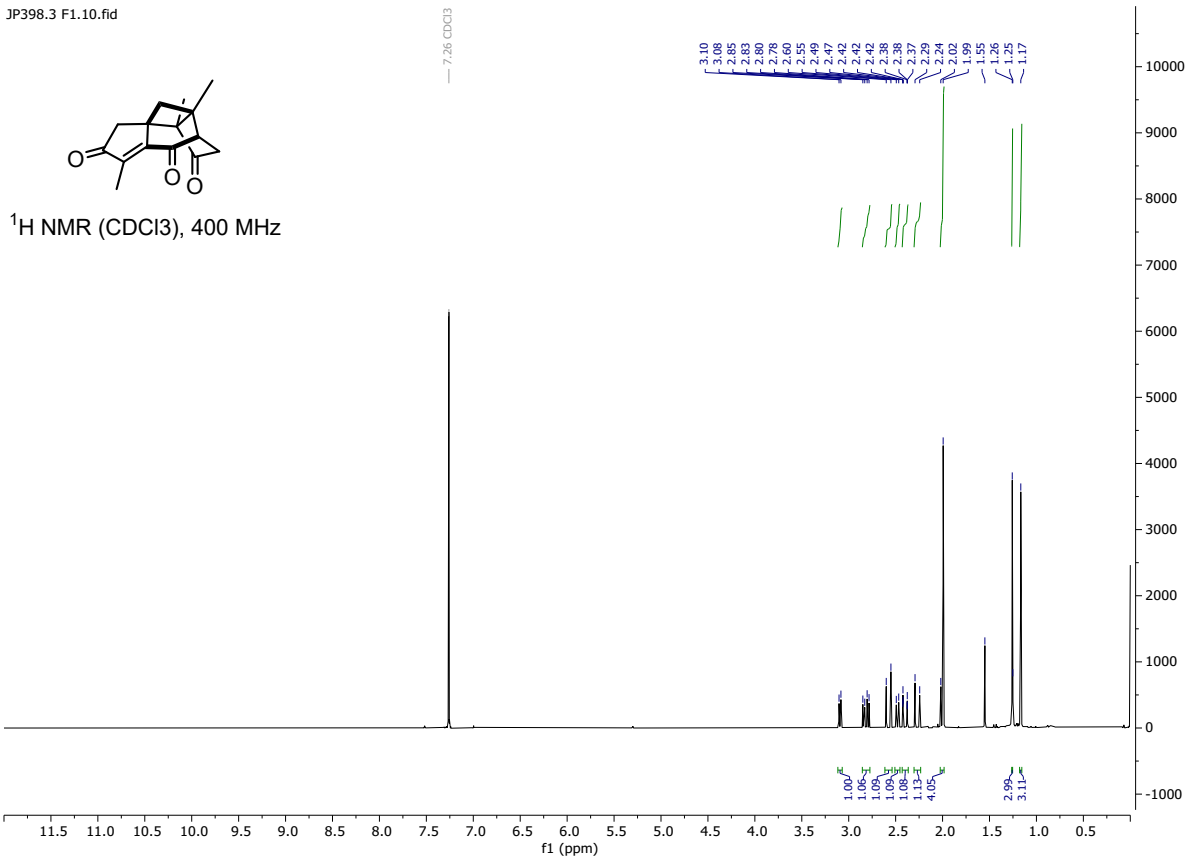

^{1}H NMR (CDCl3), 400 MHz

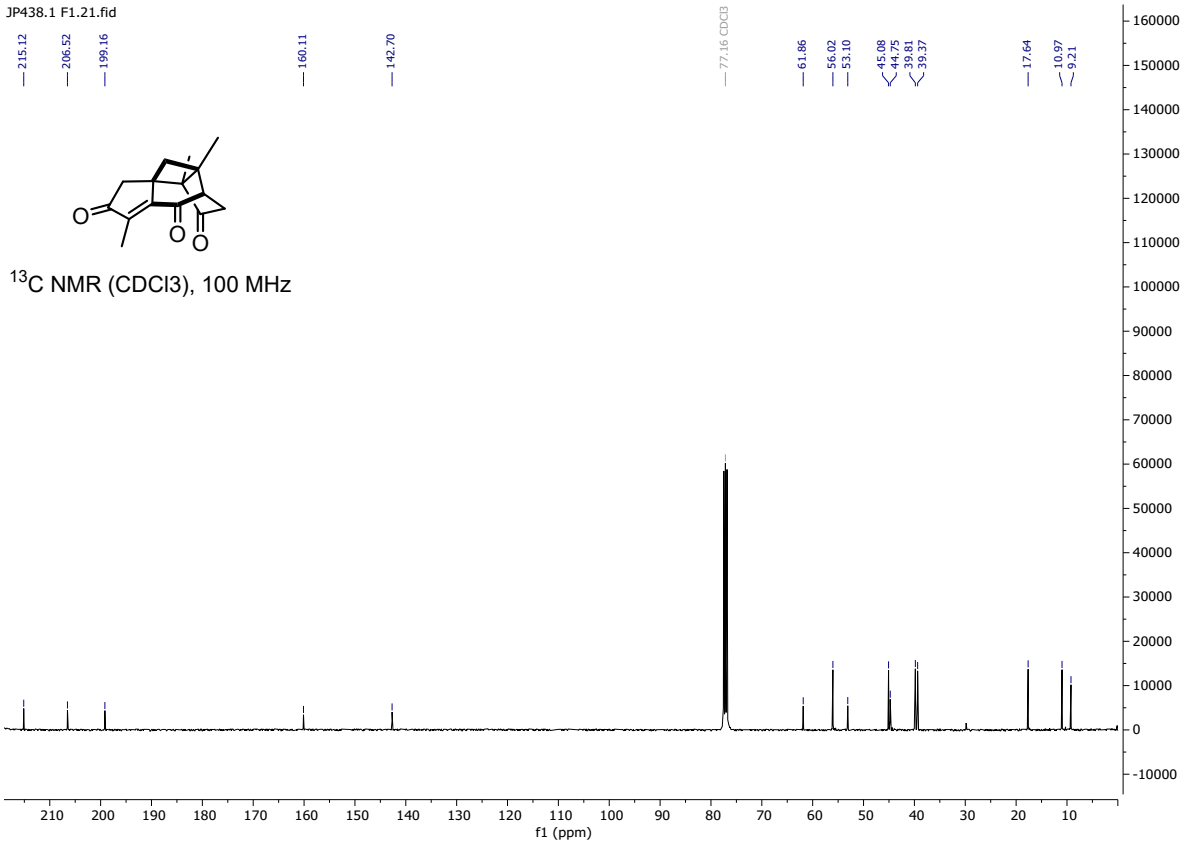

^{13}C NMR (CDCl3), 100 MHz

JP438.1 F1

Analysed on 26/02/2025

m/z mesured	Ion formula	Theoretical m/z	Error (ppm)	Score
245.1168	$C_{15}H_{17}O_3^+$	245.1172	1.8	100

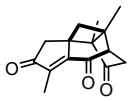

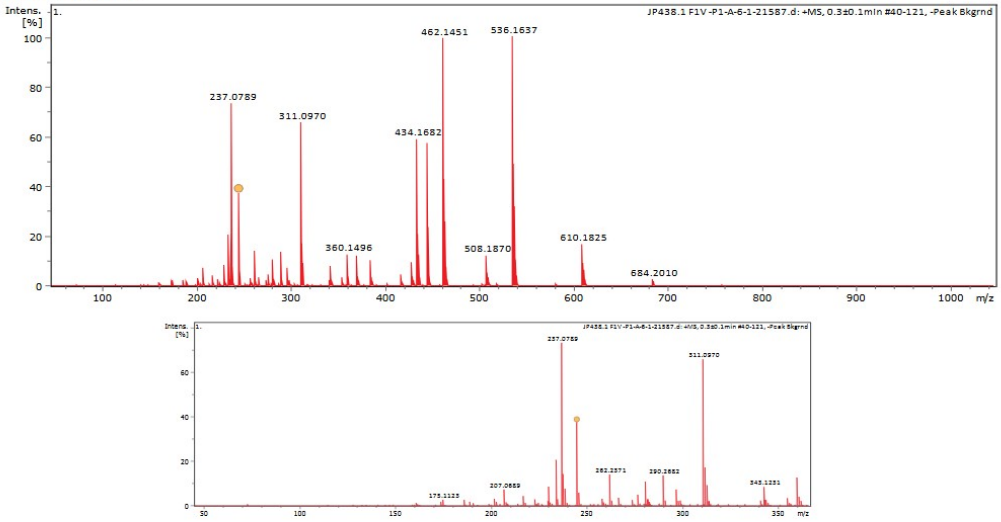

Mass spectrometry experiments was performed on a tims-TOF mass spectrometer (Bruker) in Laboratoire de Chimie Moléculaire (Ecole polytechnique, CNRS, Palaiseau, France). Electrospray source has been used in positive mode. Samples was prepared in acetonitri acid, introduced at a 5 µL/min flow rate into the interface of the instrument. Capillary and end plate voltages were set at 4.5 kV and 0.7 kV . Nitrogen was used as the nebulizer and drying gas at 2.5 bar and 3 L/min, respectively, with a drying temperature of 180°C. Tu used for calibration. The elemental compositions of all ions were determined with the instrument software Data Analysis, the precision of mass measurement was less than 3 ppm.

Compound 13

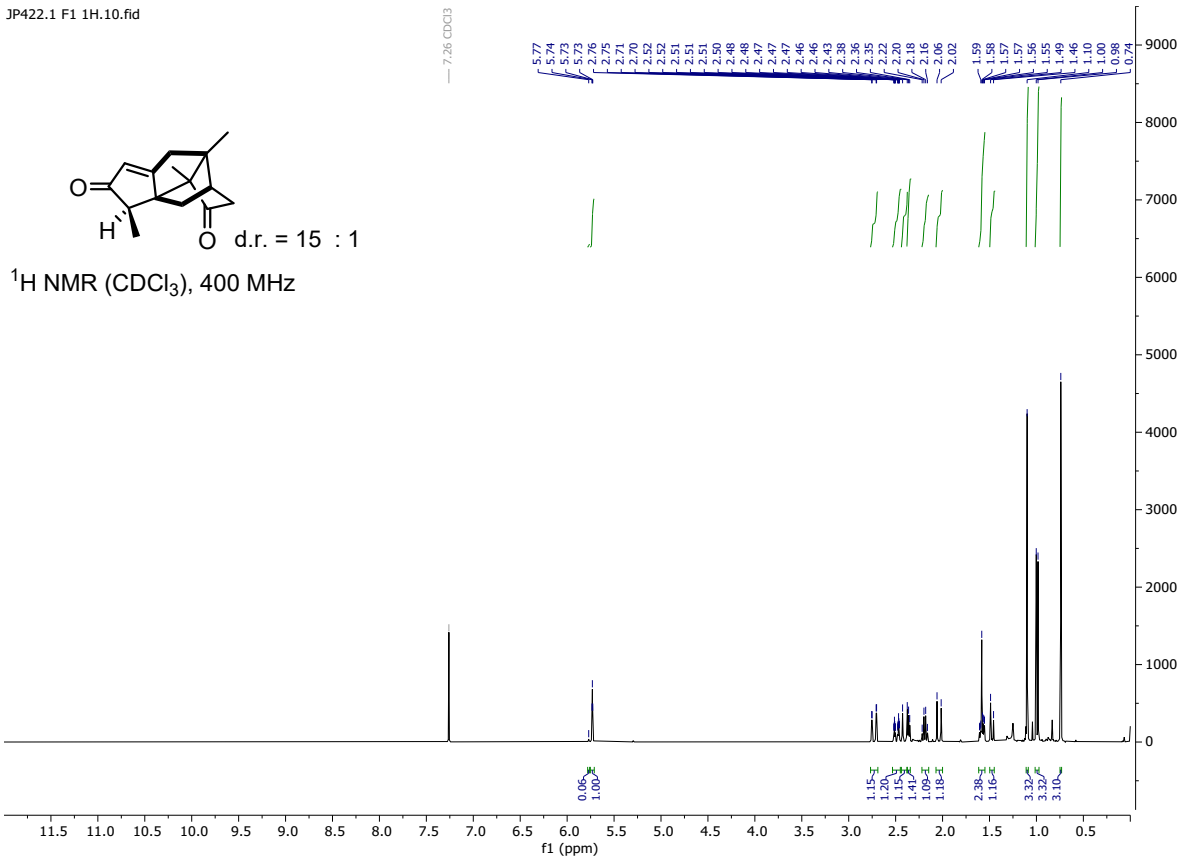

^{1}H NMR ($CDCl_3$), 400 MHz

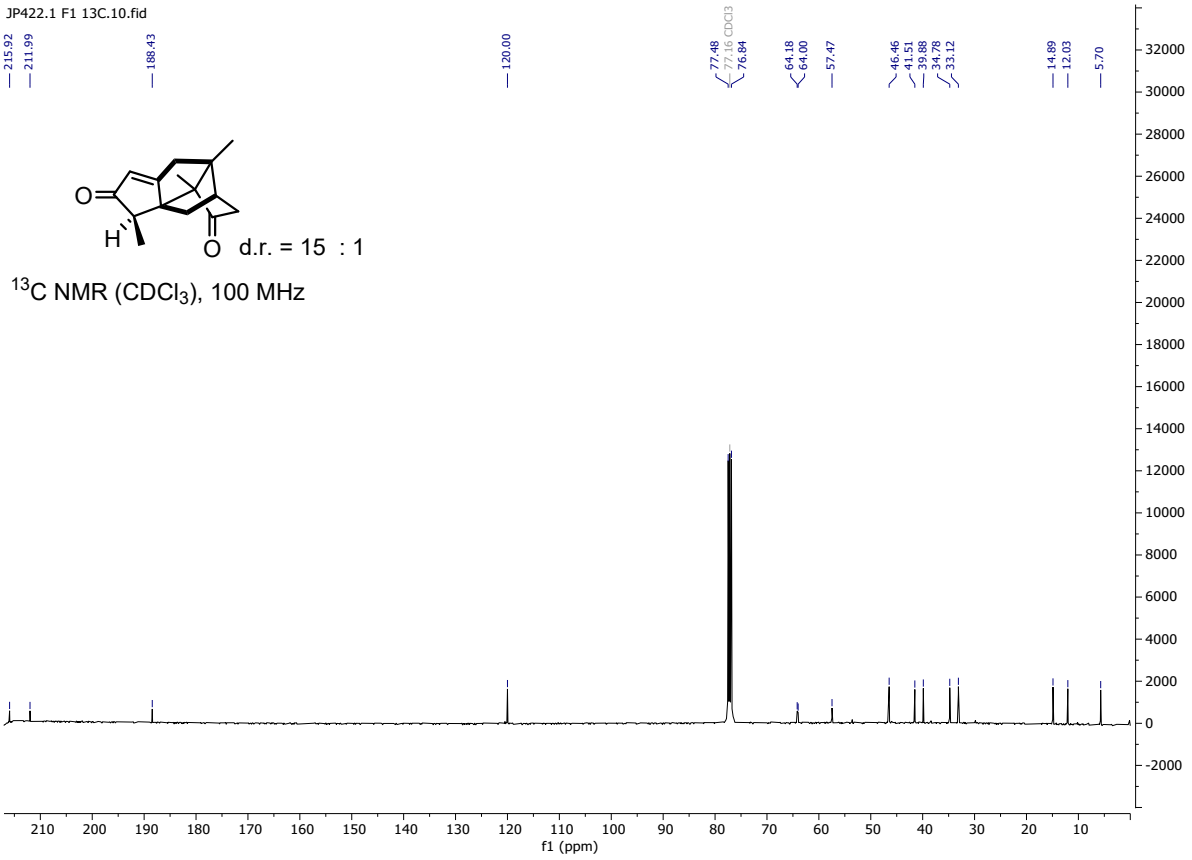

^{13}C NMR ($CDCl_3$), 100 MHz

JP422.1 F1

m/z mesured	Ion formula	Theoretical m/z	Error (ppm)	Score
231.1378	$C_{15}H_{19}O_2^+$	231.138	0.5	100

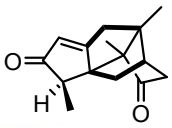

Analysed on 26/02/2025

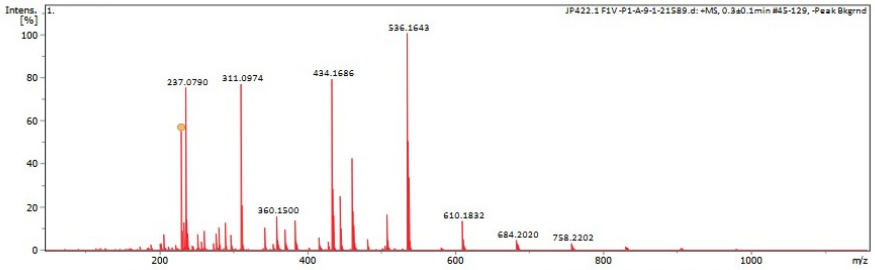

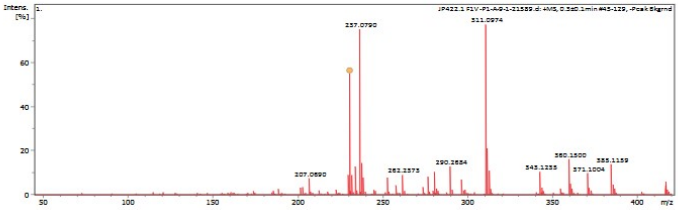

Mass spectrometry experiments was performed on a tims-TOF mass spectrometer (Bruker) in Laboratoire de Chimie Moléculaire (Ecole polytechnique, CNRS, Palaiseau, France). Electrospray source has been used in positive mode. Samples was prepared in acetonitri acid, introduced at a 5 µL/min flow rate into the interface of the instrument. Capillary and end plate voltages were set at 4.5 kV and 0.7 kV . Nitrogen was used as the nebulizer and drying gas at 2.5 bar and 3 L/min, respectively, with a drying temperature of 180°C. Tu used for calibration. The elemental compositions of all ions were determined with the instrument software Data Analysis, the precision of mass measurement was less than 3 ppm.

Compound 1 (daphnepapytone A)

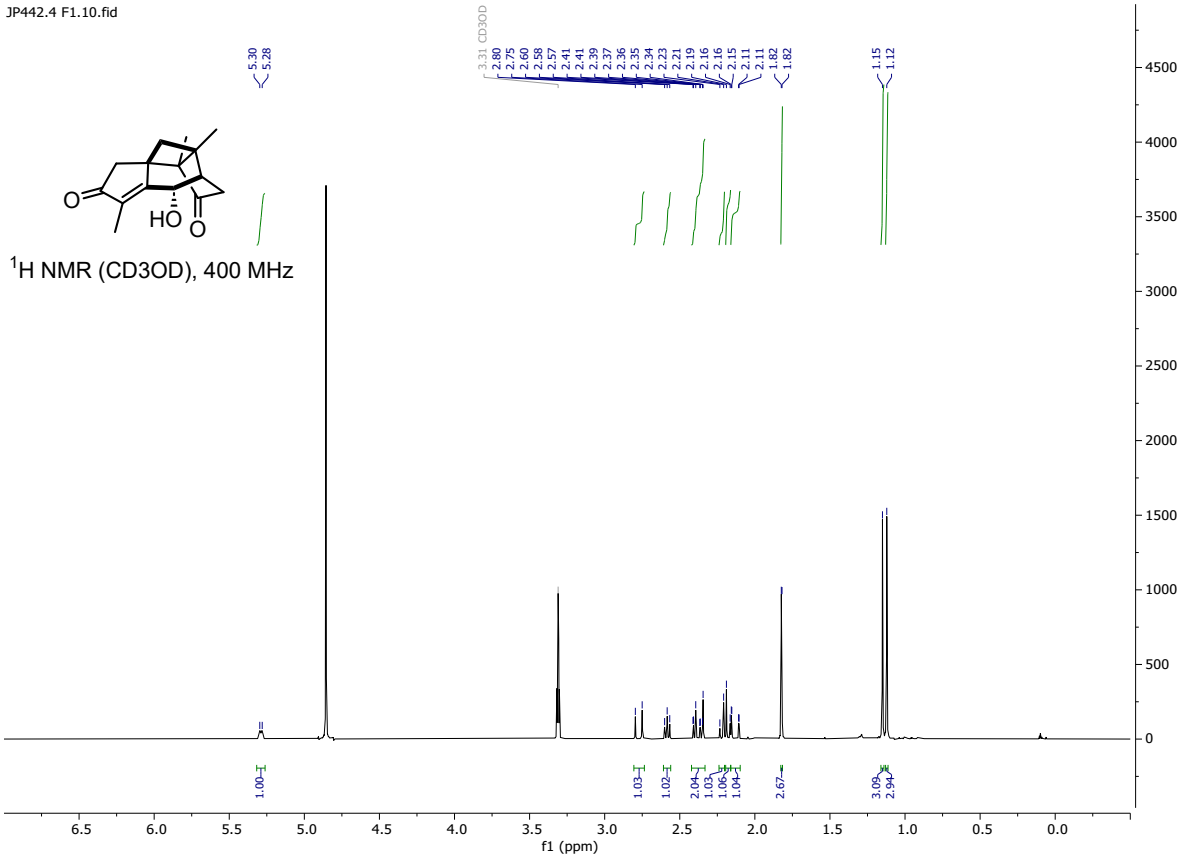

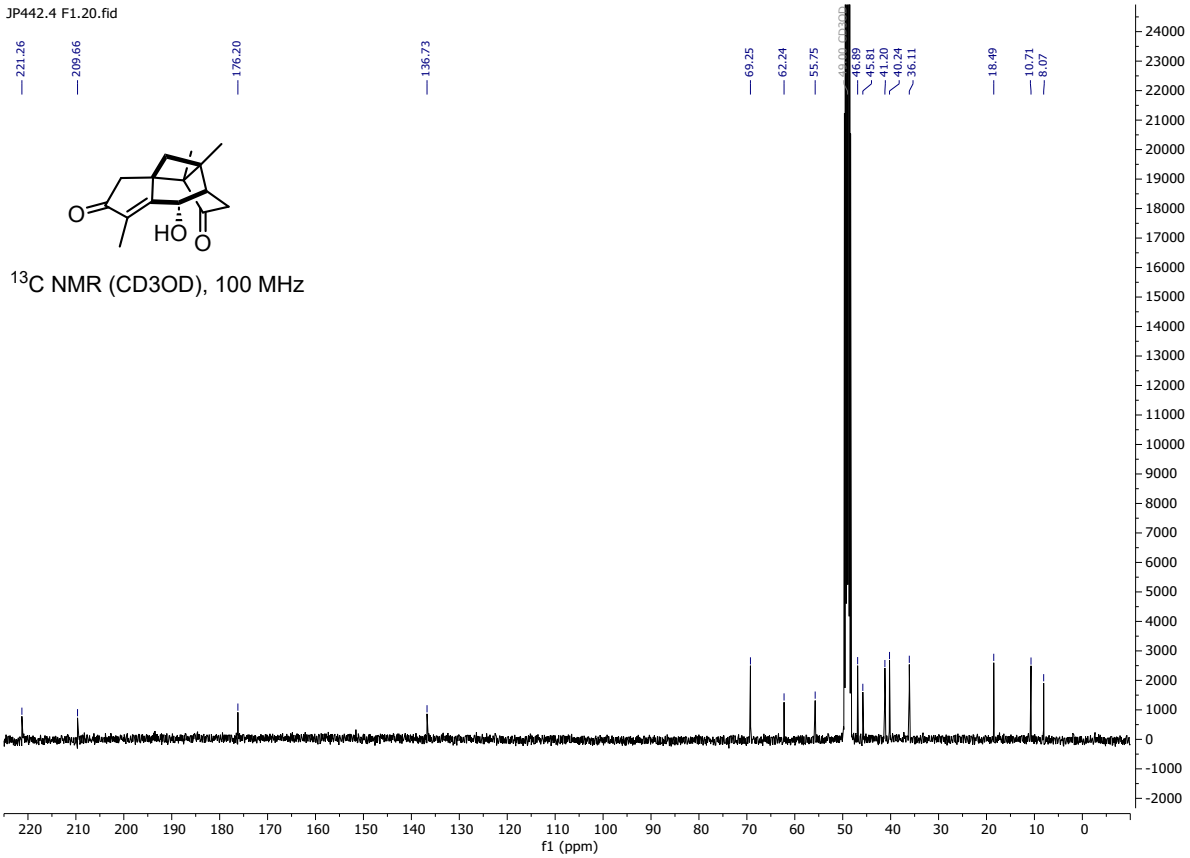

JP442.1 F1

m/z mesured	Ion formula	Theoretical m/z	Error (ppm)	Score
247.1326	$C_{15}H_{19}O_3^+$	247.1329	1	100

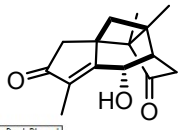

Analysed on 26/02/2025

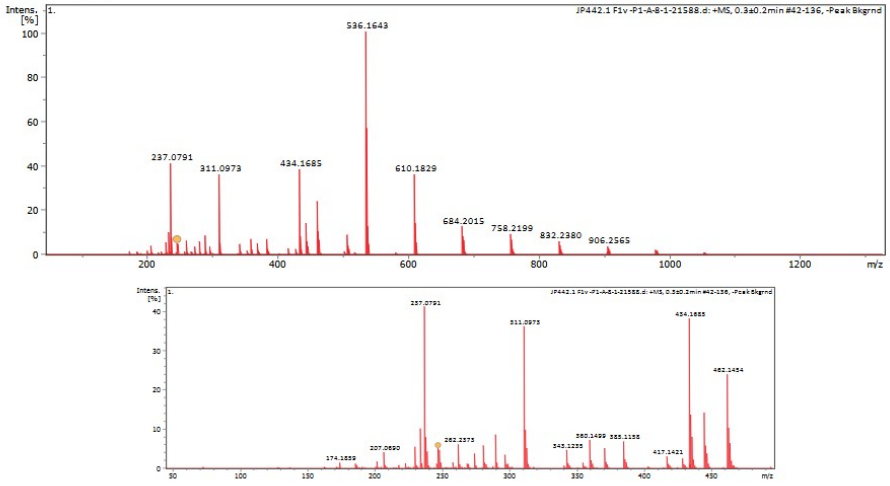

Mass spectrometry experiments was performed on a tims-TOF mass spectrometer (Bruker) in Laboratoire de Chimie Moléculaire (Ecole polytechnique, CNRS, Palaiseau, France). Electrospray source has been used in positive mode. Samples was prepared in acetonitri acid, introduced at a 5 µL/min flow rate into the interface of the instrument. Capillary and end plate voltages were set at 4.5 kV and 0.7 kV . Nitrogen was used as the nebulizer and drying gas at 2.5 bar and 3 L/min, respectively, with a drying temperature of 180°C. Tu used for calibration. The elemental compositions of all ions were determined with the instrument software Data Analysis, the precision of mass measurement was less than 3 ppm.

Compound 19[a]

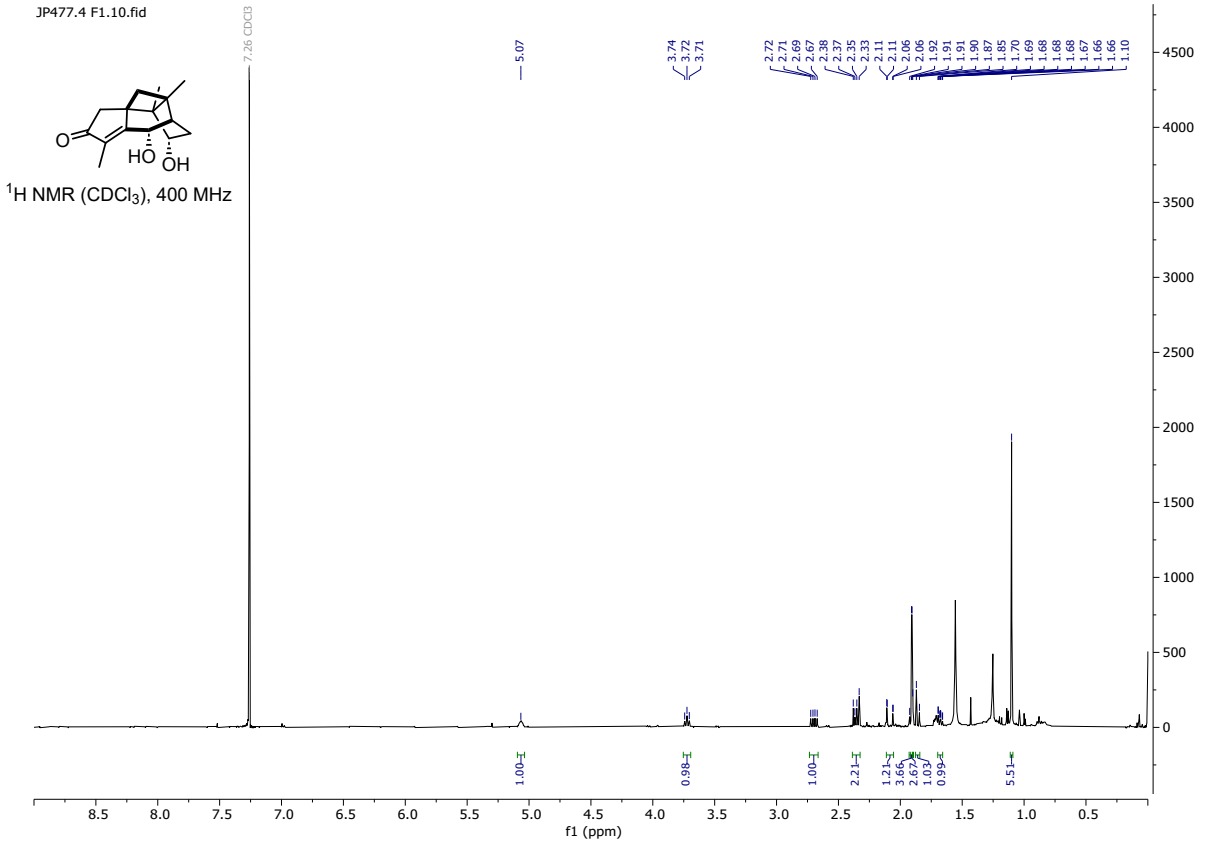

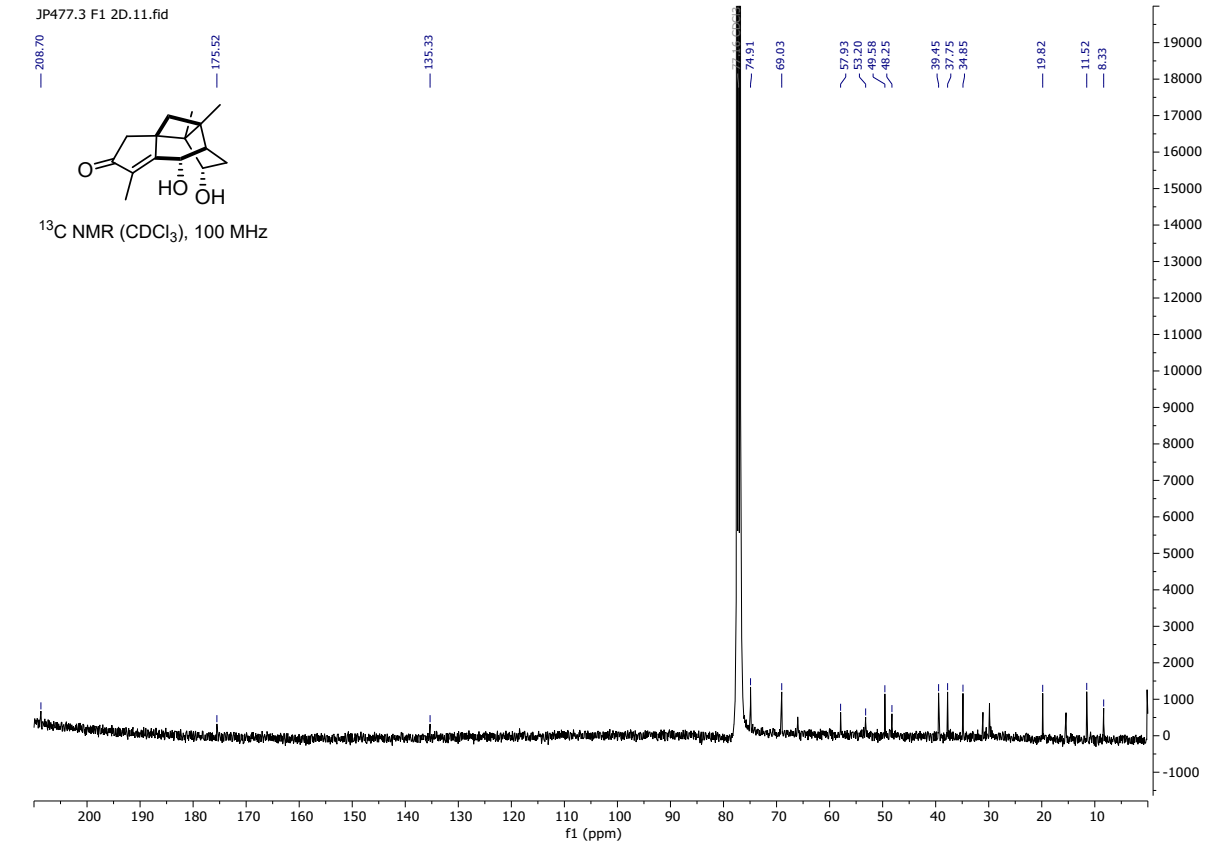

[a] This compound was obtained in very low quantity and the spectra are contaminated with traces of acetone, Et_2O, CH_2Cl_2 and BHT, more visible on the ^{13}C NMR spectrum.

JP477.4 F1

Analysed on 26/02/2025

m/z mesured	Ion formula	Theoretical m/z	Error (ppm)	Score
249.1483	$C_{15}H_{21}O_3^+$	249.1485	0.9	100

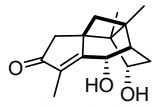

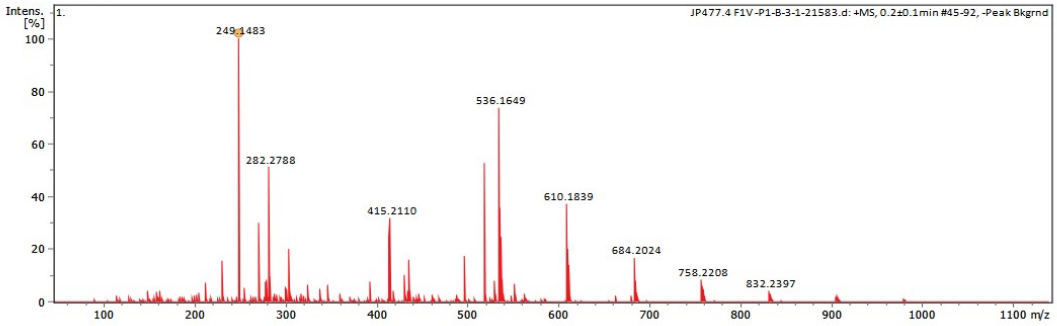

Mass spectrometry experiments was performed on a tims-TOF mass spectrometer (Bruker) in Laboratoire de Chimie Moléculaire (École polytechnique, CNRS, Palaiseau, France). Electrospray source has been used in positive mode. Samples was prepared in acetonitri acid, introduced at a 5 µL/min flow rate into the interface of the instrument. Capillary and end plate voltages were set at 4.5 kV and 0.7 kV . Nitrogen was used as the nebulizer and drying gas at 2.5 bar and 3 L/min, respectively, with a drying temperature of 180°C. Tu used for calibration. The elemental compositions of all ions were determined with the instrument software Data Analysis, the precision of mass measurement was less than 3 ppm.

7 References

1 T. Shibata, S. Kadowaki, M. Hirase and K. Takagi, *Synlett*, 2003, 0573–0575.
2 K. M. Brummond, J. Lu and J. Petersen, *J. Am. Chem. Soc.*, 2000, **122**, 4915–4920.
3 B. Alcaide, P. Almendros and C. Aragoncillo, *Chem. – Eur. J.*, 2002, **8**, 1719–1729.
4 H. Taninaka, Y. Takaishi, G. Honda, Y. Imakura, E. Sezik and E. Yesilada, *Phytochemistry*, 1999, **52**, 1525–1529.
5 D.-X. Sun, D. Zhao, H.-Y. Wei, X.-L. Ma, L.-L. Shi and J. Zhang, *Molecules*, 2018, **23**, 1383.
6 P. Zhao, B.-S. Xin, S.-Y. Qin, Z.-Y. Li, B. Lin, G.-D. Yao, S.-J. Song and X.-X. Huang, *Org. Chem. Front.*, 2022, **9**, 6213–6222.
7 C.-Y. Zheng and J.-M. Yue, *Nat. Commun.*, 2023, **14**, 2399.
8 A. L. García-Cabeza, R. Marín-Barrios, R. Azarken, F. J. Moreno-Dorado, M. J. Ortega, H. Vidal, J. M. Gatica, G. M. Massanet and F. M. Guerra, *Eur. J. Org. Chem.*, 2013, **2013**, 8307–8314.
9 S.-Z. Huang, Q. Wang, J.-Z. Yuan, C.-H. Cai, H. Wang, A. Mándi, T. Kurtán, H.-F. Dai and Y.-X. Zhao, *J. Nat. Prod.*, 2022, **85**, 3–14.
10 X-Ray and model structures were generated with CYLview20, C. Y. Legault, Université de Sherbrooke, 2020 (http://www.cylview.org).
11 Z. Meng and A. Fürstner, *J. Am. Chem. Soc.*, 2019, **141**, 805–809.
12 M. Wang, S. Khan, E. Miliordos and M. Chen, *Adv. Synth. Catal.*, 2018, **360**, 4634–4639.
13 A. W. Schuppe, D. Huang, Y. Chen and T. R. Newhouse, *J. Am. Chem. Soc.*, 2018, **140**, 2062–2066.
14 M. J. Frisch, G. W. Trucks, H. B. Schlegel, G. E. Scuseria, M. A. Robb, J. R. Cheeseman, G. Scalmani, V. Barone, G. A. Petersson, H. Nakatsuji, X. Li, M. Caricato, A. V. Marenich, J. Bloino, B. G. Janesko, R. Gomperts, B. Mennucci, H. P. Hratchian, J. V. Ortiz, A. F. Izmaylov, J. L. Sonnenberg, D. Williams-Young, F. Ding, F. Lipparini, F. Egidi, J. Goings, B. Peng, A. Petrone, T. Henderson, D. Ranasinghe, V. G. Zakrzewski, J. Gao, N. Rega, G. Zheng, W. Liang, M. Hada, M. Ehara, K. Toyota, R. Fukuda, J. Hasegawa, M. Ishida, T. Nakajima, Y. Honda, O. Kitao, H. Nakai, T. Vreven, K. Throssell, J. A. Montgomery Jr., J. E. Peralta, F. Ogliaro, M. J. Bearpark, J. J. Heyd, E. N. Brothers, K. N. Kudin, V. N. Staroverov, T. A. Keith, R. Kobayashi, J. Normand, K. Raghavachari, A. P. Rendell, J. C. Burant, S. S. Iyengar, J. Tomasi, M. Cossi, J. M. Millam, M. Klene, C. Adamo, R. Cammi, J. W. Ochterski, R. L. Martin, K. Morokuma, O. Farkas, J. B. Foresman and D. J. Fox, *Gaussian, Inc., Wallingford CT, Gaussian 16, Revision C.01*, 2016.
15 A. D. Becke, *Phys. Rev. A*, 1988, **38**, 3098–3100.
16 A. D. Becke, *J. Chem. Phys.*, 1993, **98**, 5648–5652.
17 C. Lee, W. Yang and R. G. Parr, *Phys. Rev. B*, 1988, **37**, 785–789.
18 Y. Suzuki, D. Kaneno and S. Tomoda, *J. Phys. Chem. A*, 2009, **113**, 2578–2583.
19 P. Patel, S. Lingayat, N. Gulvi and P. Badani, *Chem. Phys.*, 2018, **504**, 13–21.
20 S. Grimme, J. Antony, S. Ehrlich and H. Krieg, *J. Chem. Phys.*, 2010, **132**, 154104.
21 R. Krishnan, J. S. Binkley, R. Seeger and J. A. Pople, *J. Chem. Phys.*, 1980, **72**, 650–654.
22 A. D. McLean and G. S. Chandler, *J. Chem. Phys.*, 1980, **72**, 5639–5648.
23 T. Clark, J. Chandrasekhar, G. W. Spitznagel and P. V. R. Schleyer, *J. Comput. Chem.*, 1983, **4**, 294–301.
24 A. V. Marenich, C. J. Cramer and D. G. Truhlar, *J. Phys. Chem. B*, 2009, **113**, 6378–6396.
25 P. Song, M. Ruan, X. Sun, Y. Zhang and W. Xu, *J. Phys. Chem. B*, 2014, **118**, 10224–10231.
26 J. N. Harvey, F. Himo, F. Maseras and L. Perrin, *ACS Catal.*, 2019, **9**, 6803–6813.
27 D. Rodrigues Silva, L. A. Zeoly, P. Vermeeren, R. A. Cormanich, T. A. Hamlin, C. Fonseca Guerra and M. P. Freitas, *J. Phys. Org. Chem.*, 2023, **36**, e4556.
28 S. Grimme, *Chem. – Eur. J.*, 2012, **18**, 9955–9964.
29 G. Luchini, J. V. Alegre-Requena, I. Funes-Ardoiz and R. S. Paton, *F1000Research*, 2020, preprint, F1000Research:9:291, DOI: 10.12688/f1000research.22758.1.
30 N. Tarannam, N. Alassad, N. G. Lemcoff and S. Kozuch, *J. Chem. Theory Comput.*, 2023, **19**, 5024–5035.

31 O. V. Dolomanov, L. J. Bourhis, R. J. Gildea, J. a. K. Howard and H. Puschmann, *J. Appl. Crystallogr.*, 2009, **42**, 339–341.
32 G. M. Sheldrick, *Acta Crystallogr. Sect. Found. Adv.*, 2015, **71**, 3–8.
33 G. M. Sheldrick, *Acta Crystallogr. Sect. C Struct. Chem.*, 2015, **71**, 3–8.